11-1-2003

Field Instrumentation and Long-Term Monitoring of the FRP Bridge over Dubois Creek in Great Bend, PA

Ian C. Hodgson

Robert J. Connor

Greg C. Parent

FIELD INSTRUMENTATION AND LONG-TERM MONITORING OF THE FRP BRIDGE OVER DUBOIS CREEK IN GREAT BEND, PENNSYLVANIA

by

Ian C. Hodgson

Robert J. Connor

Greg C. Parent

FINAL REPORT

ATLSS Report No. 03-28

November 2003

ATLSS is a National Center for Engineering Research on Advanced Technology for Large Structural Systems

117 ATLSS Drive
Bethlehem, PA 18015-4729

Phone: (610)758-3525
Fax: (610)758-5902

www.atlss.lehigh.edu
Email: inatl@lehigh.edu

1.0 Introduction

This Final Report discusses and summarizes the results of the field testing and monitoring of the Dubois Creek FRP bridge in Great Bend Township, in Susquehanna County, Pennsylvania.

This bridge, which replaced an existing steel stringer bridge, has recently been constructed. The slab structure is composed of fiber-reinforced polymer (FRP) material. Although developed many years ago, the use composite materials for bridge applications is extremely limited. As part of a pilot program initiated by PennDOT and FHWA, it was decided to replace the existing steel bridge with a new FRP slab bridge at the same location. In order to better understand the behavior of this bridge structure, a instrumentation and testing program was developed and implemented. This consisted of performing controlled static and dynamic load tests, in addition to remote long-term monitoring. Strains and displacements in the FRP material and the concrete parapet were monitored. The testing and monitoring discussed in this report consisted of three phases. Phase 1 testing was conducted between July and August 2002. Phase 2 testing was conducted between February and April 2003. Finally, Phase 1 testing was conducted between August and October 2003.

In this report, the results of Phase 1 are treated as a baseline for comparison for the results of the Phases 2 and 3. Comparison of results from the subsequent test phases to a common reference facilitates the identification of trends (if they exist), potentially caused by changes in behavior over time.

1.1 Bridge Description

The bridge carries SR1037 over Dubois Creek, and can be seen in Figure 1.1. The bridge spans 21 feet 6 inches, and is skewed 70 degrees. The overall bridge width is 32 feet, with two traffic lanes. There are cast-in-place concrete parapets on either side of the bridge. The thickness of the FRP slab varies from a maximum of approximately 24 inches at the centerline to 20 inches at the edges. The slab itself is composed of two FRP panels placed side-by-side with a longitudinal joint between. Each panel consists of an FRP top and bottom plate, connected by FRP webs at 8 inches on center in both directions. The void spaces are filled with non-structural foam “bottles.” The concrete parapets are attached to the slab with reinforcement steel. The bridge substructure consists of reinforced concrete abutments supported on spread footings. The FRP slab rests on 1 inch neoprene bearing pads.

The FRP slab is topped with an epoxy overlay with a thickness of 3/8 inch. The epoxy overlay is Transpo T-48 manufactured by Castek. There have been a significant number of repairs made to this overlay since the original application, due to various types of failures. The epoxy overlay was removed in October 2003, and replaced with a bituminous overlay. A complete description of the failures and repairs can be found in Appendix B.

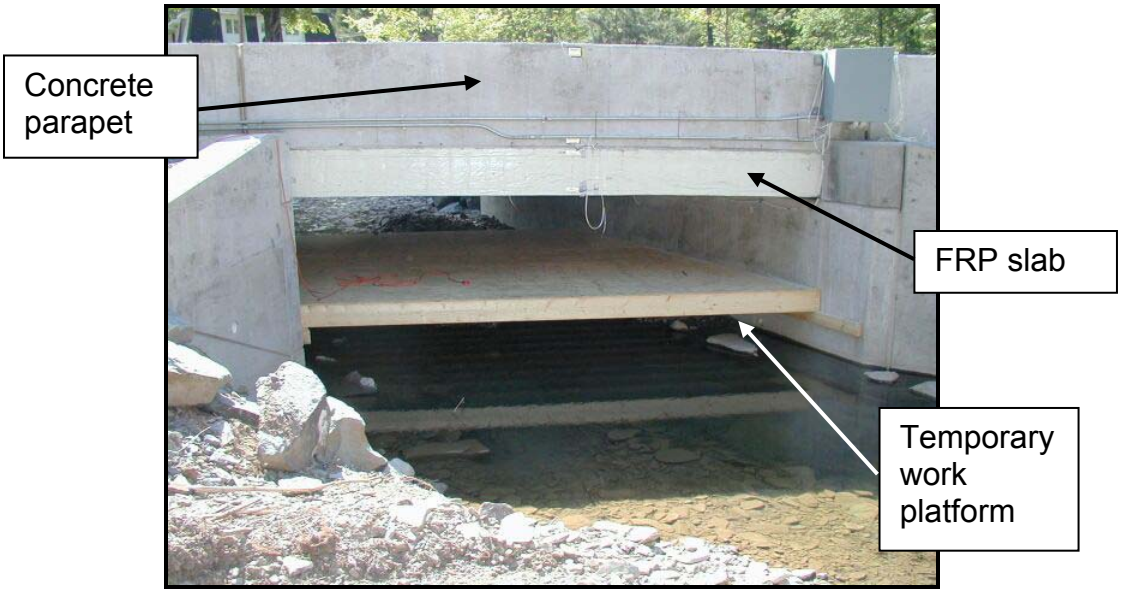

Figure 1.1 – Photograph of FRP bridge over Dubois Creek in Great Bend Twp., PA

1.2 Design Criteria

The FRP slab was designed such that the maximum deflection due to full service load plus impact (with an impact factor of 1.3) does not exceed L/800. Furthermore, the maximum stress under full dead plus live load was not to exceed 20 percent of the minimum guaranteed failure stress of the FRP material as well as the bond and joint lines. The design stresses for this bridge are summarized in Table 1.1 [Ref. 1]. For the top and bottom slab plates, the warp direction runs parallel to traffic, while for the webs, the warp direction runs vertically, through the slab thickness.

Stress Direction	Design Stress (psi)
Warp Tension (0°)	9,515
Warp Compression (0°)	9,908
Fill Tension (90°)	9,058
Fill Compression (90°)	6,555
Short Beam Shear (0°)	1,102
Short Beam Shear (90°)	928
In-Plane Shear	3,323

Table 1.1 – Summary of FRP slab design stresses

2.0 Instrumentation Plan and Data Acquisition

The following section describes the instrumentation plan used during the field testing and monitoring program. "As built" strain gage plans detailing the locations of all strain gages installed on both structures are provided in Appendix A.

2.1 Strain Gages

Strain gages were placed at locations chosen to establish the global and local behavior of the structure.

Several types of strain gages were used. Prior to construction of the FRP slab, strain rosettes were embedded in the fiberglass fabric. These rosettes were produced by Measurements Group Inc. and were 45 degree rosettes, with 0.25 inch gage length type CEA-06-250UR-350. Rosettes were placed in the top FRP plate and in selected FRP webs. These rosettes were pre-embedded because field installation was not possible.

At the underside of the FRP slab and on the concrete parapets, uniaxial bondable strain gages were used. These gages have an active grid length of two inches. Hence the strain is measured over a length of two inches. The strain measured is the average over the two-inch gage length. Gages of this type are appropriate for use on non-homogenous materials such as the FRP or concrete. In some locations, two gages were used and oriented in a "T" configuration, as shown in Figure 2.1. These gages were produced by Measurements Group Inc., and are type N2A-06-20CBW-350.

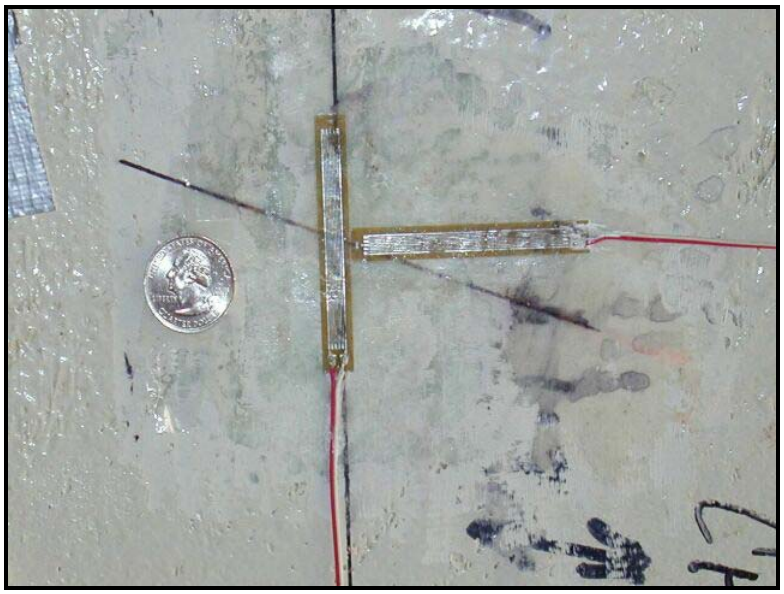

Figure 2.1 – Bondable strain gages in a "T" configuration

The gage resistance was 350Ω and an excitation voltage of 10 Volts was used. All gages were protected with a multi-layer system and then sealed with a silicon type agent. Where required, wire connections were soldered and electrically insulated with heat shrink tube. The majority of the sensors were operational throughout the monitoring period. However, three individual gages of the embedded rosettes were damaged during the construction process.

2.2 Summary of Instrumentation Layout

The following section summarizes the instrumentation plan. Strain gages, thermocouples, and displacement sensors were included in the plan. Only the downstream panel and parapet were instrumented. The detailed instrumentation plan, showing the locations of all sensors is provided in Appendix A.

2.2.1 Strain Gages on Top of Slab

As indicated previously, strain rosettes were embedded in the top surface of the FRP slab. Rosettes were located on three transverse lines, and two longitudinal lines, for a total of six rosettes (see Appendix A). The rosettes were oriented such that the arms of the rosette are aligned parallel to the longitudinal and transverse directions of the bridge, and at 45 degrees.

2.2.2 Strain Gages on Bottom of Slab

Uniaxial two-inch bondable strain gages were installed on the same longitudinal and transverse lines used to locate the rosettes on the top surface of the slab (six locations total). At the two transverse lines closest to the abutments, a single longitudinal gage was installed at each location. At the transverse line at the centerline of the span, two gages were installed at each location in a "T" configuration (see Figure 2.1), with legs parallel to the longitudinal and transverse bridge directions.

2.2.3 Strain Gages on Bottles

The strain gages described in Sections 2.2.1 and 2.2.2 were installed to investigate the global response of the FRP slab structure to load. Additional rosettes were installed around a selected bottle in the slab. Two rosettes were installed in the top and two webs of one bottle (three rosettes). The webs of two adjacent bottles were also instrumented. The webs of these bottles were adjacent to the webs of the bottle with three strain gages. The rosettes of each pair are embedded in adjacent layers of FRP (the webs, top and bottom plate are composed of multiple layers of FRP material). Hence bend and axial strains in the webs could be calculated.

Since each pair of rosettes are located at the same position in the plane of the FRP, the state of strain through the thickness of a given FRP layer can be determined. Using these data an understanding of the local behavior of the FRP slabs when subjected to concentrated loads is obtained.

2.2.4 Strain Gages on Parapet

Uniaxial two-inch bondable strain gages were placed on the downstream concrete parapet, on both sides, near the top and bottom, at the centerline of the bridge span. Additional longitudinal gages were installed on the side of the FRP slab at the centerline of the bridge span.

The location of the neutral axis at the parapet can be estimated using the data from these gages. Weak axis bending of the parapet (if present) can also be detected since gages are located on both faces.

2.2.5 Displacement Sensors at Bottom of Slab

Vertical displacements of the FRP slab were measured during Phase 1 and 3 testing (these measurements were not made during Phase 2 due to weather constraints). During Phase 1 testing, three displacement sensors were used. The sensors were located along the midspan of the bridge, beneath the parapet, at the bridge centerline, and halfway between these two locations. Linear Variable Differential Transformers (LVDTs) were used and were mounted to the temporary work platform beneath the bridge, as shown in Figure 2.2. For Phase 3, the sensors were mounted to a steel support frame (see Section 11.2).

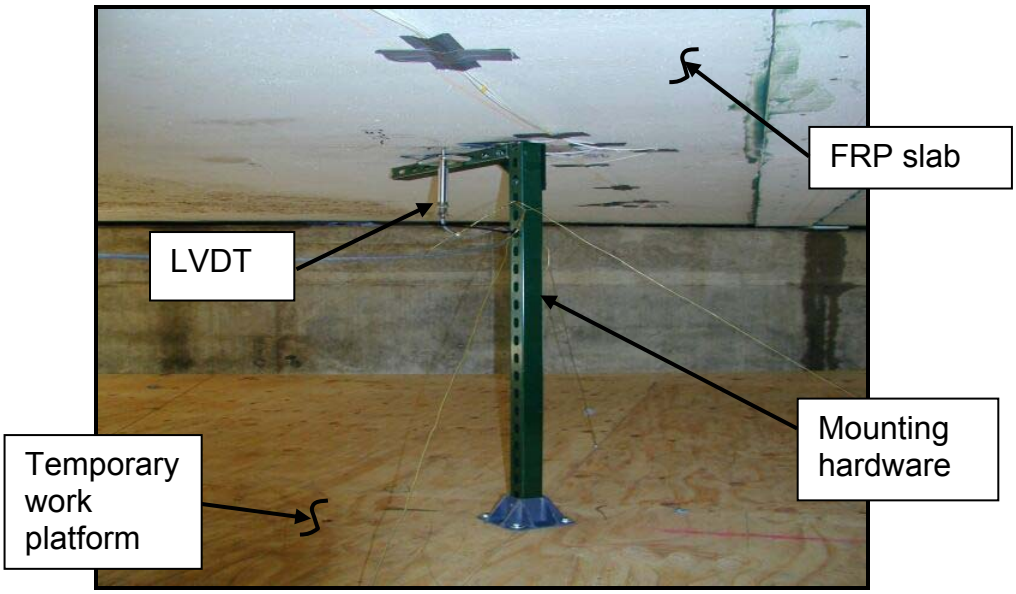

Figure 2.2 – Vertical displacement sensor (LVDT) mounted beneath the bridge slab (Phase 1 tests only)

2.2.6 Thermocouple Layout

Temperature sensors were added for the long-term monitoring phase of the project. Thermocouples were installed at the bottom and top surface of the FRP slab. The locations of these sensors can be seen in Appendix A. An additional thermocouple was used to record ambient air temperature.

2.3 Data Acquisition

2.3.1 On-site Controlled Testing

Data were collected using a Campbell Scientific CR9000 Data Logger. This is a high-speed, multi-channel, 16-bit digital data acquisition system. In order to ensure a stable, noise-free signal, analog and digital filtering were employed. Using a laptop computer, real-time review of the data was possible during all tests. Hence, sensors could be checked in real-time to ensure proper operation. A photograph of the data acquisition system can be seen in Figure 2.3.

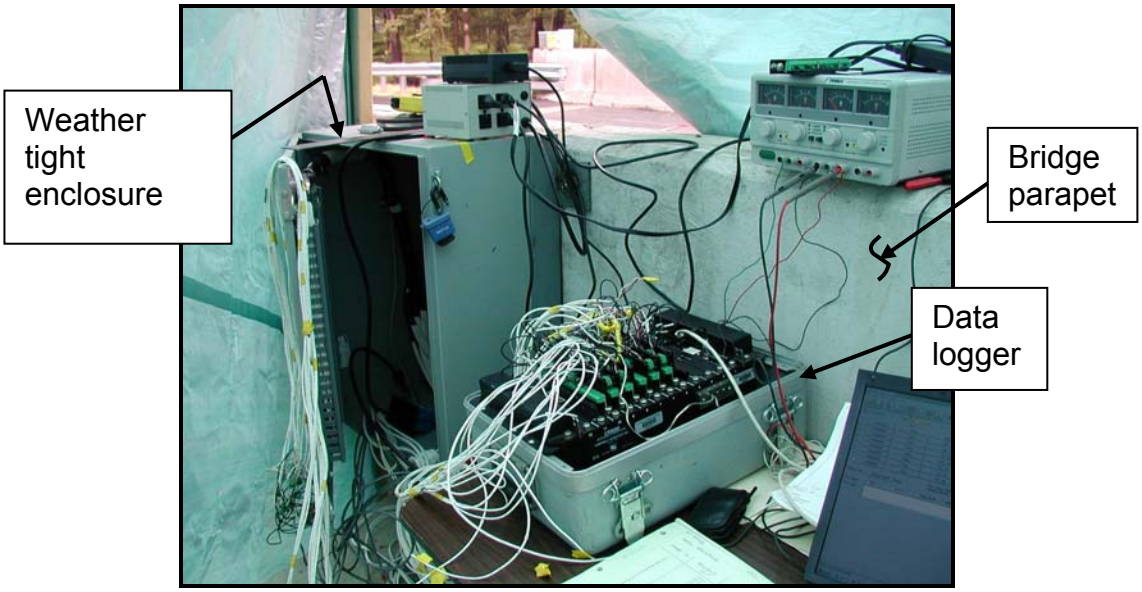

Figure 2.3 – Data acquisition system used for the on-site controlled load testing

2.3.2 Remote Long-term Monitoring

Remote long-term monitoring of selected gages was also conducted using a CR9000 Data Logger. The monitoring began after an initial review of the measurements taken during the controlled static and dynamic tests was completed. The data logger was stored in a weather tight enclosure mounted to the bridge parapet (Figure 2.3).

Remote communication with the Data Logger was made using an analog telephone line provided by Penn DOT. Program upload and data download was performed remotely from the ATLSS laboratories in Bethlehem, PA.

3.0 Phase 1 Test Program – Summary

The test program included controlled load tests using a test truck of known weight and geometry. Various travel speeds and truck locations were used. During the tests, time-history data from all sensors were recorded. In addition, long-term monitoring of the bridge was conducted. When predefined strain thresholds were exceeded, limited time-history data were recorded to facilitate characterization of the loading event. These tests and the data collected are discussed below.

3.1 Controlled Load Tests

In order to measure in-situ response of the bridge to load and to validate analytical models of the bridge, a series of controlled load tests were conducted using a test truck of known load and geometry. A photograph of the test truck can be seen in Figure 3.1. Several types of load tests were conducted. These included park, crawl, and dynamic tests.

Figure 3.1 – Photograph of test truck utilized during the controlled load tests

The gross vehicle weight (GVW) of the truck was approximately 52,800 pounds. The truck was provided by the general contractor. Tables 3.1 and 3.2 summarizes the axle loads and geometry of the truck.

It should be noted that during tests, only one truck was used. Therefore the results obtained from these tests do not represent the full live load on the bridge. Future testing will utilize two test trucks.

Test Description	Rear Axle Type	Front Axle Load (lb)	Rear Tandem Load (lb)	GVW[1] (lb)	Date of Tests
Controlled Load Tests	Tandem	13,700	39,120	52,820	June 5, 2002

Note:
1. GVW = Gross Vehicle Weight

Table 3.1 – Test truck axle load data

Rear Axle	L1 (in)	L2 (in)	W_f (in)	W_r (in)	A[1] (in)	B (in)	C (in)	D[1] (in)	E (in)
Tandem	192	50	84	72	-	16	24	-	11.5

Note:
1. This dimension was not measured.

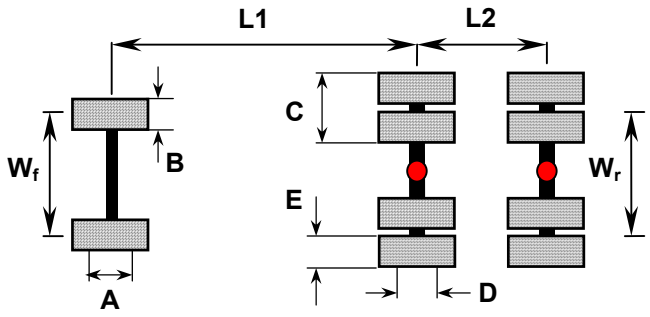

Table 3.2 - Geometry of test truck used for controlled load tests

Since the total number of channels in the instrumentation plan was larger than the available capacity of the data logger, two separate setups were required. The first excluded all rosettes on the instrumented bottles, as previously stated. These rosettes were installed to recover local response of the FRP slab. The remaining gages provide data related to the global response of the bridge. The controlled load tests for this setup are summarized in Table 3.3. It should be noted that the **bold** test names represent the data set selected for each test configuration used in the data analysis, as will be discussed in Section 4. The various test truck positions for each of the controlled load tests are illustrated in Figure 3.2.

For the second test setup, the bottle gages were then connected. The controlled load tests for this second setup are summarized in Table 3.4.

Test #	File Name	Test Type	Travel Dir.[1]	Lane[2]	Truck Dir.[3]	Comment
1	**CRL_US1.DAT**	**Crawl**	**S**	**US**	**F**	**57" from CL right dual to FF PPT.**
2	CRL_US2.DAT	Crawl	N	US	R	57" from CL right dual to FF PPT.
3	CRL_US3.DAT	Crawl	S	US	F	57" from CL right dual to FF PPT.
4	**CRL_DS1.DAT**	**Crawl**	**S**	**DS**	**F**	**CL right dual over rosettes A, B, C**
5	CRL_DS2.DAT	Crawl	N	DS	R	CL right dual over rosettes A, B, C
6	CRL_DS3.DAT	Crawl	S	DS	F	CL right dual over rosettes A, B, C
7	**CRL_DS4.DAT**	**Crawl**	**S**	**DS**	**F**	**CL left dual over rosettes D, E, F**
8	CRL_DS5.DAT	Crawl	N	DS	R	CL left dual over rosettes D, E, F
9	CRL_DS6.DAT	Crawl	S	DS	F	CL left dual over rosettes D, E, F
10	**CRL_PPT1.DAT**	**Crawl**	**N**	**DS**	**R**	**Left tires 4"-6" off FF DS PPT.**
11	CRL_PPT2.DAT	Crawl	N	DS	R	Left tires 4"-6" off FF DS PPT.
12	CRL_PPT3.DAT	Crawl	N	DS	R	Left tires 4"-6" off FF DS PPT.
13	**PRK_RT1.DAT**	**Park**	**S**	**DS**	**F**	**CL right dual over rosettes A, B, C**
14	PRK_RT2.DAT	Park	S	DS	F	CL right dual over rosettes A, B, C
15	**PRK_LT1.DAT**	**Park**	**S**	**DS**	**F**	**CL left dual over rosettes D, E, F**
16	PRK_LT2.DAT	Park	S	DS	F	CL left dual over rosettes D, E, F
17	DYN_LT1.DAT	Dynamic	S	DS	F	Approx. speed = 23 mph; truck approx. centered in normal DS travel lane
18	**DYN_LT2.DAT**	**Dynamic**	**S**	**DS**	**F**	**Approx. speed = 23 mph; truck approx. centered in normal DS travel lane**
19	**DYN_RT1.DAT**	**Dynamic**	**S**	**US**	**F**	**Approx. speed = 23 mph; truck approx. centered in normal US travel lane**
20	DYN_RT2.DAT	Dynamic	S	US	F	Approx. speed = 23 mph; truck approx. centered in normal US travel lane

Note:
1. N = north, S = south
2. DS = downstream, US = upstream
3. F= forward, R = reverse

Table 3.3 – Summary of controlled load tests (SETUP #1)

Test #	Filename	Test Type	Travel Dir	Lane	Truck Dir.	Comment
21	CRL_CLB1.DAT	Crawl	S	DS	F	CL left dual 2-3" US of CL instrumented bottle
22	**CRL_CLB2.DAT**	**Crawl**	**S**	**DS**	**F**	**CL left dual 2-3" US of CL instrumented bottle**
23	CRL_CLB3.DAT	Crawl	S	DS	F	CL left dual 2-3" US of CL instrumented bottle
24	**CRL_DSB1.DAT**	**Crawl**	**S**	**DS**	**F**	**CL left dual 9-10" DS of CL instrumented bottle**
25	CRL_DSB2.DAT	Crawl	S	DS	F	CL left dual 12" DS of CL instrumented bottle
26	CRL_DSB3.DAT	Crawl	S	DS	F	CL left dual 10" DS of CL instrumented bottle
27	CRL_USB1.DAT	Crawl	S	DS	F	CL left dual 13" US of CL instrumented bottle
28	CRL_USB2.DAT	Crawl	S	DS	F	CL left dual 14" US of CL instrumented bottle
29	**CRL_USB3.DAT**	**Crawl**	**S**	**DS**	**F**	**CL left dual 14" US of CL instrumented bottle**

Note:
1. N = north, S = south
2. DS = downstream, US = upstream
3. F= forward, R = reverse

Table 3.4 – Summary of controlled load tests (SETUP #2)

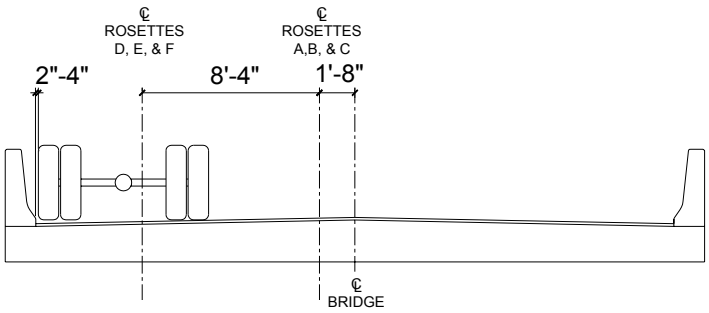

(a) Tests CRL PPT1 to CRL PPT3

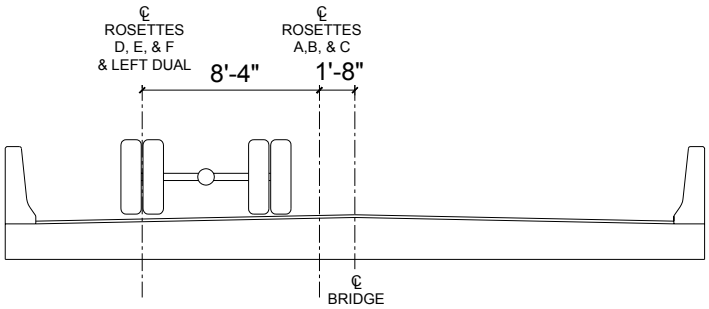

(b) Tests CRL DS4 to CRL DS6

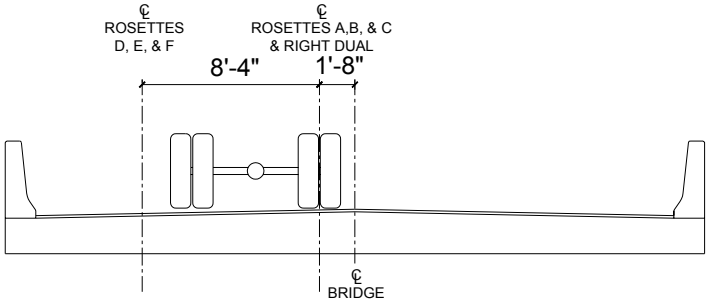

(c) Tests CRL DS1 to CRL DS3

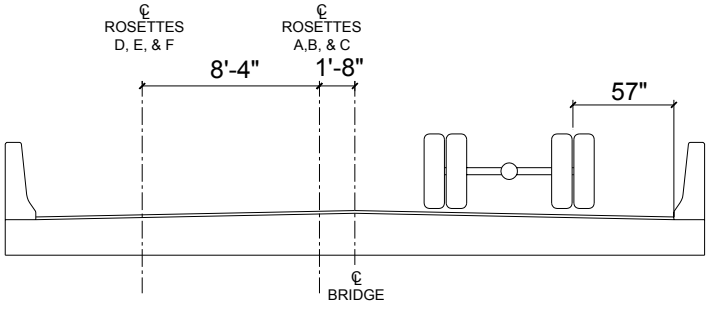

(d) Tests CRL US1 to CRL US3

Figure 3.2 – Location of test truck for the various load tests
(a) CRL_PPT1 (b) CRL_DS4 (c) CRL_DS1 (d) CRL_US1

3.2 Remote Monitoring Program

The type of data collected during the long-term monitoring program is summarized in this section. To reduce the amount of data collected, only critical strain gages were selected to be included in the long-term monitoring program. These strain gages were selected based on a review of the controlled load test data. Displacements of the bridge slab were not monitored. Twelve strain gages were selected. Table 3.5 presents the strain gages included in the long-term monitoring program. In addition to strain gages, the three thermocouples described in Section 2.2.6 were monitored.

Monitored Channel No.	Strain Gage	Location
1	CH_38	Bottom of slab; near centerline; longitudinal @ midspan
2	CH_40	Bottom of slab; near centerline; longitudinal @ 1/4 span
3	CH_42	Bottom of slab; in downstream lane; longitudinal @ midspan
4	CH_44	Bottom of slab; in downstream lane; longitudinal @ 1/4 span
5	CH_39	Bottom of slab; near centerline; transverse @ midspan
6	CH_43	Bottom of slab; in downstream lane; transverse @ midspan
7	CH_22	Top of slab; near centerline; longitudinal @ midspan
8	CH_31	Top of slab; in downstream lane; longitudinal @ midspan
9	CH_32	Top of slab; in downstream lane; 45 deg. @ midspan
10	CH_33	Top of slab; in downstream lane; transverse @ midspan
11	CH_45	Top of parapet; longitudinal; @ midspan
12	CH_50	Bottom of parapet; longitudinal @ midspan

Table 3.5 - Summary of strain gages selected for remote long-term monitoring program

4.0 Results of Controlled Load Tests

The results of the controlled static and dynamic load tests are discussed in this section

4.1 General Response

Several interesting observations related to overall behavior of the bridge were made during the controlled load tests. First, it is clear from the measured data that the parapets act as deep concrete beams spanning between abutments. The parapets are connected to the FRP slab and carry a significant portion of the load. The parapets are also very stiff compared to the FRP slab and provide a certain level of support at the edges of the slab. As a result, the FRP slab is effectively supported by the abutments and to a certain degree by the parapets (*i.e., on all four edges*). Therefore, a comparison of stresses in the slab assuming simply supported conditions does not correlate well with measured data. (*It is recognized that even in absence of the parapets, plate action of the slab results in a complicated distribution of two-way bending moments. This is further aggravated by the aspect ratio and skew of the bridge. Nevertheless, the parapets greatly influence the response of the structure, especially near the upstream and downstream edges.*)

The measurements also suggest the behavior of the FRP slab is influenced (*and complicated*) by the longitudinal joint located at the centerline of the bridge. At this joint, the two FRP panels are "butted" together and adhesively bonded. This connection does not appear to provide full moment continuity across the joint. However, shear forces appear to be adequately transmitted across the joint (this will be discussed further in Section 4.4.2.

In general, measured displacements for all positions of the test truck on the bridge were very low. As a result of the participation with the parapets and the overall geometry of the structure, the bridge experienced bending in both longitudinal and transverse directions. Measured strains resulting from the test truck loading were also low.

4.2 Repeatability of Data

As indicated in Tables 3.3 and 3.4, each test was repeated multiple times. Review of data from the same test type indicates that the data are consistent and repeatable. Therefore only one data set for each test type will be reviewed in the this report. This data set for each test type is indicated in bold typeface in Tables 3.3 and 3.4.

4.3 Vertical Displacements

As stated, the vertical displacements for all load configurations were very low. Three displacement sensors were used during the controlled load testing. LVDT's were installed along the midspan of the downstream FRP panel, as shown in Figure 4.1. As shown in the figure, CH_51 is located near the bridge centerline, CH_53 is beneath the downstream parapet, and CH_52 is approximately halfway in between. Table 4.1 contains a summary of the peak displacements for the four different static crawl tests performed. Note that for all loading cases the peak displacements are significantly less than the design maximum of L/800. It should be noted that the testing was done with one truck only, and therefore does not represent the full design live load.

Data Channel	Location	Peak Vertical Displacement (mils) (negative down)			
		CRL_PPT1	CRL_DS4	CRL_DS1	CRL_US1
CH_51	Centerline	-35.4 *(L/7290)*	-54.2 *(L/4760)*	-66.1 *(L/3900)*	-39.0 *(L/6620)*
CH_52	1/4 pt.	-57.6 *(L/4480)*	-63.6 *(L/4060)*	-58.8 *(L/4390)*	-13.9 *(L/18560)*
CH_53	Parapet	-24.8 *(L/10400)*	-16.3 *(L/15820)*	-9.8 *(L/26330)*	-0.8 *(L/322500)*

Table 4.1 – Summary of peak vertical displacements
measured during static crawl tests (PHASE 1)

Figures 4.2 through 4.5 contain plot of vertical displacement versus time for the load tests CRL_PPT1, CRL_DS4, CRL_DS1, and CRL_US1, respectively. The inset in these figures indicates the truck position during testing. During test CRL_PPT1, the test truck was as close as possible to the downstream parapet. With the successive tests shown in Figures 4.3 through 4.5, the truck position was progressively further away from the parapet.

With the exception of test CRL_PPT1, the truck was moving forward in the downstream lane (right to left in Figure 4.1). For test CRL_PPT1, the truck backed up along the parapet (left to right in Figure 4.1). As a result, the general shape of the plot in Figure 4.2 (test CRL_PPT1) appears to be a mirror image of the remaining plots.

For all tests, the peak displacements at each sensor do not occur simultaneously. This is due to the skewed position of the displacement sensors and the geometry of the bridge. It can be seen that when the truck is moving forward (Figures 4.3 through 4.5), CH_51 reaches its peak displacement first, followed by CH_52 and CH_53. Furthermore, each plot has two maxima. The smaller represent the passing of the front axle, while the larger represents the rear tandem axle.

4.3.1 Test CRL_PPT1 (Wheel adjacent to downstream parapet)

It is evident from each of these plots that the displacements beneath the parapet were always lower than at the other points beneath the slab. The largest parapet displacement relative to the other displacements occurred during test CRL_PPT1 (Figure 4.2). This is expected, as the truck was as close as possible to the parapet. The peak

displacement for this test occurred at the middle of the panel (CH_52), and was approximately 55 mils. The peak displacement at the parapet was approximately 25 mils.

4.3.2 Test CRL_DS4 (Wheel 60 inches from face of downstream parapet)

Examination of Figure 4.3 (test CRL_DS4, the next successive load position) reveals that although the peak displacement occurred at CH_52 in the middle of the panel (60 mils), the displacement was nearly the same at CH_51 at the bridge centerline. Displacement at the parapet remained small at 15 mils.

4.3.3 Test CRL_DS1 (Wheel 88 inches from face of downstream parapet)

During test CRL_DS1, with the truck closer to the bridge centerline (see Figure 4.4), the peak displacement occurred near the bridge centerline (CH_51) unlike the previous two tests. However, the magnitude of the displacements at CH_51 and CH_52 were approximately the same.

4.3.4 Test CRL_US1 (Wheel 57 inches from face of upstream parapet)

Finally, when the truck was in the upstream lane (Figure 4.5), the peak displacement occurred at the bridge centerline (CH_51), however, the magnitude was lower at approximately 40 mils. The displacement at the parapet (CH_53) was negligible.

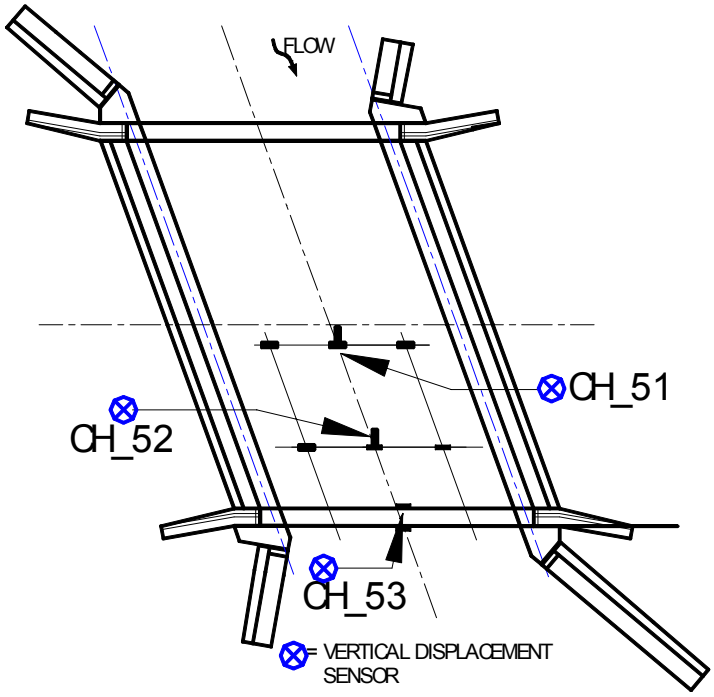

Figure 4.1 – Locations of vertical displacement sensors (used for Phase 1) located on the underside of the bridge slab. Noted CH_53 is located underneath the downstream parapet

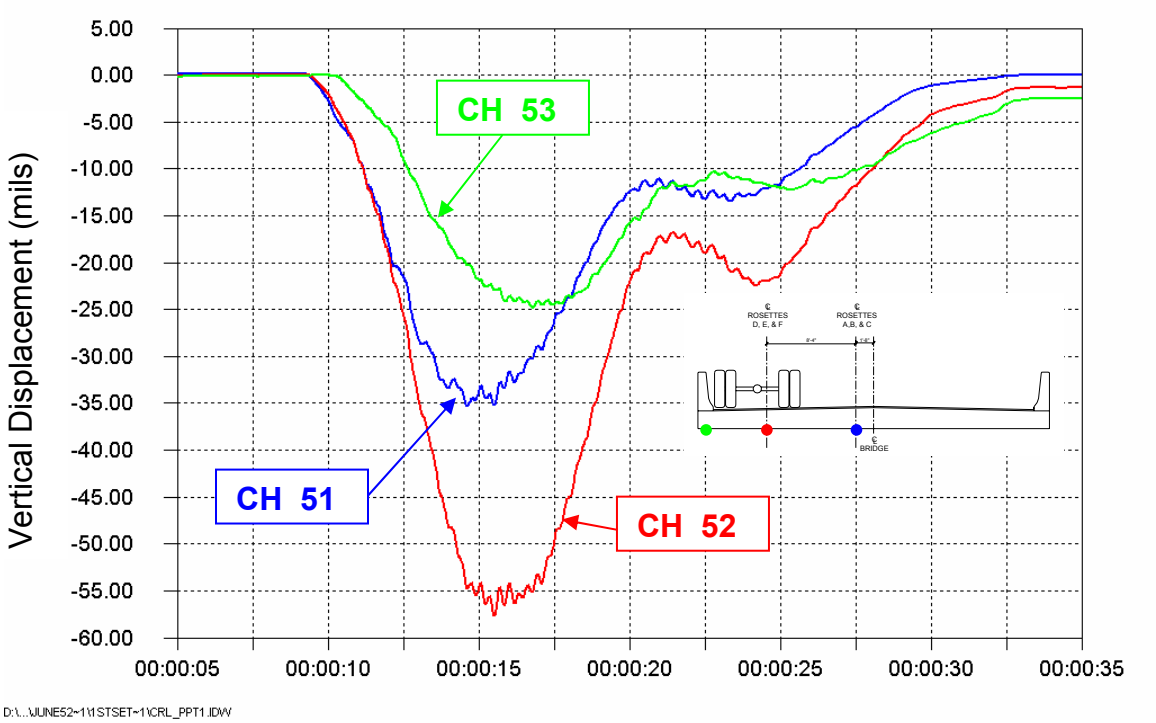

Figure 4.2 – Vertical displacement time-history for load test CRL_PPT1
(Test truck located as close as possible to downstream
parapet)

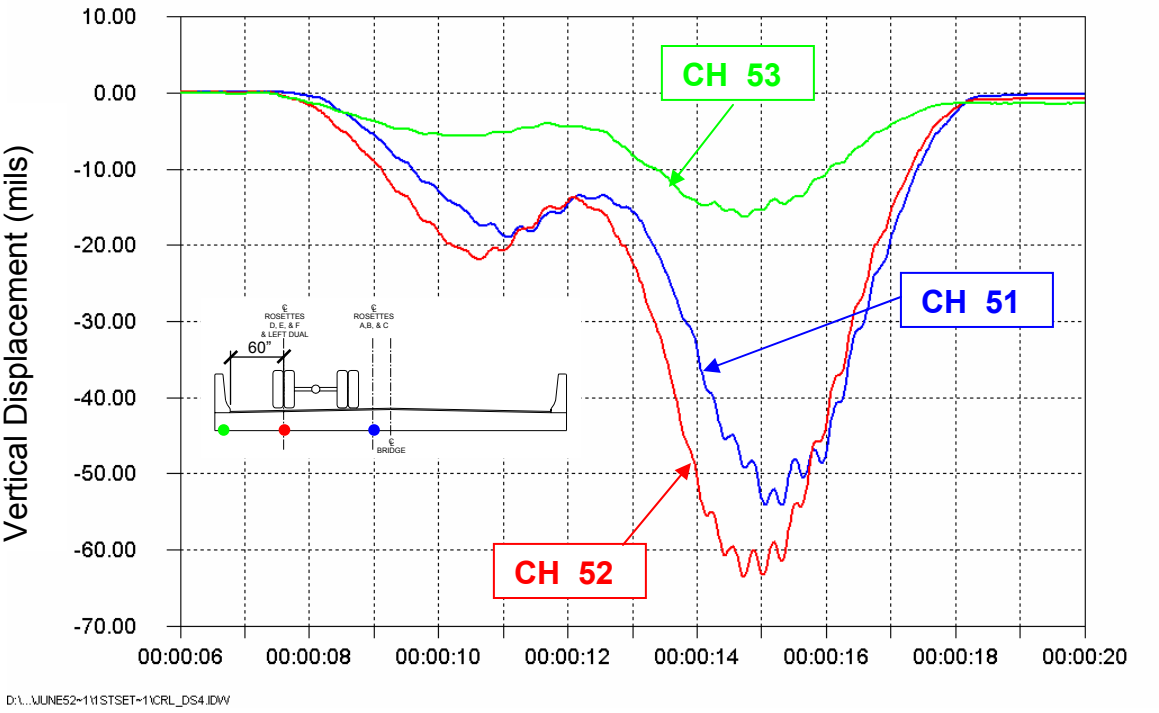

Figure 4.3 – Vertical displacement time-history for load test CRL_DS4
(Test truck located with centerline of right dual over rosettes D, E, F)

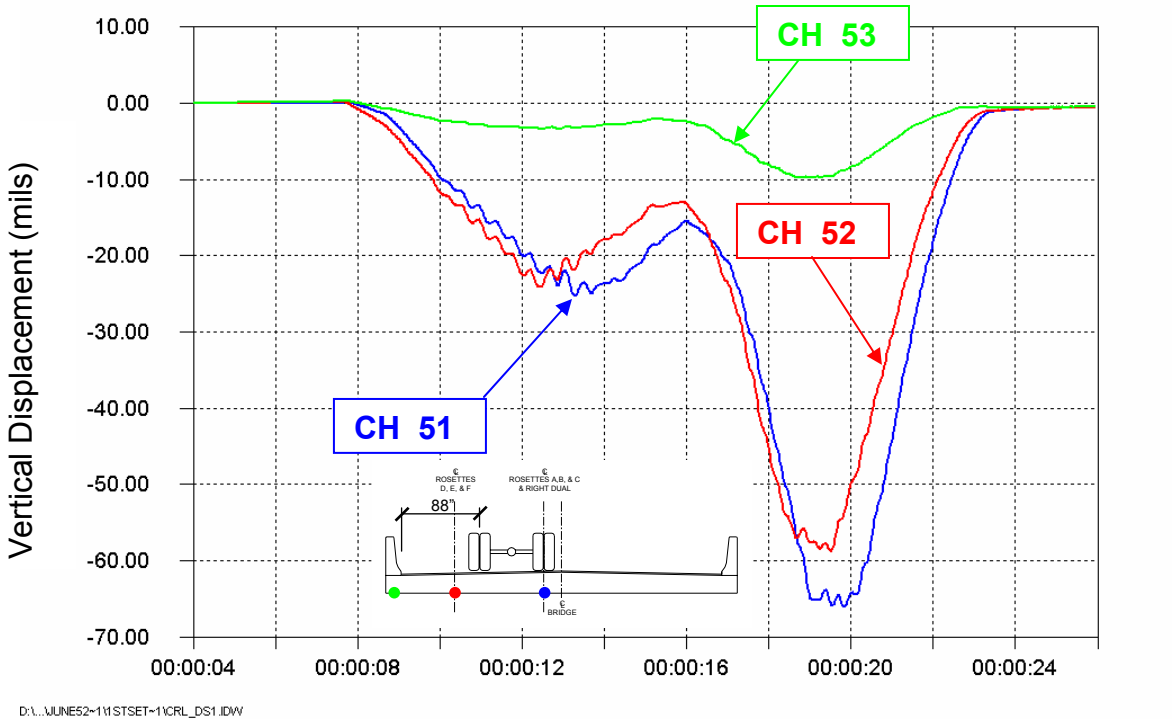

Figure 4.4 – Vertical displacement time-history for load test CRL_DS1
(Test truck located with centerline of right dual over rosettes A, B, C)

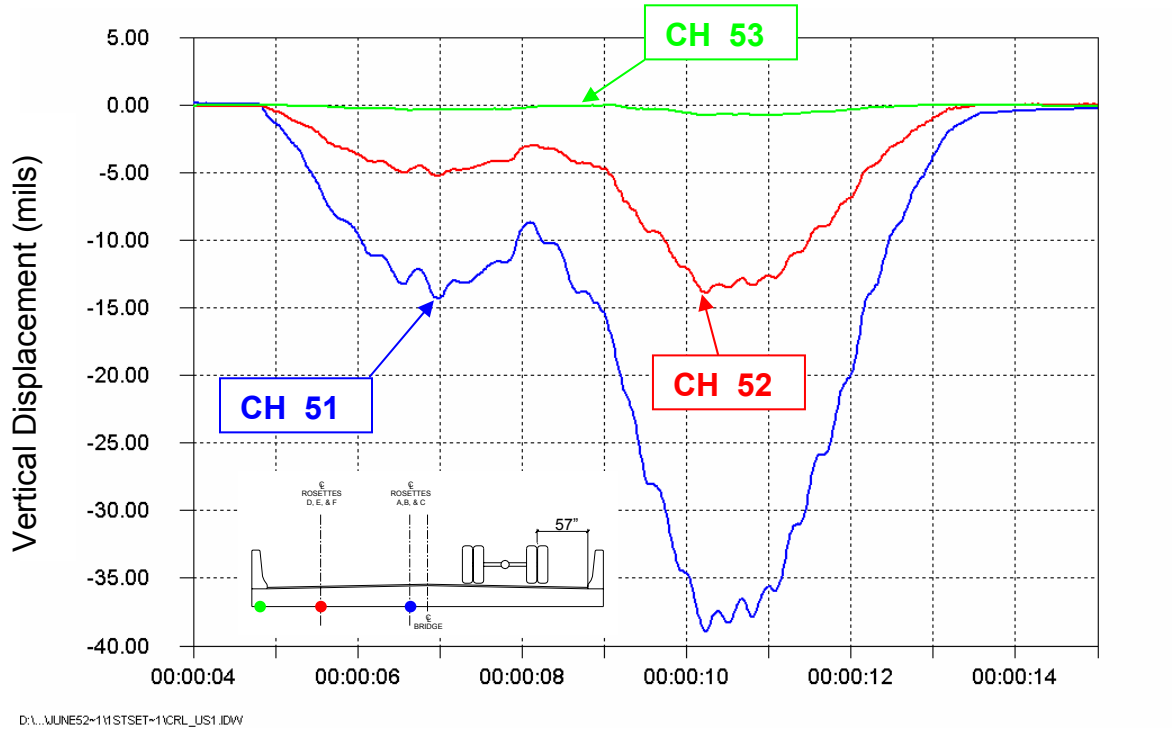

Figure 4.5 – Vertical displacement time-history for load test CRL_US1
(Test truck located in upstream lane)

4.4 Strains in the FRP Slab

As a result of the stiffening effect of the parapet, the FRP slab clearly behaves as a two-way element, bending in both the longitudinal and transverse directions. Evidence of this behavior is seen in the displacement data discussed in Section 4.3. This section will examine a portion of the FRP slab strain gage data. A summary of the peak strains at selected gages for the four different types of crawl tests is contained in Table 4.2. It is evident that the strains induced in the FRP slab and parapet by the test truck are low.

Figure 4.6 contains a partial gage plan of the FRP slab, indicating location and channels of strain data that will be discussed below. Figure 4.7 contains a strain gage plan of the parapet at midspan.

Data Channel	Location	Direction	Peak Strain (με)			
			CRL_PPT1	CRL_DS4	CRL_DS1	CRL_US1
CH_22	Top of FRP Slab	Longitudinal	-54.8	-80.5	-122.5	-63.8
CH_24		Transverse	-4.8	-28.8	-74.9	5.4
CH_31		Longitudinal	-62.1	-97.5	-60.2	-14.6
CH_33		Transverse	-49.5	-93.2	-42.2	9.3
CH_38	Bottom of FRP Slab	Longitudinal	54.9	84.8	118.5	69.6
CH_39		Transverse	5.4	26.9	78.2	-8.5
CH_42		Longitudinal	100.4	126.4	88.1	18.2
CH_43		Transverse	79.0	119.7	61.9	-11.1
CH_45	Parapet	Top - Long	-46.0	-30.7	-18.2	-1.9
CH_50		Bot - Trans	69.1	49.7	35.4	5.2

Table 4.2 – Summary of peak strains measured during **PHASE 1** static crawl tests

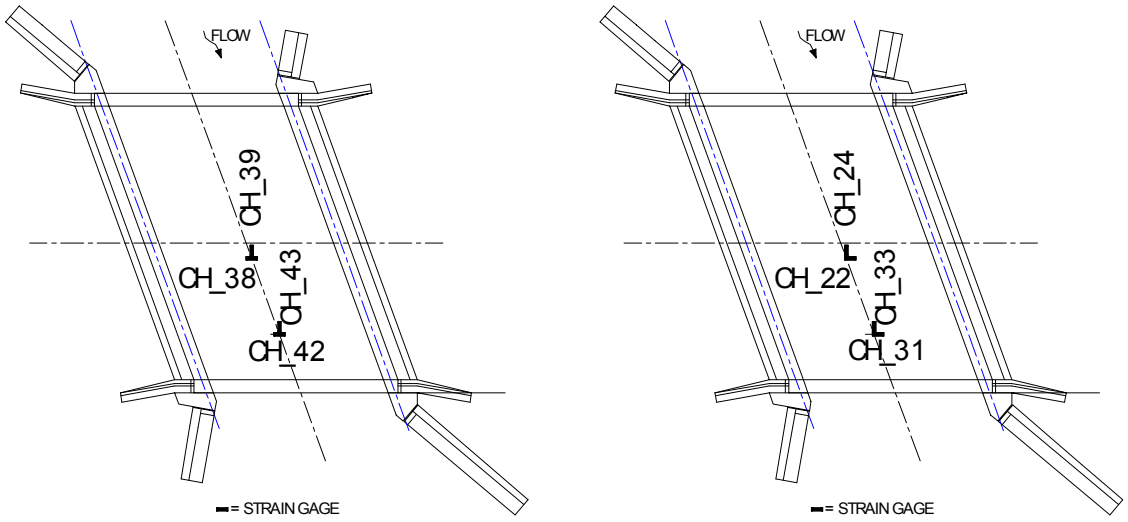

(a) bottom surface of slab (b) top surface of slab

Figure 4.6 – Partial strain gage plan of FRP slab

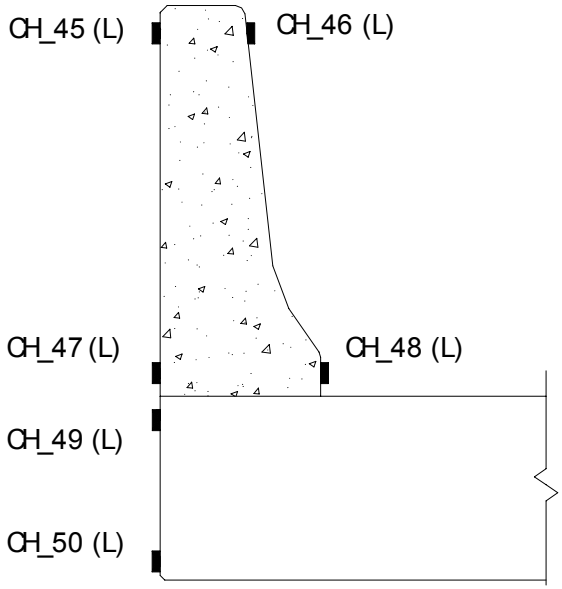

Figure 4.7 – Strain gage plan of parapet (section is at midspan; L denotes longitudinal)

4.4.1 Longitudinal Bending

A plot of longitudinal strain versus time for controlled load test CRL_DS1 is contained in Figure 4.8 and in Figure 4.6. The centerline of the right dual was centered over gage CH_22, as indicated in the figure inset and in Figure 4.6. This is evident in the strain history for CH_22. The passing of the single front and dual rear axles can clearly be seen in the plot. These spikes are evidence of local bending of the FRP slab top plate due to the concentrated wheel load.

Furthermore, as with the displacement data, it can be seen that the peak strain in gages CH_31 and CH_42 occurs prior to the peaks in gages CH_22 and CH_38. This is also the result of the skewed geometry of the bridge

Note that gage pair CH_38 and CH_22 are located on the bottom and top of the slab, respectively, directly opposite each other. As such, comparing the data from these sensors provides an indication of the amount of bending and axial load in the slab structure. The same is true for the pair of CH_42 and CH_31. Examining the data from these two pairs of gages separately, it can be seen that they are symmetric. That is, the magnitudes of the strains in one pair are roughly equal and opposite, indicating nearly pure bending in the slab. The only exception to this is the spikes in the data of channel CH_22, which are the result of local bending, as described above.

Furthermore, the slab experiences positive longitudinal bending with the passing of the test truck. That is, the top of the slab (CH_22 and CH_31) is put into compression, while the bottom of the slab (CH_38 and CH_42) is put into tension.

Peak strains in the FRP material due the test truck loading at CH_38 and CH_22 were around 100 microstrain. This corresponds to a very low stress, less than 0.5 ksi. The strains and stresses at CH_42 and CH_31 are approximately 80% of the values at the bridge centerline.

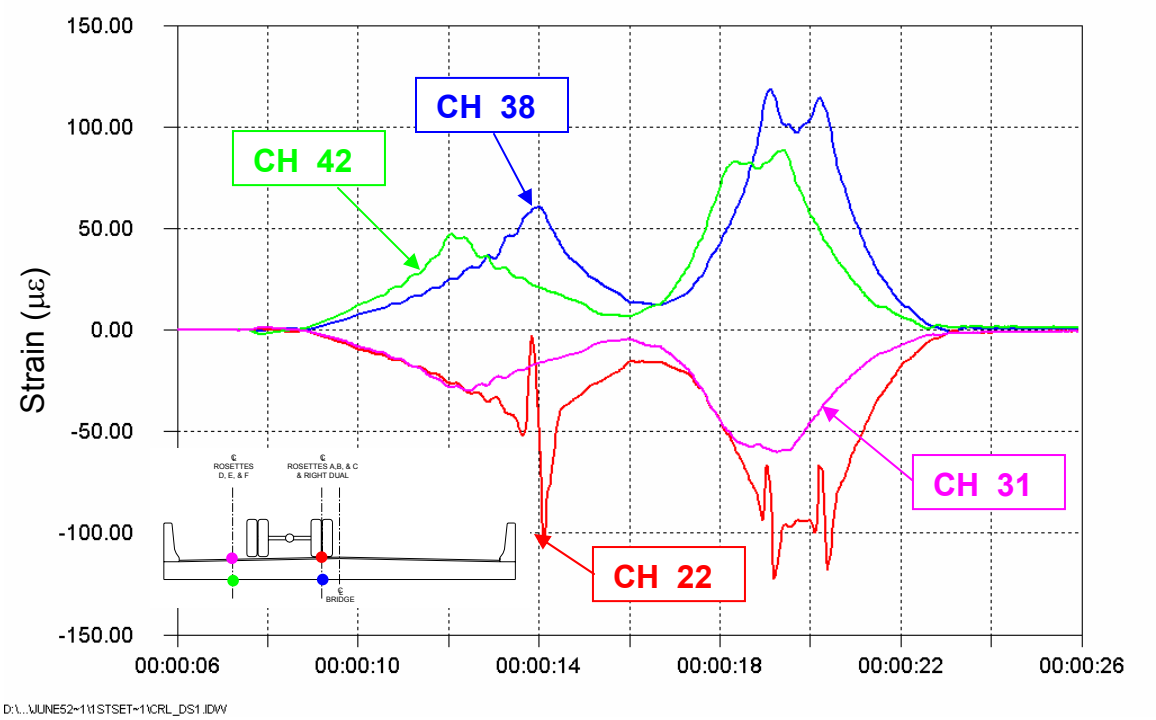

Figure 4.8 – Longitudinal strain history at midspan for load test CRL_DS1 (Centerline right dual over CH_22)

4.4.2 Transverse Bending

A plot of strain versus time for transverse strain gages for load test CRL_DS1 is contained in Figure 4.9. These gages are oriented in the transverse direction along the midspan of the bridge. As above, there are two pairs of gages, located on directly opposite sides of the FRP slab.

As before, the centerline of the right rear dual was located over gage CH_24. The spikes in the data are again the result of local bending in the FRP slab plate. Also, comparing CH_24 with CH_39 and CH_33 with CH_43, it can be seen that the magnitudes are approximately equal and opposite. Furthermore, peaks at the two gaged locations do not occur simultaneously, again due to the skewed geometry of the bridge. Finally, the slab experiences positive bending with the passing of the test truck since the top of the slab (CH_24 and CH_33) is in compression, while the bottom of the slab is in tension (CH_39 and CH_43).

Although the strain magnitudes are less than those in the longitudinal direction, these plots indicate that there is significant bending of the FRP slab in the transverse direction.

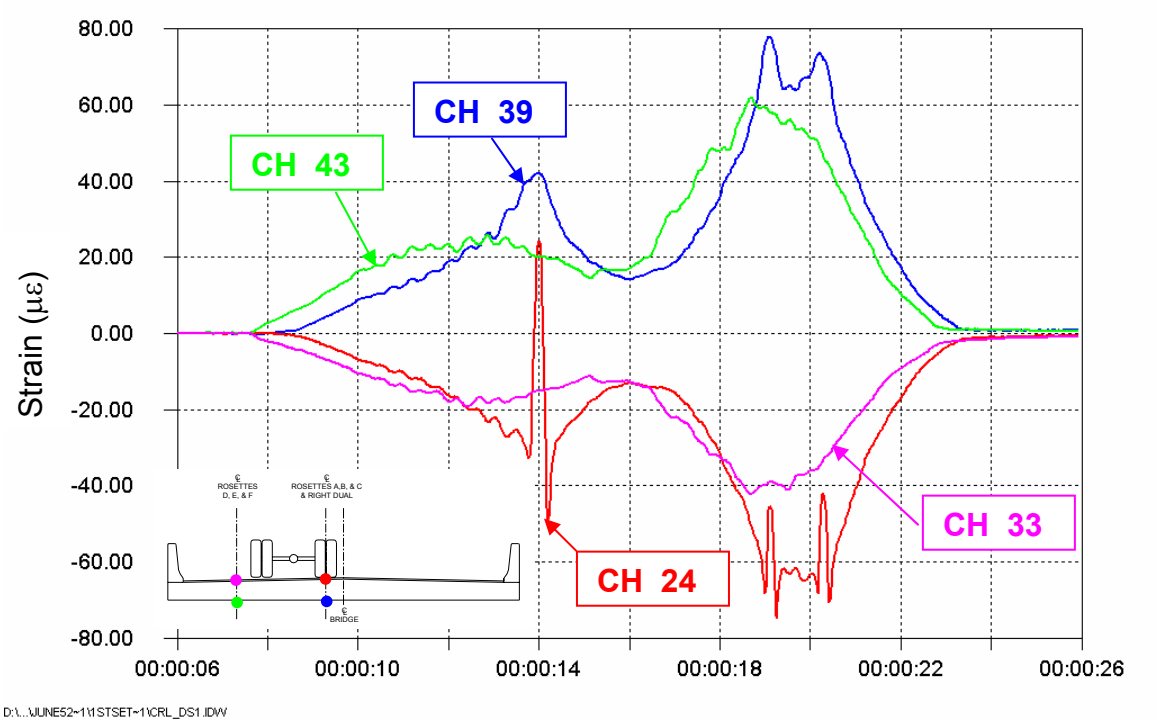

Figure 4.9 – Transverse strain history at midspan for load test CRL_DS1 (Centerline right dual over CH_22)

As discussed in Section 4.1, it appears that the longitudinal joint does not provide full moment continuity between the two FRP panels, yet it does appear to provide shear continuity. This is demonstrated by comparing the transverse strain data near the centerline of the bridge for tests CRL_DS4 and CRL_US1. During these two tests, the test truck was centered in the downstream and upstream lanes, respectively. Referring to Table 4.2, it can be seen that the peak strains at transverse gages CH_24 (top of slab) and CH_39 (bottom of slab) are –28.8 με and +26.9 με, respectively, for test CRL_DS4. However, these values are +5.4 με and –8.5 με, respectively, for test CRL_US1. Since the gages are located near the centerline, and the truck positions for the two tests are symmetric with respect to the bridge centerline, the strain values are expected to be similar. It is believed that this discrepancy is caused by a lack of bending continuity across the joint.

The presence of shear continuity can also be demonstrated by the strain data in Table 4.2 from the same two tests (CRL_DS4 and CRL_US1). The peak strains for longitudinal gages CH_22 (top of slab) and CH_38 (bottom of slab) are –80.5 με and 84.8 με, respectively, for test CRL_DS4. These peak strains are –63.8 με and 69.6 με, respectively, for test CRL_US1. These strains are comparable in magnitude (unlike the transverse gages), and suggest that shear forces are transferred across the joint which cause longitudinal bending strains in the FRP slab. The difference in values (approximately 20%) may be due to the fact that the truck may not have been exactly symmetrically placed, and the gages are offset slightly from the centerline.

This behavior could be better defined with additional instrumentation placed on the upstream FRP panel.

4.5 Stresses in the FRP Slab

As indicated in the instrumentation plan (see Appendix A), 45 degree strain rosettes were embedded within the top plate of the FRP slab at six locations to measure global stresses in the FRP slab. Additional rosettes were placed in the webs and top plate of one particular bottle to measure local response of the FRP material to concentrated load, and will be discussed subsequently.

The six rosettes used to measure the global response of the bridge are labeled A through F. All three arms of the rosette were operating correctly only at rosettes C, D, and E. These rosettes are indicated in Figure 4.10.

Using established equations from mechanics or experimental stress analysis and assuming a state of plane stress, the stresses can be determined from the measured strains in the three arms of the rosette. The required material properties for the composite material were obtained from the Hardcore Composites report, *"Analysis of Dubois Creek Bridge, Susquehanna County Analysis Report, Rev. B,"* dated July 10, 2001.

Table 4.3 contains the results of the rosette data reduction. Figure 4.10 indicates the locations of the rosette as well as the coordinate system used for reporting stress directions.

Rosette Name		CRL_PPT1			CRL_DS4			CRL_DS1			CRL_US1		
		σ_x (ksi)	σ_y (ksi)	τ_{xy} (ksi)	σ_x (ksi)	σ_y (ksi)	τ_{xy} (ksi)	σ_x (ksi)	σ_y (ksi)	τ_{xy} (ksi)	σ_x (ksi)	σ_y (ksi)	τ_{xy} (ksi)
C	Max	0.00	0.04	0.02	0.01	0.01	0.02	**0.25**	0.00	0.17	0.00	0.04	0.01
	Min	-0.17	-0.02	-0.03	-0.26	-0.06	-0.05	-0.14	-0.09	-0.03	-0.11	-0.03	-0.08
D	Max	0.01	0.00	0.00	0.00	0.16	0.02	0.00	0.00	0.02	0.00	0.06	0.02
	Min	-0.30	-0.16	-0.02	**-0.52**	-0.29	-0.11	-0.15	-0.07	-0.01	-0.06	0.00	0.00
E	Max	0.00	0.00	0.00	0.00	0.00	0.00	0.00	0.00	0.01	0.00	0.02	0.00
	Min	-0.30	-0.20	-0.03	-0.47	-0.35	-0.22	-0.14	-0.08	-0.02	-0.05	0.00	-0.02

Table 4.3 – Summary of peak rosette stresses measured during static crawl tests
(Peak stresses are indicated in bold)
PHASE 1 DATA

The stresses caused in the FRP slab by the passing of the test truck are very low as indicated in the table. This confirms the strain data presented in Section 4.4. Peak stresses are 0.5 ksi in compression and 0.3 ksi in tension.

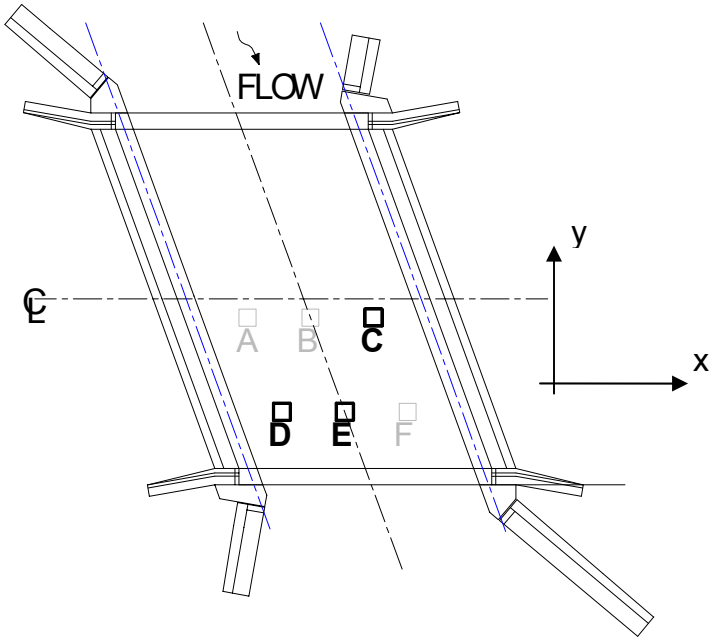

Figure 4.10 – Locations of rosettes on top of FRP slab and coordinate system

4.6 Neutral Axis Shifting in the FRP Slab

As a result of the stiffening effect of the parapet, skewed geometry (*i.e., the aspect ratio*), and 2-D plate behavior, the slab cannot be idealized as a simply supported beam. Furthermore, if the entire bridge cross-section is analyzed, the assumption that plane sections will remain plane may not be valid. By examining the strains throughout the cross-section, the variation of the location of the neutral axis can be examined.

Since the parapet is connected to the FRP slab with steel reinforcement, it is reasonable to assume that the parapet is fully composite with the FRP slab. This case is illustrated in Figure 4.11(a). The other extreme is the case in which there is no composite action. This case is illustrated in Figure 4.11 (b). The actual behavior appears to be bounded by these extremes.

Figure 4.12 shows the experimentally obtained strains in the parapet and supporting FRP slab at a section at one instant in time, for test CRL_DS1. The behavior of the parapet is similar for the other tests. Shown on this plot are the longitudinal strain measurements and a best-fit straight-line strain distribution using a least-squares approach. This provides an estimate of the location of the neutral axis. Note that on the diagram, the outside face of the parapet represents the zero strain line. Values to the left are in compression, while values to the right are in tension. The neutral axis occurs where the linear regression line crosses the zero strain line, any part of the parapet above this point is in compression and any point below is in tension.

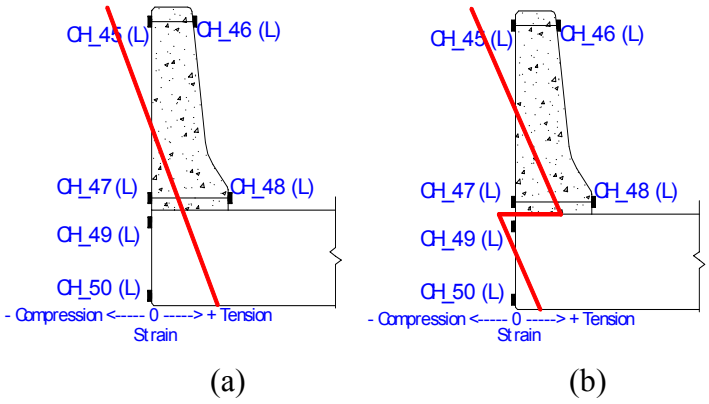

Figure 4.11 – Idealized strain distribution through the parapet assuming (a) fully-composite behavior; (b) non-composite behavior

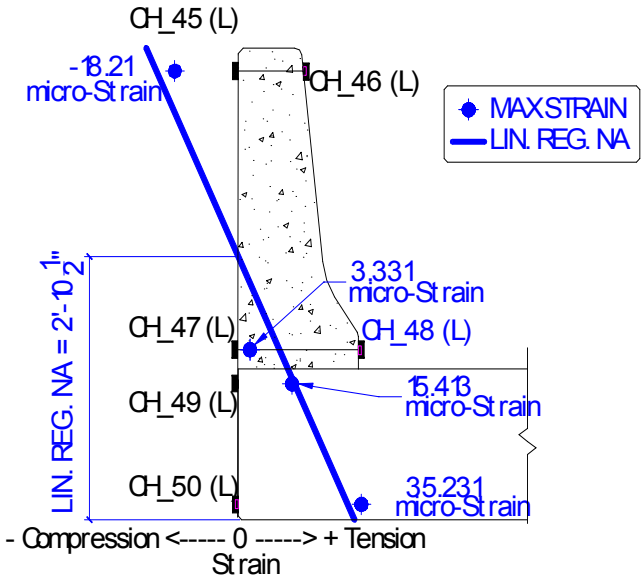

Figure 4.12 – Best fit straight line of measured strain values in parapet and FRP slab
Note: (L) denotes longitudinal gage

It is apparent from Figure 4.12 that the neutral axis occurs within the parapet. However, the strain gages further from the parapet on the FRP slab indicate that the neutral axis is located within the FRP slab itself. This indicates that the neutral axis location varies with transverse position in the bridge cross-section. Figure 4.13 shows an estimate of the location of the neutral axis throughout the slab. Known points at the parapet and at two locations within the slab are determined using measured data. The dashed line has been drawn to illustrate the variation of the neutral axis location. This indicates that the common assumption of plane sections remaining plane is not valid in this case.

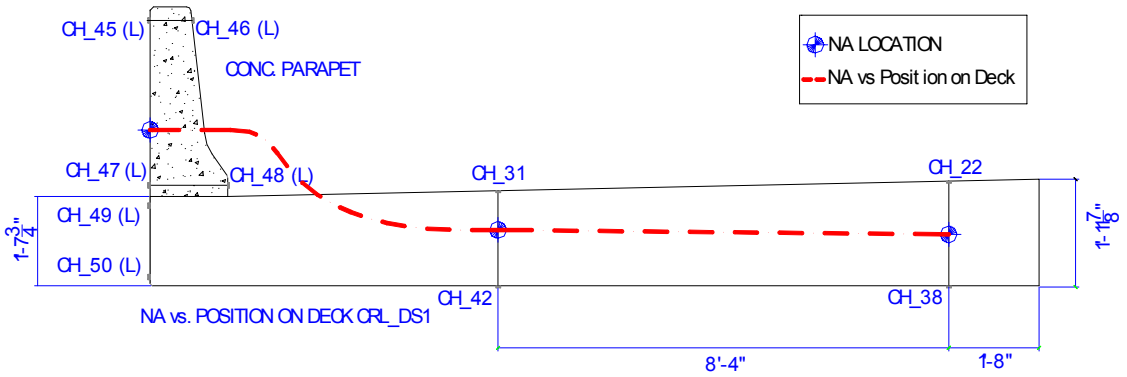

Figure 4.13 – Estimated variation of neutral axis location with transverse position using measured strain data

4.7 Dynamic Tests

Dynamic load tests were performed to determine the response of the bridge to dynamic loading. The test truck was driven across the bridge at approximately 25 miles per hour, in both the downstream and upstream traffic lanes. The truck was always driven from north to south. Each test was repeated twice. Table 3.3 contains a summary of the dynamic tests. Dynamic test DYN_LT2 was selected for data reduction and analysis. The test truck was in the downstream (instrumented) lane during this test.

A comparison will be made between data collected during a static crawl test and a dynamic test. The test truck position for crawl test CRL_DS1 is roughly the same as that for the dynamic test DYN_LT2 and will be used for comparison.

Figure 4.14 contains a strain time-history plots of CH_38 and CH_39 for the crawl test CRL_DS1. These gages are located on the underside of the FRP slab and the center of bridge, as indicated on Figure 4.6. An identical plot for the test DYN_LT2 is shown in Figure 4.15. Since these gages are located on the underside of the slab, the local effects of the passing of the test truck are minimal. The predominant response shown in each of these figures therefore is global response.

A comparison of the two figures reveals that the peak strains are similar for static and dynamic loading rates. Therefore, it can be stated that there is negligible dynamic amplification of the FRP slab strains at the bottom plate of the slab. Furthermore, it can be suggested that the dynamic amplification is negligible for global strain response. This statement will only be true as long as the wearing surface and approach roadways remain in good condition.

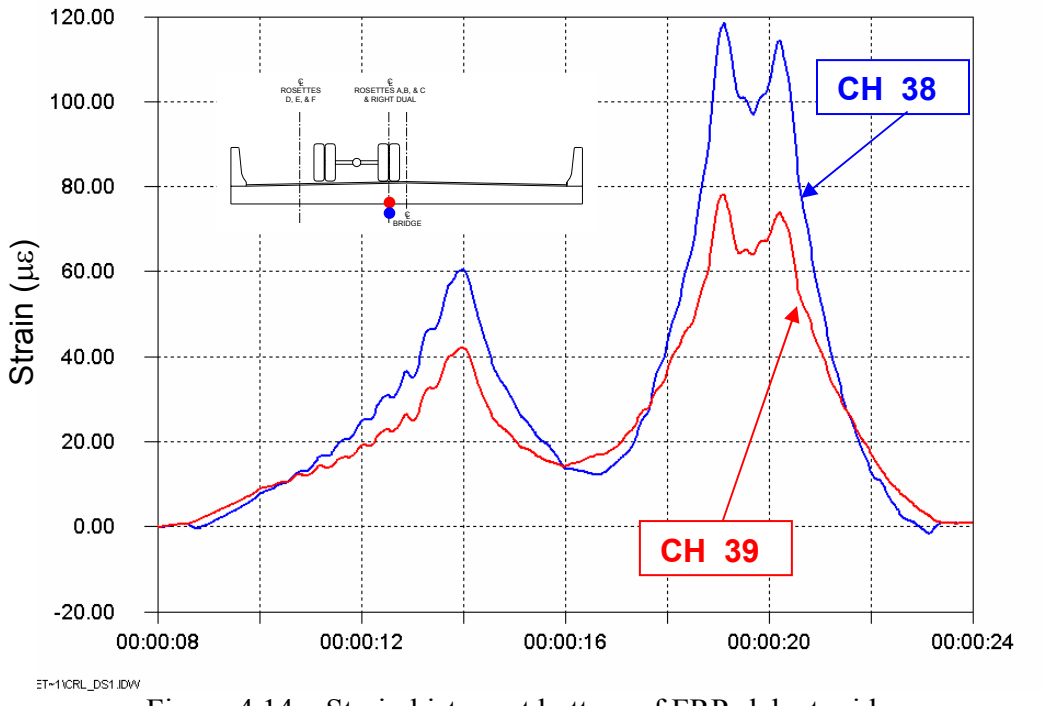

Figure 4.14 – Strain history at bottom of FRP slab at midspan
for static load test CRL_DS1
(CH_38 is longitudinal, CH_39 is transverse)

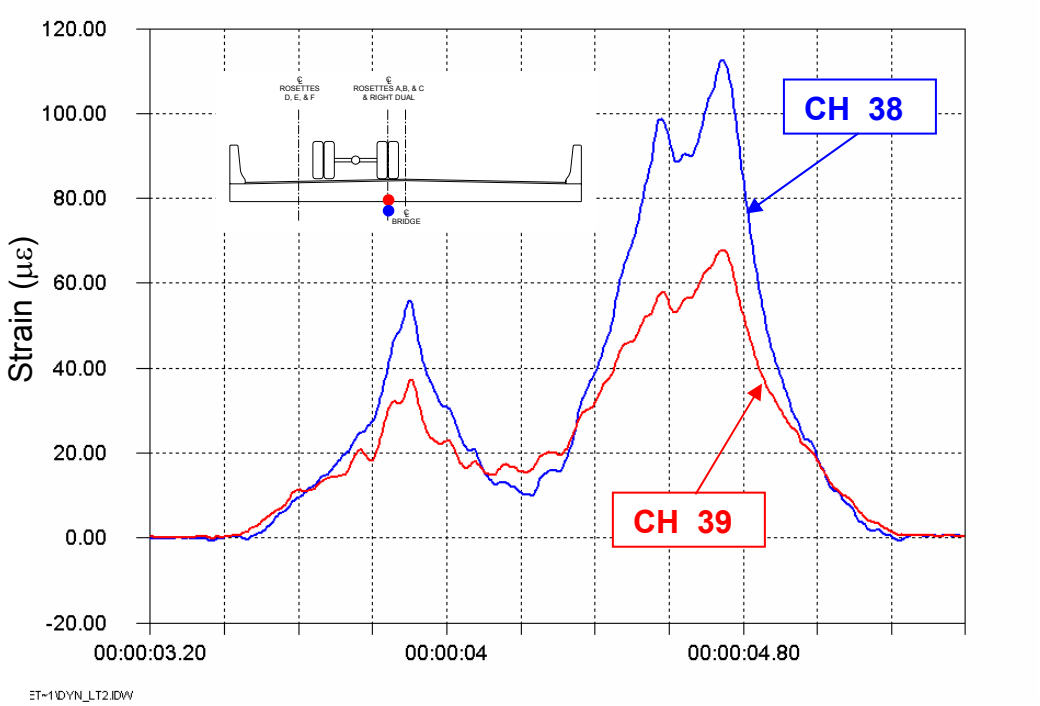

Figure 4.15 – Strain history at bottom of FRP slab at midspan
for dynamic load test DYN_LT2
(CH_38 is longitudinal, CH_39 is transverse)

A similar comparison can be made for the corresponding strain gages on the top surface of the FRP slab. Figures 4.16 and 4.17 contain strain time-history plots at the top of the slab for the static and dynamic tests, respectively.

It can be seen from these plots that unlike the gages on the bottom of the slab, these strain gages are subjected to local bending due to the concentrated load of the individual truck wheels, as indicated by the spikes in the curve.

The peak values of strain are higher for the dynamic test data. However, the baseline strain values (ignoring the peaks) for the two tests are similar. The peaks in the stress time-histories are the result of local bending of the FRP web and flange plates. The baseline strain variation is due to the global bending of the FRP slab. It appears that dynamic loading only affects the strains caused by local deformation of the FRP slab.

The peak strain at CH_22 during the static test is approximately 120 microstrain (Figure 4.16). The corresponding peak strain from the dynamic test is approximately 150 microstrain (Figure 4.17). This is a dynamic amplification of approximately 25%. It must be noted that part of the difference may be attributed to variations in the transverse position of the wheel.

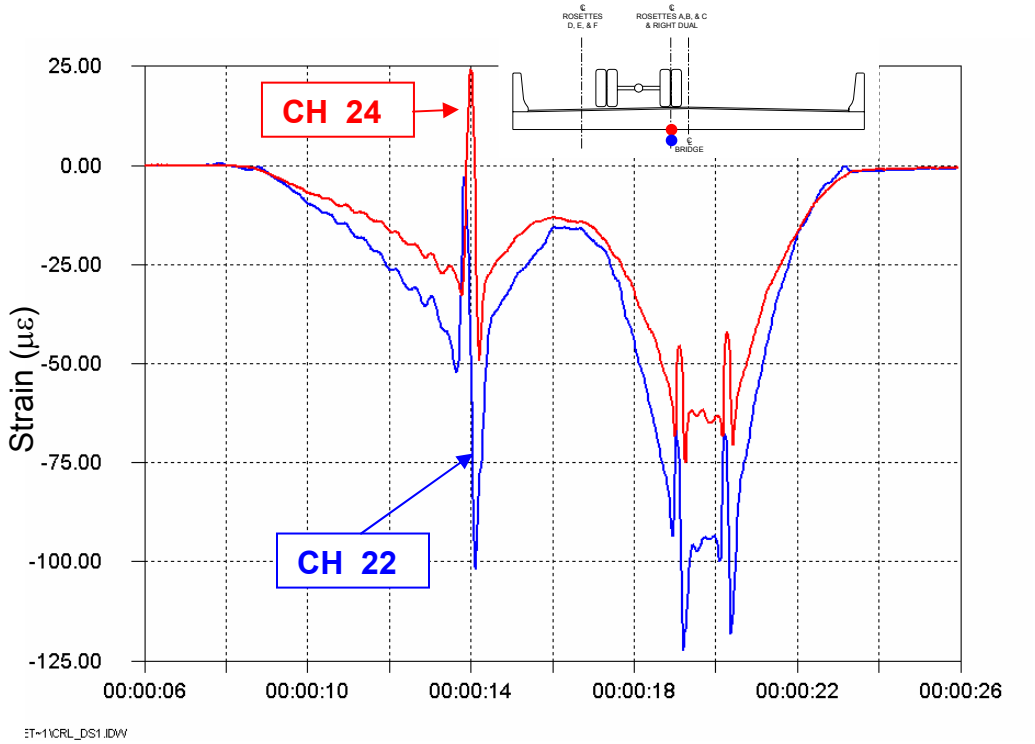

Figure 4.16 – Strain history at top of FRP slab at midspan
for static load test CRL_DS1
(CH_22 is longitudinal, CH_24 is transverse)

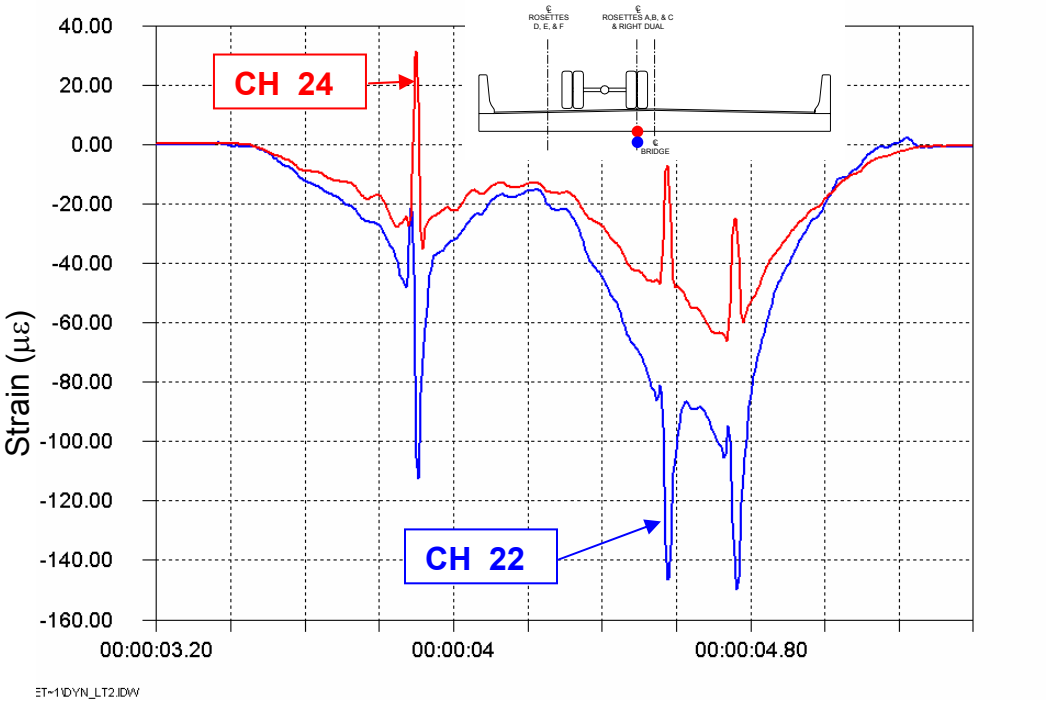

Figure 4.17 – Strain history at top of FRP slab at midspan
for dynamic load test DYN_LT2
(CH_22 is longitudinal, CH_24 is transverse)

4.8 Local Behavior of the FRP Slab

As described in the previous sections, the FRP slab experiences considerable two-way bending due to the rigidity of the concrete parapets, which behave as structural components of the bridge. The stresses and strains experienced by the FRP slab as a result of this two-way bending are low. These stresses discussed thus far are global stresses, resulting from deformation of the FRP slab acting as a unit. However, when subjected to a point load, such as that resulting from a truck tire, there is local bending of the FRP top plate and webs.

4.8.1 Bottle Instrumentation

The FRP slab is manufactured around a series of non-structural foam bottles. In order to investigate the local behavior of the FRP slab, 45 degree rosettes were placed on two webs and the top plate around one foam bottle. This is a total of three locations. There were two rosettes at each of these locations. This permits the determination of the strain distribution through the thickness of the FRP plates at each location. Examination of these data provides a means to investigate the presence of bending in these plates.

Figure 4.18 contains a plan view drawing of the FRP slab. Indicated on this plan is the location of the instrumented bottle. Figure 4.19 is a detailed plan of the instrumented bottle. The various rosettes and coordinate system for each rosette are shown in the figure.

4.8.2 Test Description

Three test types were performed to investigate local behavior of the FRP slab. For each test, the truck was driven across the bridge at very low speed. The centerline of the left dual was centered over the instrumented bottle, then centered 12 inches downstream and upstream of the instrumented bottle. Each test was repeated three times for a total of nine tests. These tests are summarized in Table 3.4. The data acquisition system was connected to gages included in test setup #2.

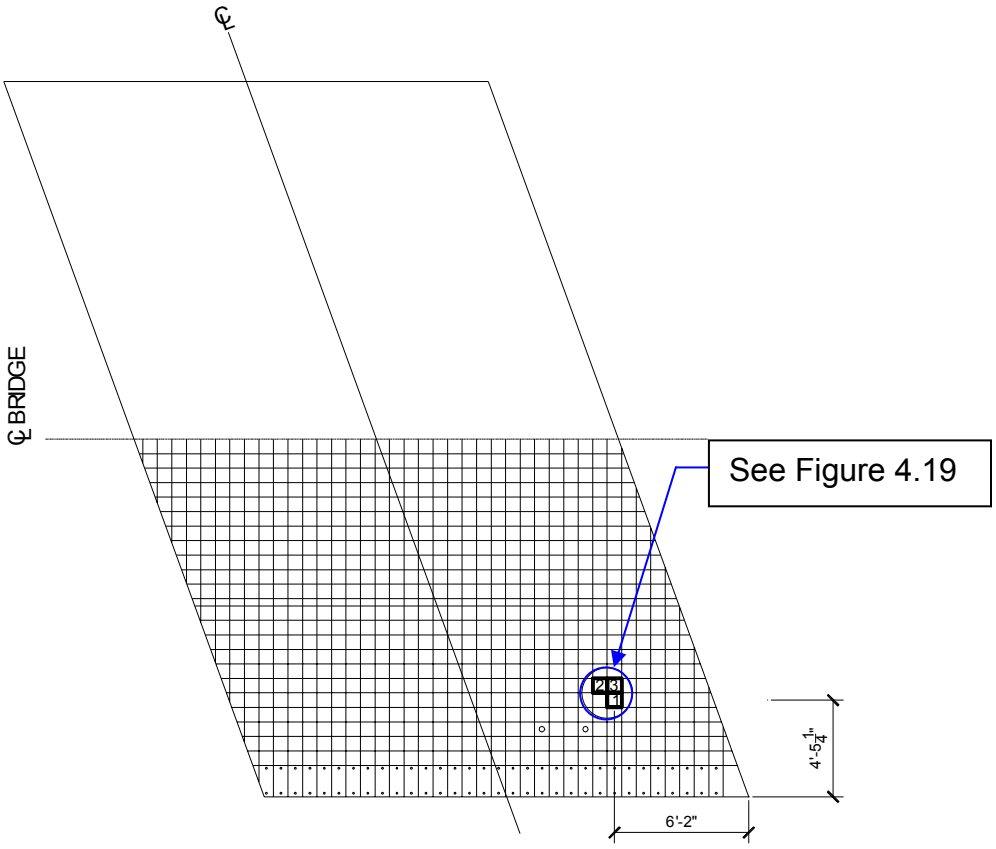

Figure 4.18 – Location plan of instrumented bottle

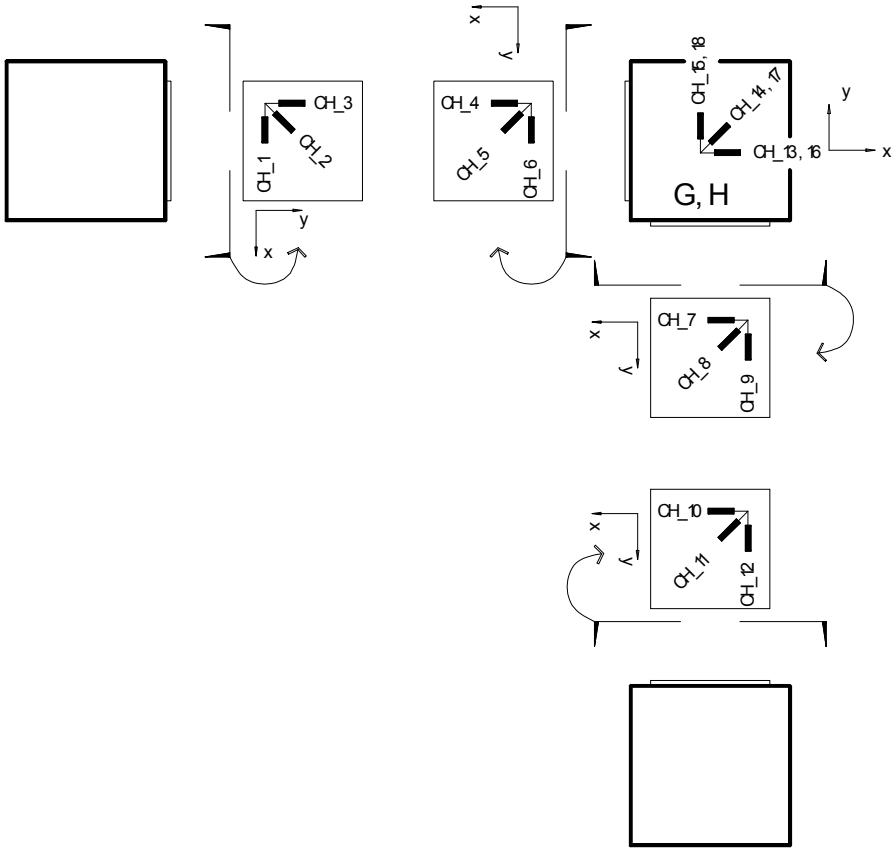

Figure 4.19 – Rosette configuration on instrumented bottle
(Coordinate system of each rosette is indicated)

4.8.3 Peak Stresses

The stresses in the bottles can be determined given the strain data from these rosettes and the material properties of the FRP slab. The peak stresses in these six rosettes for the three static crawl tests performed are contained in Table 4.4. The peak tensile and compressive stresses are shown in boldface type. The peak tensile stress is 4.6 ksi, while the peak compressive stress is –5.3 ksi.

Rosette		*Test CRL_CLB2*			*Test CRL_DSB1*			*Test CRL_USB3*		
		σ_x (ksi)	σ_y (ksi)	τ_{xy} (ksi)	σ_x (ksi)	σ_y (ksi)	τ_{xy} (ksi)	σ_x (ksi)	σ_y (ksi)	τ_{xy} (ksi)
Rosette 123	*Max*	0.5	0.2	0.0	0.5	0.1	0.1	0.0	0.4	0.0
	Min	0.0	**-5.3**	-0.3	-0.1	-4.8	-0.3	-0.1	0.0	-0.2
Rosette 456	*Max*	0.1	0.2	0.1	0.1	0.2	0.1	0.0	0.0	0.0
	Min	-1.4	-0.2	-0.1	-1.3	-0.2	0.0	0.0	-0.2	-0.2
Rosette 789	*Max*	0.0	0.2	0.4	0.1	0.2	0.4	0.0	0.1	0.1
	Min	-0.3	-3.1	-0.3	-0.2	-2.1	-0.3	-0.1	0.0	-0.1
Rosette 101112	*Max*	0.4	0.3	0.3	0.3	0.3	0.3	0.1	0.1	0.0
	Min	-0.1	-3.1	-0.5	-0.4	-2.1	-0.4	0.0	0.0	-0.2
Rosette G	*Max*	**4.6**	2.3	0.0	4.0	2.0	0.0	0.0	0.0	0.0
	Min	-0.5	-0.3	-0.6	-0.5	-0.3	-0.6	-0.3	-0.2	-0.1
Rosette H	*Max*	0.1	0.0	0.1	0.0	0.0	0.1	0.0	0.0	0.0
	Min	-0.2	-0.3	-0.2	-0.2	-0.3	-0.2	-0.2	-0.2	-0.1

Table 4.4 – Summary of peak stresses in the bottle rosettes for static load tests
Maximum tensile and compressive stresses are indicated in bold. (Test Setup #2)
PHASE 1 DATA

4.8.4 Local Bending of FRP Plates

Figure 4.20 contains a simplified gage plan for the bottle rosettes which will be used in the following discussion. The FRP slab is composed of webs in both directions connected to a top and bottom plate by the resin. Analysis of such a structure is complicated, as is the interpretation of limited strain data. Nevertheless, certain general observations can be made.

The FRP slab structure is three dimensional, however for the purposes of this discussion, the slab will be considered as a two dimensional structure, in the longitudinal and transverse directions, separately.

Figure 4.21 contains a strain history plot for the longitudinal "frame" consisting of the web and top plate gages (see the figure inset). This event represents the passing of the front wheel of the truck. It can be seen that the magnitude of the strains are an order of magnitude larger than those observed during global response to load. The peak strain occurs at the underside of the top plate, with a magnitude of approximately 1000 microstrain. This occurs at the underside of the top plate (CH_13) as the wheel load passes above. The top plate is in positive bending since this strain is tensile (positive). It is also evident that CH_16 shows a low positive tensile strain. Comparable compressive

strain is not measured since this rosette was installed close to the mid-thickness of the top plate.

The web gages (CH_3 and CH_4) both indicate compressive strains, which is the result of the vertical concentrated force above. The webs act as stiffeners under such loading. Furthermore, it can be seen that there is significant bending strain in comparison to the average strain in the web. The average strain is a measure of the axial component of force in the web plate.

Figure 4.22 contains a similar plot for the transverse "frame." The magnitudes of strain in the transverse direction are approximately half of those in the longitudinal direction. The peak stress occurs at the underside of the top plate, as in the longitudinal direction (Figure 4.21). However, the web gages indicate that there is very little bending, due to the fact that the two web gages (CH_9 and CH_12) have comparable magnitudes.

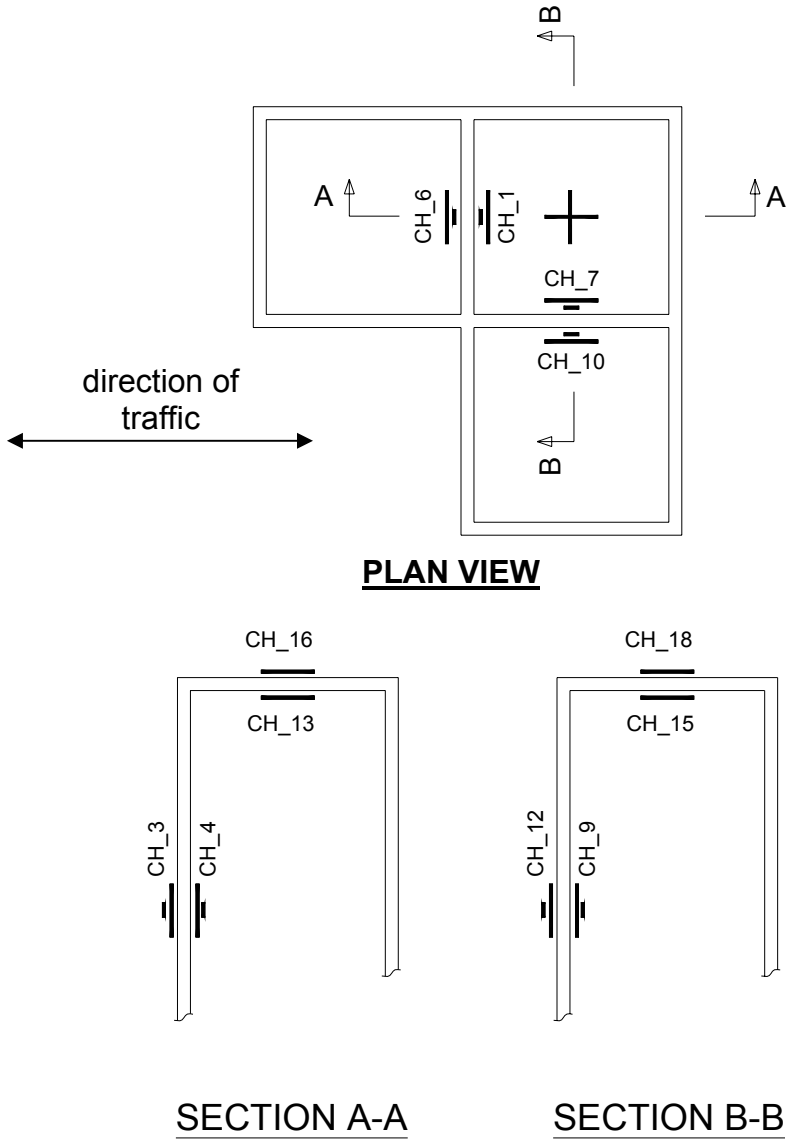

Figure 4.20 – FRP bottle rosette configuration

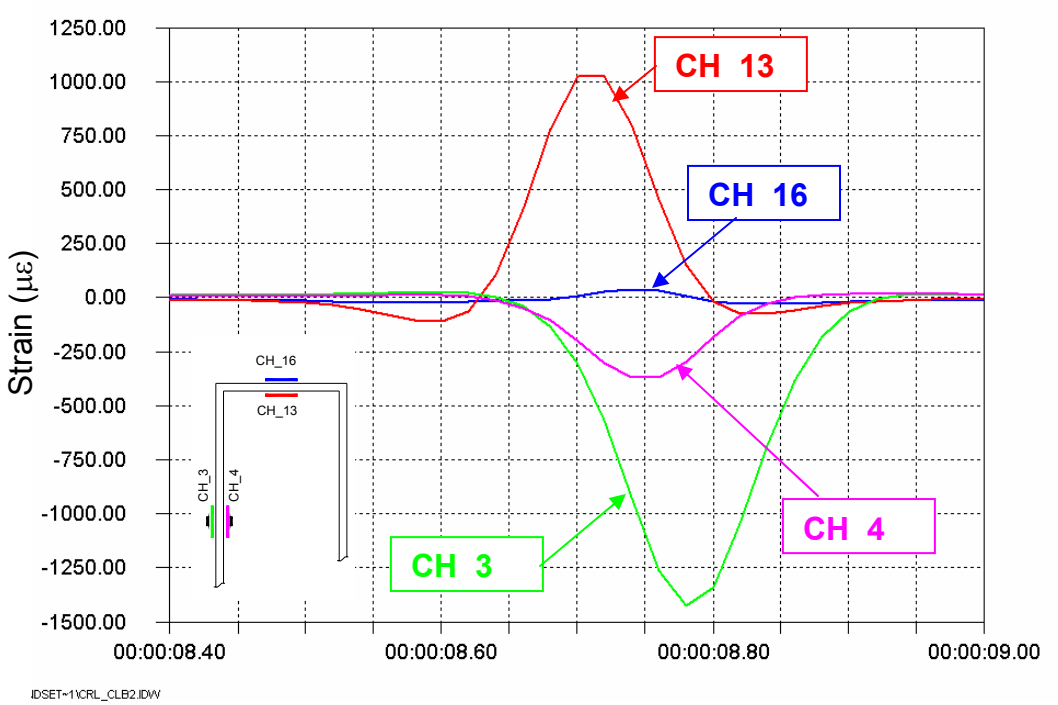

Figure 4.21 – Strain history in top plate of bottle for longitudinal "frame" action (see section A-A of Figure 4.20)

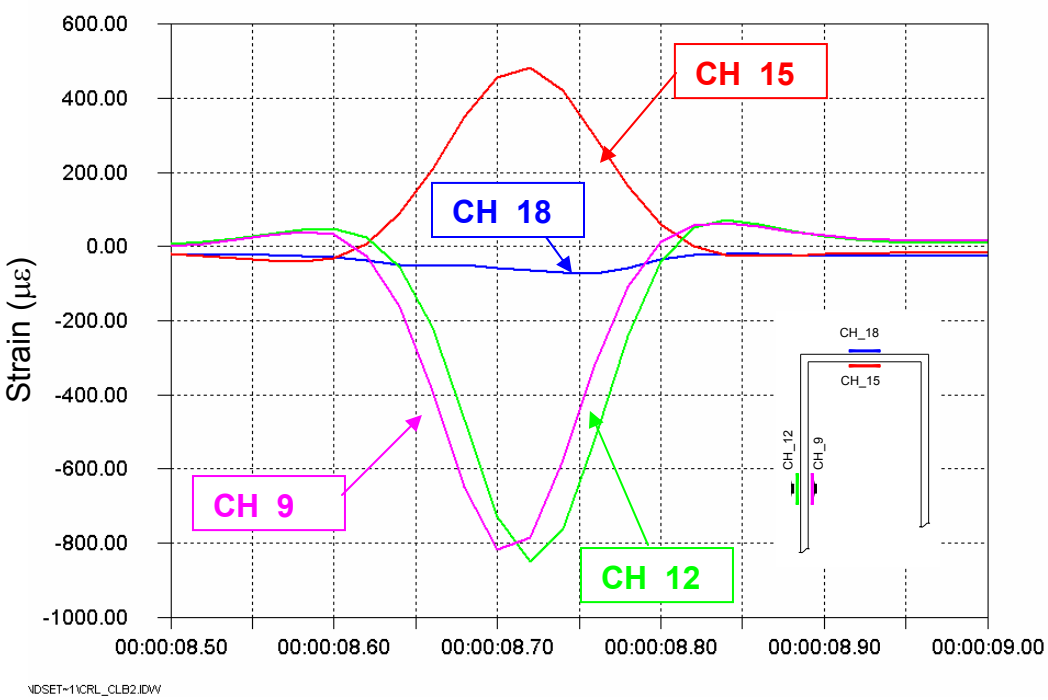

Figure 4.22 – Strain history in top plate of bottle for transverse "frame" action (see section B-B of Figure 4.20)

Finally, Figure 4.23 contains strain history plots for the four horizontal gages mounted to the web plates (see the figure inset). This direction of bending is caused by the restraint at the sides of the web plate. Due the fact that FRP slab is a three dimensional structure (and not two dimensional frames as considered above), a point load at the center of the top plate (between webs) causes bending in both directions in the web plates it is attached to. Furthermore, for the wheel load of the test truck considered, these strains are significant.

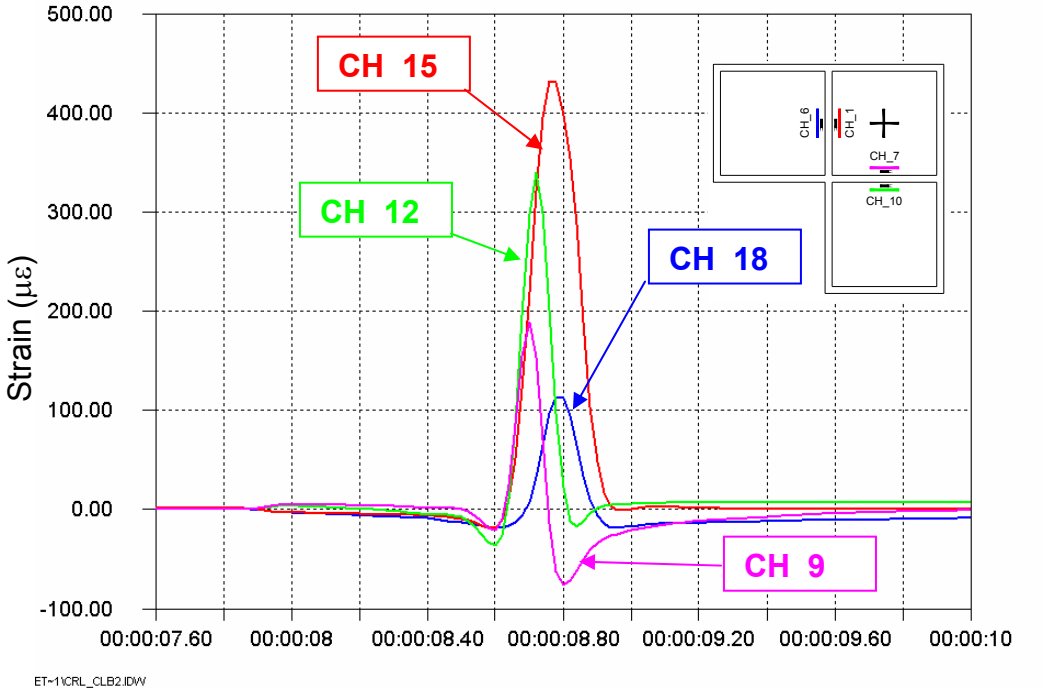

Figure 4.23 – Strain history in webs of bottle for bending
in the plane of the FRP slab
(see plan view of Figure 4.20)

4.9 Out-of-Plane Bending of the Parapet

As discussed above, the concrete parapet behaves as a structural component of the bridge. When the test truck is on the bridge, the parapet is strained due to in-plane bending, as the parapet acts as a deep beam spanning between the abutments. However, due to the eccentricity of the load and the fact that there appears to be rotational continuity between the FRP slab and the parapet, the parapet appears to experience some out-of-plane bending, in addition to the in-plane component. The magnitude of this out-of-plane bending can be estimated by comparing strains on either side of the parapet.

Figures 4.24 through 4.27 contain strain histories of the two strain gages at the top of the parapet on the exterior (CH_45) and interior (CH_46) faces, for the static crawl tests CRL_PPT1, CRL_DS4, CRL_DS1, and CRL_US1, respectively.

Under positive in-plane bending, the top of the parapet is put into compression. However, in each of the four plots, it can be seen that the compressive strain at exterior face of the parapet (CH_45) is larger than the strain at the interior. This would imply that the out-of-plane moment acts in the direction which would cause the top of the parapet to deflect inwards towards the bridge.

In each of the tests, the magnitude of the bending strains is approximately the same and low, equal to approximately 1-2 microstrain. However, as the test truck moves away from the parapet, the in-plane bending strain becomes lower, and therefore the out-of-plane bending strain component becomes a larger percentage of the total strain.

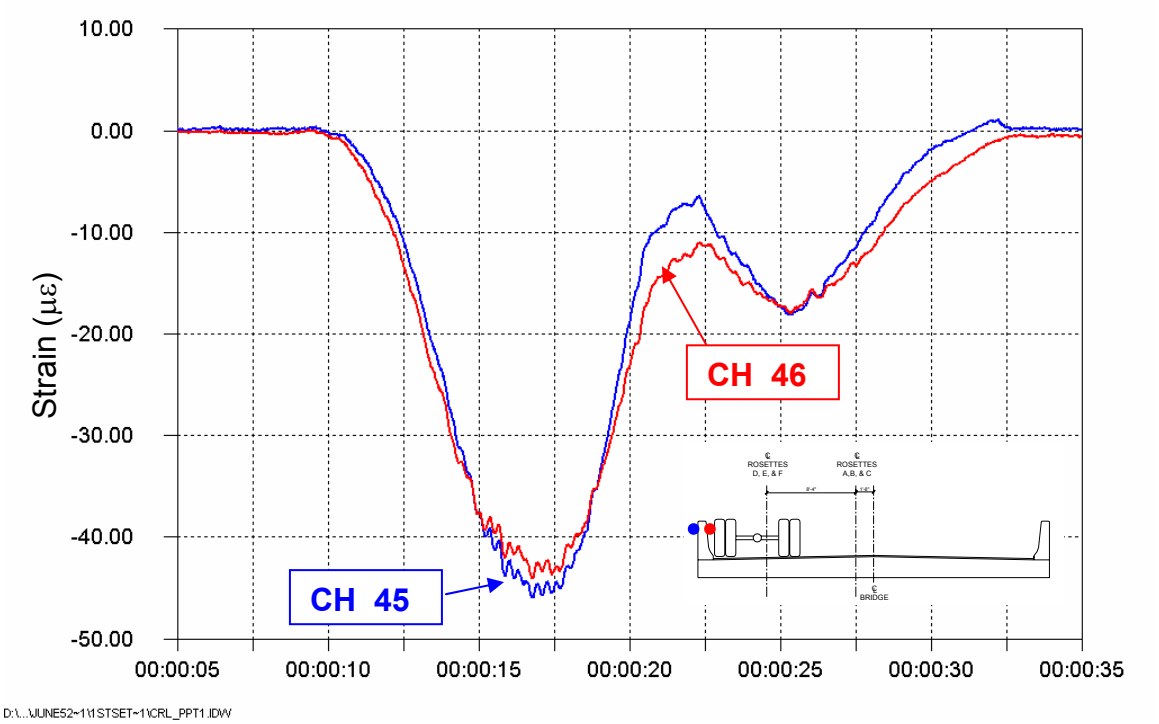

Figure 4.24 – Strain history at top of parapet for test CRL_PPT1
(CH_45 is exterior face; CH_46 is interior face)

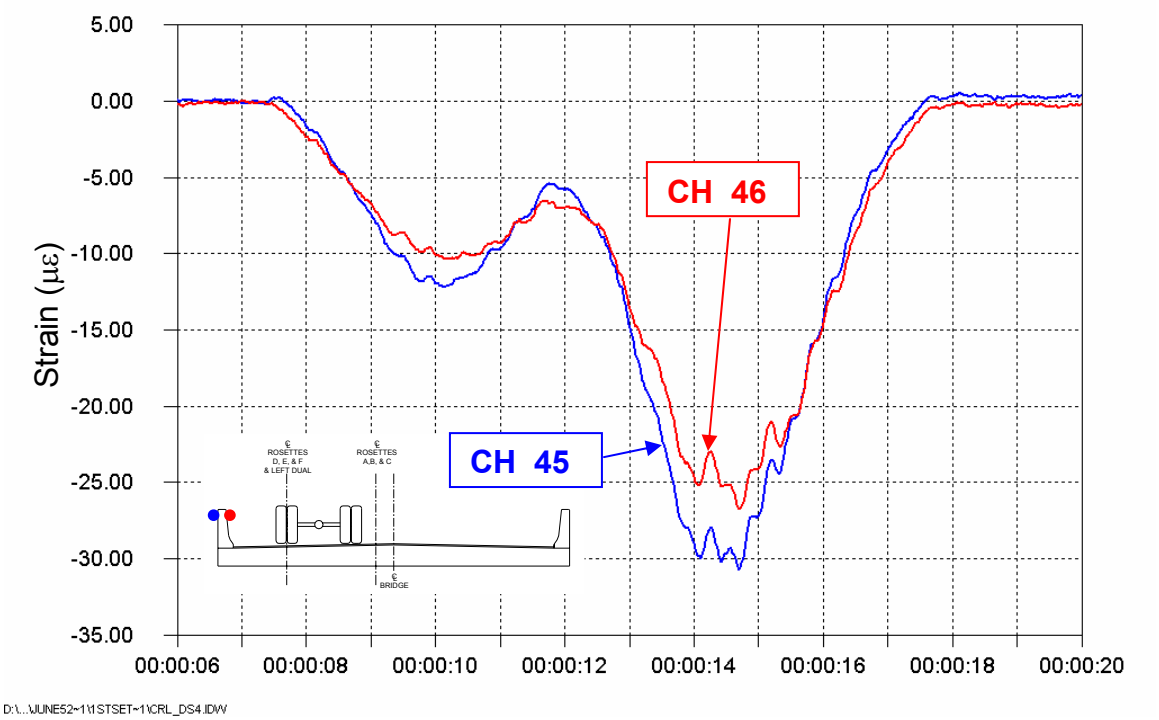

Figure 4.25 – Strain history at top of parapet for test CRL_DS4
(CH_45 is exterior face; CH_46 is interior face)

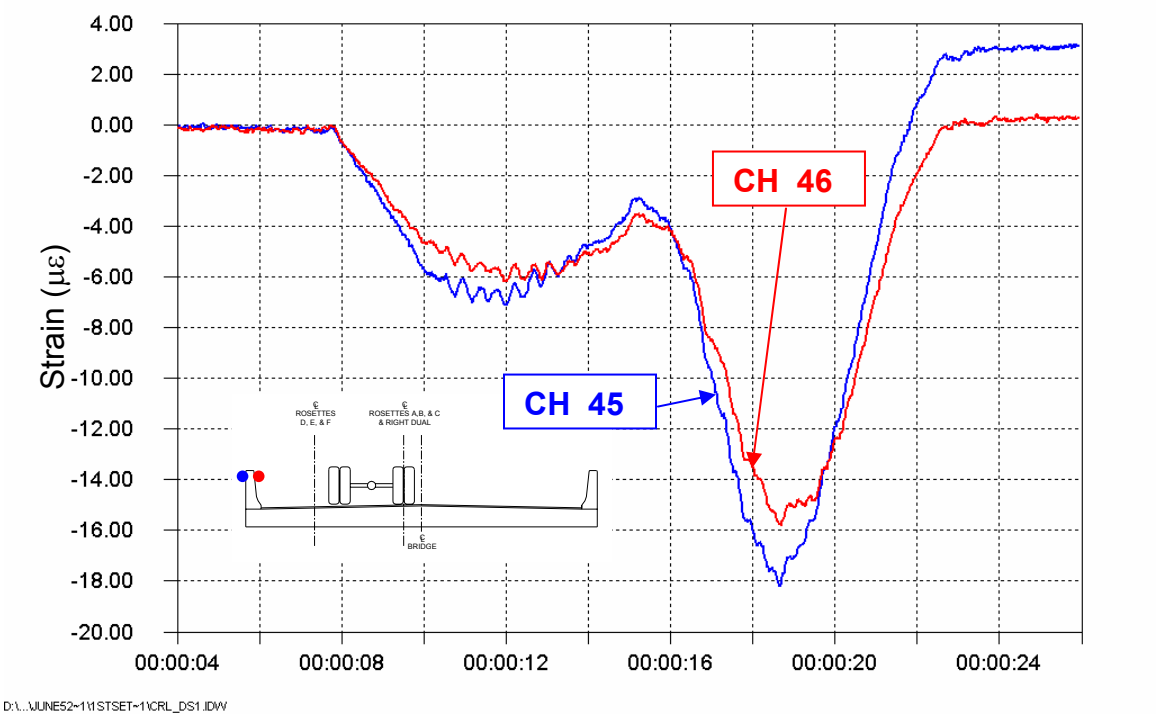

Figure 4.26 – Strain history at top of parapet for test CRL_DS1
(CH_45 is exterior face; CH_46 is interior face)

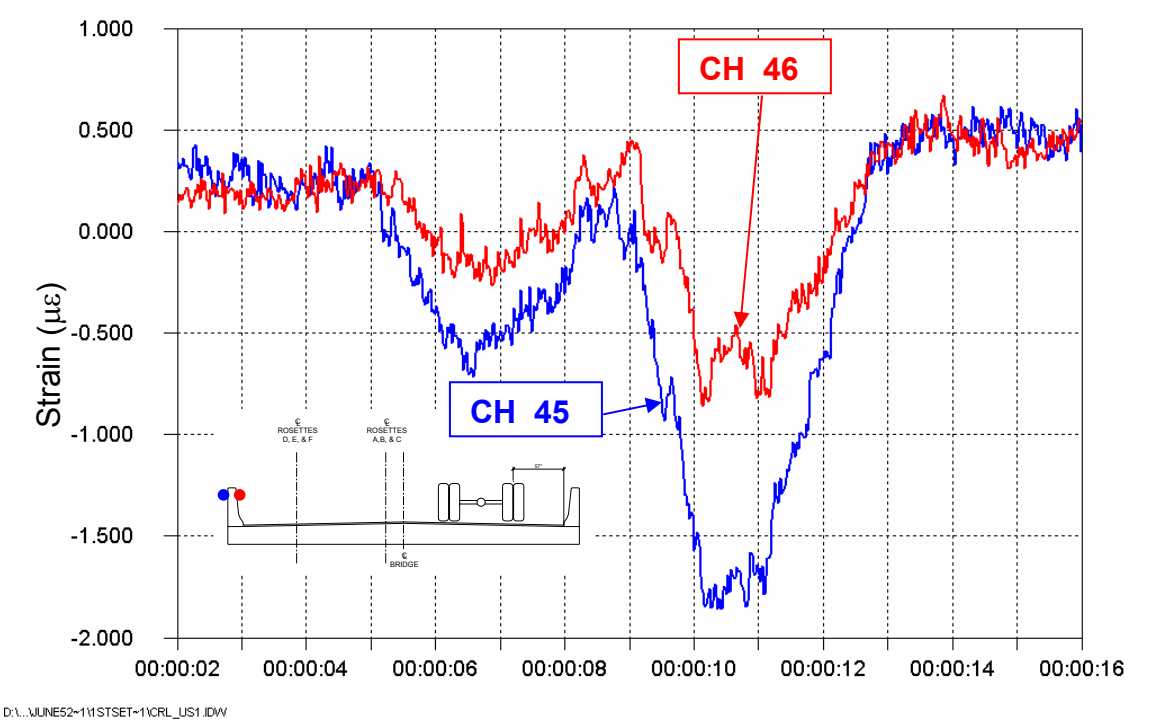

Figure 4.27 – Strain history at top of parapet for test CRL_US1
(CH_45 is exterior face; CH_46 is interior face)

5.0 Long-Term Monitoring

The first phase of the long-term monitoring of the FRP bridge was conducted from July 1, 2002 to August 12, 2002. A reduced number of strain gages were selected for long-term monitoring, based on a review of the controlled load test data. These channels are listed in Table 3.5. Temperature data were also monitored. Thermocouples were installed in the bottom and top plates of the FRP slab. An additional thermocouple was used to record the ambient air temperature.

During monitoring, the data logger constantly checks the strain gages to determine if predefined triggers or strain thresholds have been exceeded, indicating the presence of a heavy vehicle. At that point, the data logger records time-history data for a predefined period of time. The data from two gages, CH_22 and CH_38, were used for the triggers. When the strain at CH_22 exceeded 25 microstrain in compression and the strain at CH_38 exceeded 25 microstrain in tension, five seconds of data prior to and five seconds following the trigger event were recorded for all monitored channels. Use of this type of trigger (i.e. top plate in compression, bottom plate in tension) ensures that the time-history data recorded represent a real event and not an erroneous event, such as a noise spike.

Temperature data were constantly monitored. Five-minute averages of all temperature data were recorded.

5.1 Strain Magnitudes

A review of all data collected during the monitoring period provides an estimate of the magnitude of stresses caused by normal traffic to which the bridge is subjected during its service life. Table 5.1 contains a summary of the peak strains recorded at each of the monitored strain gages during the monitoring period. Although the maximum strains are greater than produced by the test truck, it should also be noted that the number of triggered events was small. Figure 5.1 presents a plot of all triggered events recorded during the entire monitoring period. During this interval, there were 90 vehicles that crossed on the downstream side of the bridge which exceed the trigger threshold (about 2.4 per day). It can also be seen from the figure that there were only eight vehicles that crossed the bridge during the monitoring period which caused strains higher that 100 microstrain in the either of the trigger gages. The measured peak strains are low, as shown in the table.

It is possible the largest strains measured were the result of multiple trucks on the bridge at one time. However, this is thought to be unlikely due to the very low ADT on the road.

Data Channel	Location	Peak Strain During Monitoring (με)
CH_38	Bottom of slab; near centerline; longitudinal @ midspan	132
CH_40	Bottom of slab; near centerline; longitudinal @ quarterspan	94
CH_42	Bottom of slab; in downstream lane; longitudinal @ midspan	162
CH_44	Bottom of slab; in downstream lane; longitudinal @ quarterspan	127
CH_39	Bottom of slab; near centerline; transverse @ midspan	91
CH_43	Bottom of slab; in downstream lane; transverse @ midspan	140
CH_22	Top of slab; near centerline; longitudinal @ midspan	-161
CH_31	Top of slab; in downstream lane; longitudinal @ midspan	-120
CH_32	Top of slab; in downstream lane; 45 deg. @ midspan	-191
CH_33	Top of slab; in downstream lane; transverse @ midspan	-92
CH_45	Top of parapet; longitudinal; @ midspan	-27
CH_50	Bottom of parapet; longitudinal @ midspan	62

Table 5.1 – Summary of peak strains measured during long-term monitoring

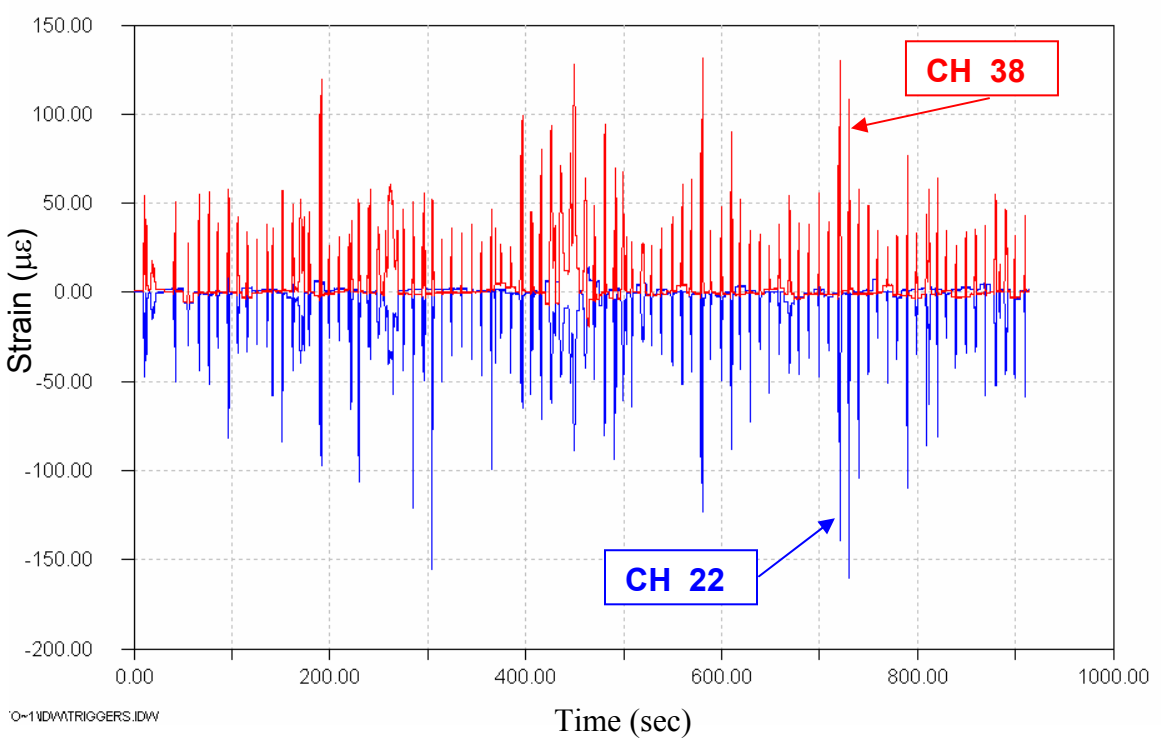

Figure 5.1 – Triggered time histories for entire monitoring period

5.2 Temperature Monitoring

Temperatures in the FRP slab and outside air were monitored. The average temperature in the top of the slab during the entire monitoring period was 84 F. At the bottom of the slab, the average temperature was 75 F. The average ambient air temperature was 74 F. Figure 5.2 presents a temperature history plot for a representative two week portion of the monitoring data.

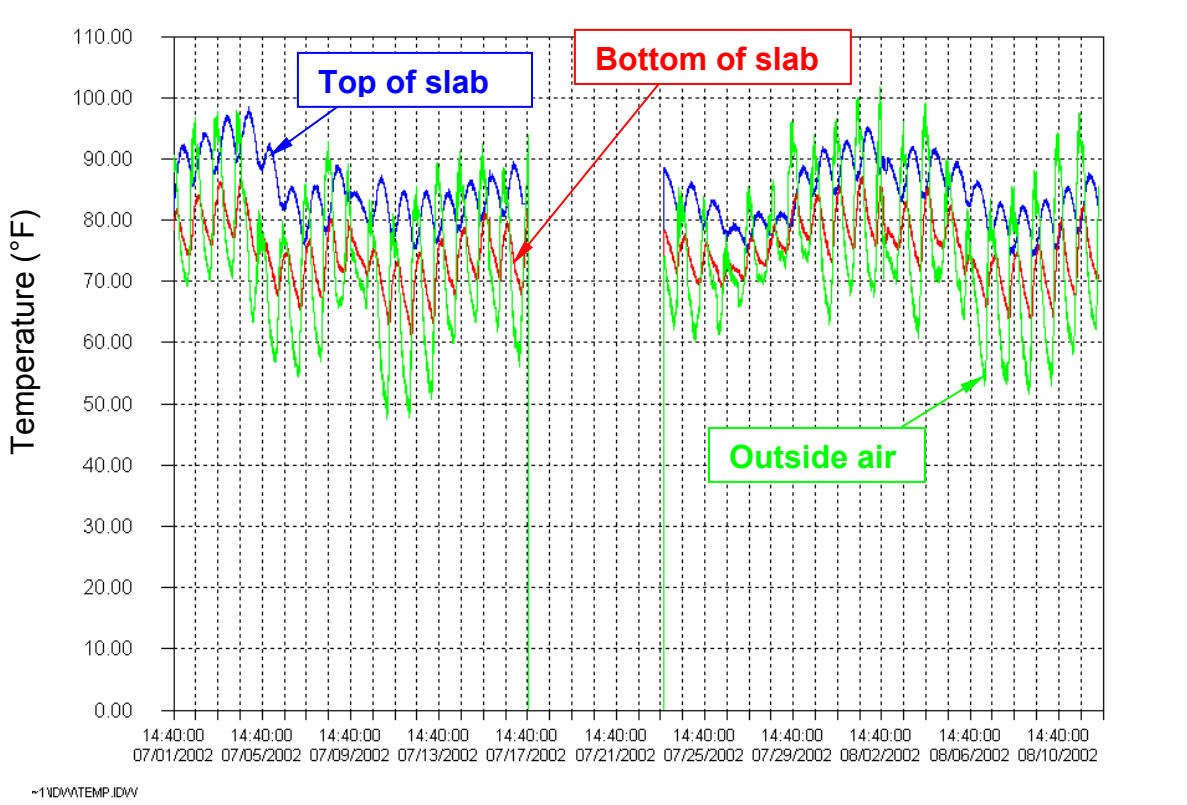

Figure 5.2 – Temperature time-histories for the entire Phase 1 monitoring period

6.0 Phase 2 Testing

This section of the report discusses the results of the second phase of controlled load-testing and long-monitoring of the Dubois Creek FRP bridge in Great Bend, PA. PennDOT comments on the draft letter report have been incorporated. Enclosed is the response to these comments.

This phase of testing was conducted on February 20, 2003, and was a follow-up to similar testing conducted in June 2002. This phase of testing was performed to investigate potential changes over time in stiffness, load distribution characteristics, or general behavior of this unique new bridge. A series of load tests were performed similar to those conducted during the first phase of testing eight months before. Details and results of the first phase of testing were earlier in this report. The results of this phase of testing are compared to those of Phase 1.

7.0 Phase 2 Test Program - Summary

7.1 Test Trucks

Two test trucks were made available for the second phase of testing. New tests were conducted utilizing both trucks to investigate the effect simultaneous loading in both vehicle lanes. Figure 7.1 contains a photograph of test truck #1. Test truck #2 is shown in Figure 7.2.

A summary of the truck weights is given in Table 7.1. The geometry of the test trucks is contained in Table 7.2.

Test truck #1 (the lighter of the trucks) was used for the majority of the static crawl tests. This was done for two reasons. First, the weight of this truck is closer to the truck used in the Phase 1 tests. The rear tandem weight of truck #1 was 5% heavier than the rear tandem of the Phase 1 truck. Secondly, test truck #2 had an interstate plow mounted to the front, which prevented the truck from getting close to the parapet.

Test truck #2 was used for all dynamic tests. The rear tandem weight of this truck was 17% higher than that of the Phase 1 test truck.

Figure 7.1 – Photograph of test truck #1 (425-8076) utilized during controlled load testing

Figure 7.2 – Photograph of test truck #2 (107-8076) utilized during controlled load testing

Test Phase.	Truck No.	Truck ID No.	Rear Axle Type	Front Axle Load (lb)	Rear Tandem Load (lb)	GVW[1] (lb)	Date of Tests
1	1	N/A	Tandem	13,700	39,120	52,820	June 5, 2002
2	1	425-8076	Tandem	16,300	41,250	57,550	February 20, 2003
2	2	107-8076	Tandem	21,750	45,650	67,400	February 20, 2003

Note:
1. GVW = Gross Vehicle Weight

Table 7.1 – Test truck axle load data

Test Phase.	Truck No.	L1 (in)	L2 (in)	W_f (in)	W_r (in)	A[1] (in)	B (in)	C (in)	D[1] (in)	E (in)
1	1	192	50	84	72	-	16	24	-	11.5
2	1	163	51	84	72	-	13	22	-	9
2	2	162	51	84	73	-	12	22	-	9

Note:
1. This dimension was not measured.

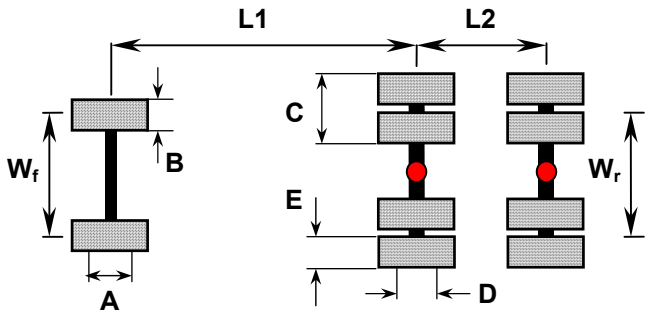

Table 7.2 - Geometry of test truck used for controlled load tests

7.2 Test Summary

In general, the same tests were conducted for the Phase 2 tests, since the purpose of this testing was to compare the behavior with the Phase 1 testing. As before, two setups were used for testing since the total number of data channels was more than could be read by the data logger at one time. Tables 7.3 and 7.4 summarize the load tests which were conducted for setup #1 and #2, respectively. The tests highlighted and bold represent the tests of each type that were selected for data analysis (each test type was repeated).

Instrumentation was kept the same, however, due to the fact that the temporary platform had been removed and the significant accumulation of snow and ice beneath the bridge, displacements were not measured. However, in the upcoming third phase of testing, a frame will be installed beneath the slab to measure displacements to assess whether the flexibility of the slab has changed over time.

Test #	File Name	Test Type	Travel Dir.[1]	Lane[2]	Truck Dir.[3]	Comment
1	**PRK_DEF.DAT**	**Park**	**S**	**US**	**F**	**CL left dual over rosettes D, E, F**
2	**PRK_CBA.DAT**	**Park**	**S**	**US**	**F**	**CL right dual over rosettes A, B, C**
3	**CRL_PPT1.DAT**	**Crawl**	**S**	**DS**	**F**	**Left tires adj. to DS PPT.**
4	CRL_PPT2.DAT	Crawl	N	DS	R	Left tires adj. to DS PPT.
5	CRL_DEF1.DAT	Crawl	S	DS	F	CL left dual over rosettes D, E, F
6	**CRL_DEF2.DAT**	**Crawl**	**S**	**DS**	**F**	**CL left dual over rosettes D, E, F**
7	**CRL_ABC1.DAT**	**Crawl**	**N**	**DS**	**R**	**CL right dual over rosettes A, B, C**
8	CRL_ABC2.DAT	Crawl	S	DS	F	CL right dual over rosettes A, B, C
9	**CRL_US1.DAT**	**Crawl**	**N**	**DS**	**R**	**Truck in upstream lane**
10	CRL_US2.DAT	Crawl	N	DS	R	Truck in upstream lane
11	**DYN_DS1.DAT**	**Dynamic**	**S**	**DS**	**F**	**Approx. speed = 27 mph; truck #2 approx. centered in normal DS travel lane**
12	DYN_DS2.DAT	Dynamic	S	DS	F	Approx. speed = 27 mph; truck #2 approx. centered in normal DS travel lane
13	**DYN_US1.DAT**	**Dynamic**	**S**	**US**	**F**	**Approx. speed = 27 mph; truck #2 approx. centered in normal US travel lane**
14	DYN_US2.DAT	Dynamic	S	US	F	Approx. speed = 27 mph; truck #2 approx. centered in normal US travel lane
15	SBS_1.DAT	Park	S	US,DS	F	Both trucks side by side
16	**SBS_2.DAT**	**Park**	**S**	**US,DS**	**F**	**Both trucks side by side**

Note:
1. N = north, S = south
2. DS = downstream, US = upstream
3. F= forward, R = reverse
4. Truck #1 was used for tests 1-10; Truck #2 was used for tests 11-14

Table 7.3 – Summary of controlled load tests (SETUP #1)

Test #	Filename	Test Type	Travel Dir	Lane	Truck Dir.	Comment
17	CRL_CLB1.DAT	Crawl	S	DS	F	CL left dual 2-3" US of CL instrumented bottle
18	**CRL_CLB2.DAT**	**Crawl**	**S**	**DS**	**F**	**CL left dual 2-3" US of CL instrumented bottle**
19	CRL_DSB1.DAT	Crawl	S	DS	F	CL left dual 9-10" DS of CL instrumented bottle
20	**CRL_DSB2.DAT**	**Crawl**	**S**	**DS**	**F**	**CL left dual 12" DS of CL instrumented bottle**
21	**CRL_USB1.DAT**	**Crawl**	**S**	**DS**	**F**	**CL left dual 13" US of CL instrumented bottle**
22	CRL_USB2.DAT	Crawl	S	DS	F	CL left dual 14" US of CL instrumented bottle

Note:
1. N = north, S = south
2. DS = downstream, US = upstream
3. F= forward, R = reverse
4. Truck #1 was used for tests 17-22

Table 7.4 – Summary of controlled load tests (SETUP #2)

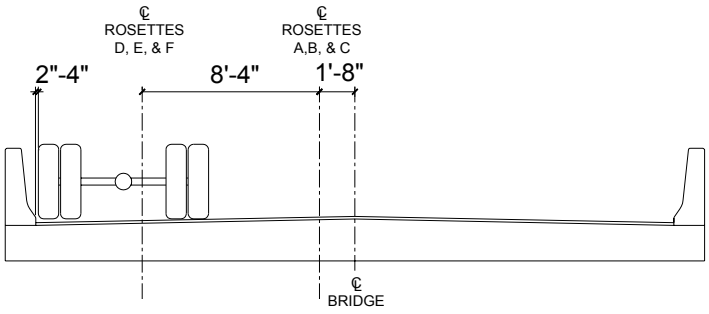

(a) Tests CRL PPT1 & CRL PPT2

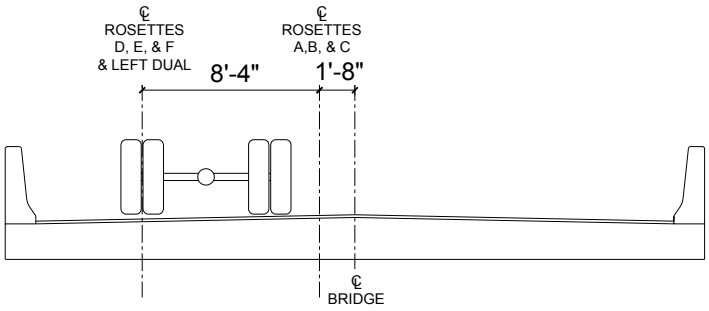

(b) Tests CRL DEF1 & CRL DEF2

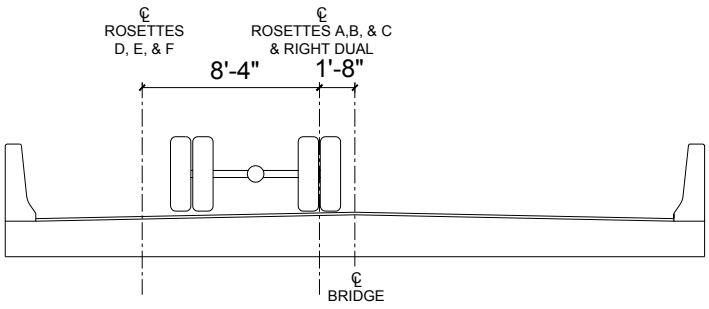

(c) Tests CRL ABC1 & CRL ABC2

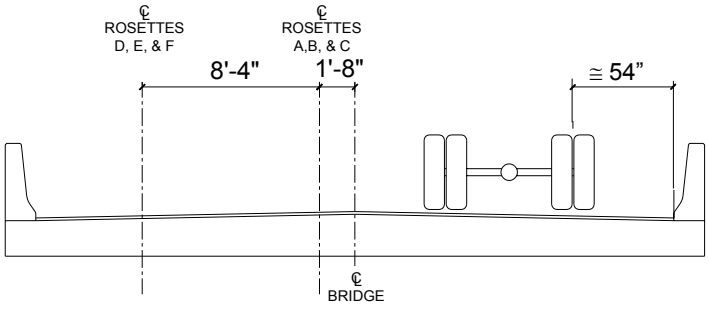

(d) Tests CRL US1 & CRL US2

Figure 7.3 – Location of test truck for the various load tests
(a) CRL_PPT1 (b) CRL_DEF2 (c) CRL_ABC1 (d) CRL_US1

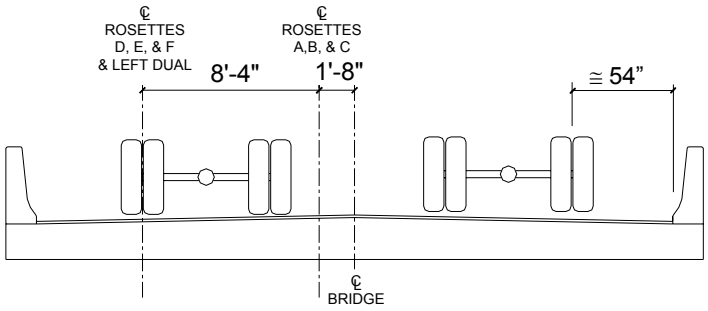

(e) Tests CRL_SBS1 & CRL_SBS2

Figure 7.3 cont'd – Location of test truck for the various load tests
(e) CRL_SBS2

Figure 4- Photograph of side-by-side static crawl test

The test truck positions were kept the same, as shown in Figure 7.3. Furthermore, tests were conducted with the trucks positioned side-by-side, as shown in Figures 7.3(e) and 7.4.

8.0 Results of Controlled Load Tests

In general, the behavior of the bridge during the Phase 2 tests was similar to that of the Phase 1 tests. Although deflections were not measured as during Phase 1, bridge displacements were not perceptible. However, this will be confirmed in the next phase of load tests when displacement sensors will be installed.

8.1 Static Load Tests

The magnitudes of measured strains due to global bending were similar from the two phases. Since there was only a 5% difference between the rear tandem axle weights

of the trucks used for the static crawl tests for the two phases, direct comparison can be reasonably made between the measured strains.

A summary of the peak strains measured in Phases 1 and 2 can be seen in Tables 8.1 and 8.2, respectively. It can be seen that in general the strain magnitudes are comparable. Table 8.3 contains a summary of the measured strains for the side-by-side test conducted during Phase 2 only. The magnitude of the measured strains during this test are not excessive.

Of interest are the data from CH_33 during test CRL_DEF2 and CH_24 during test CRL_ABC1, both from Phase 2 (Table 8.2). The number given in parenthesis is the peak positive measured strain. Although these gages are on the top of the slab, and are in a compression strain field due to global loading, there was a significantly higher strain reversal due to the passage of the wheel load than observed in the Phase 1 testing.

This can be further examined in Figures 8.1 and 8.2, which contain strain histories of four longitudinally oriented strain gages located at midspan for Phase 1 and 2, respectively. It can be seen in the figure that the global strain magnitudes from Phase 1 and 2 are comparable. However, the strain reversal on CH_22 is larger during the Phase 2 tests.

A similar observation can be made from Figures 8.3 and 8.4, which contain strain histories of four transversely oriented strain gages located at midspan for Phase 1 and 2, respectively. The strain reversal of channel CH_24 is significantly larger in the Phase 2 test. However, as for the longitudinally oriented gages, the global strain magnitudes are comparable.

Three reasons are suggested for the higher strain reversals. First, the rear tandem foot print was different for the two phases of testing. The Phase 1 test truck had a rear ire width (dimension 'E' of Table 7.2) of 11.5 inches, and a dual tire width (dimension 'C' of Table 7.2) of 24 inches. These dimensions for the Phase 2 truck were 9 and 22 inches, respectively. While these differences are small when considering their effect on global strains, they will have a large effect on the local strains, considering that the FRP webs are located on 8 inch centers. Secondly, the test trucks may not have been located at exactly the same location during the tests, despite careful setup procedures. Again the effect on global strains are most likely negligible, but is more pronounced in the local strains, as observed in strain reversals. Similar sensitivity to transverse position of the loading has been observed in tests conducted on steel orthotropic bridge decks. Hence, the observed variability in behavior is not surprising. Finally, the wearing surface may have had different behavior during the two phases of testing, both in how concentrated loads are spread to the FRP slab, and the amount of local composite behavior the topping provides. These differences may be the result of the numerous repairs made to the surface.

It is suggested that static tests be repeated several times with slightly varying lateral truck positions to for the Phase 3 tests later this summer. An assessment of the sensitivity to lateral truck position on the behavior of the bridge (both local and global) can be made by comparing the results of these tests. Furthermore, it is recommended that the Phase 3 tests be conducted with tests trucks of identical rear tandem geometry as the Phase 2 test trucks.

It is important to note in all the strain plots, that when the local strain peaks are ignored, the global strains are similar. This is consistent with the fact that the test truck from Phase 2 had a rear tandem weight that was only 5% more than that for Phase 1.

Data Channel	Location	Direction	Peak Strain (με)			
			CRL_PPT1	CRL_DS4	CRL_DS1	CRL_US1
CH_22	Top of FRP Slab	Longitudinal	-55	-81	-123	-64
CH_24		Transverse	-5	-29	*-75 (+24)*	5
CH_31		Longitudinal	-62	-98	-60	-15
CH_33		Transverse	-50	*-93 (+1)*	-42	9
CH_38	Bottom of FRP Slab	Longitudinal	55	85	119	70
CH_39		Transverse	5	27	78	-9
CH_42		Longitudinal	100	126	88	18
CH_43		Transverse	79	120	62	-11
CH_45	Parapet	Top - Long	-46	-31	-18	-2
CH_50		Bot - Trans	69	50	35	5

Table 8.1 – Summary of peak strains measured during **PHASE 1** static crawl tests

Data Channel	Location	Direction	Peak Strain (με)			
			CRL_PPT1	CRL_DEF2	CRL_ABC1	CRL_US1
CH_22	Top of FRP Slab	Longitudinal	-45	-70	-121	-65
CH_24		Transverse	-5	-36	***-50 (+80)***	-14
CH_31		Longitudinal	-42	-82	-45	-15
CH_33		Transverse	-27	***-41 (+67)***	-32	7
CH_38	Bottom of FRP Slab	Longitudinal	60	97	117	90
CH_39		Transverse	12	51	80	16
CH_42		Longitudinal	104	132	100	25
CH_43		Transverse	84	122	72	-14
CH_45	Parapet	Top - Long	-44	-26	-22	-4
CH_50		Bot - Trans	64	41	34	7

Table 8.2 – Summary of peak strains measured during **PHASE 2** static crawl tests

Data Channel	Location	Direction	Peak Strain (με)
			CRL_SBS2
CH_22	Top of FRP Slab	Longitudinal	-45
CH_24		Transverse	-5
CH_31		Longitudinal	-42
CH_33		Transverse	-27
CH_38	Bottom of FRP Slab	Longitudinal	60
CH_39		Transverse	12
CH_42		Longitudinal	104
CH_43		Transverse	84
CH_45	Parapet	Top - Long	-44
CH_50		Bot - Trans	64

Table 8.3 – Summary of peak strains measured during **PHASE 2** side-by-side static crawl test

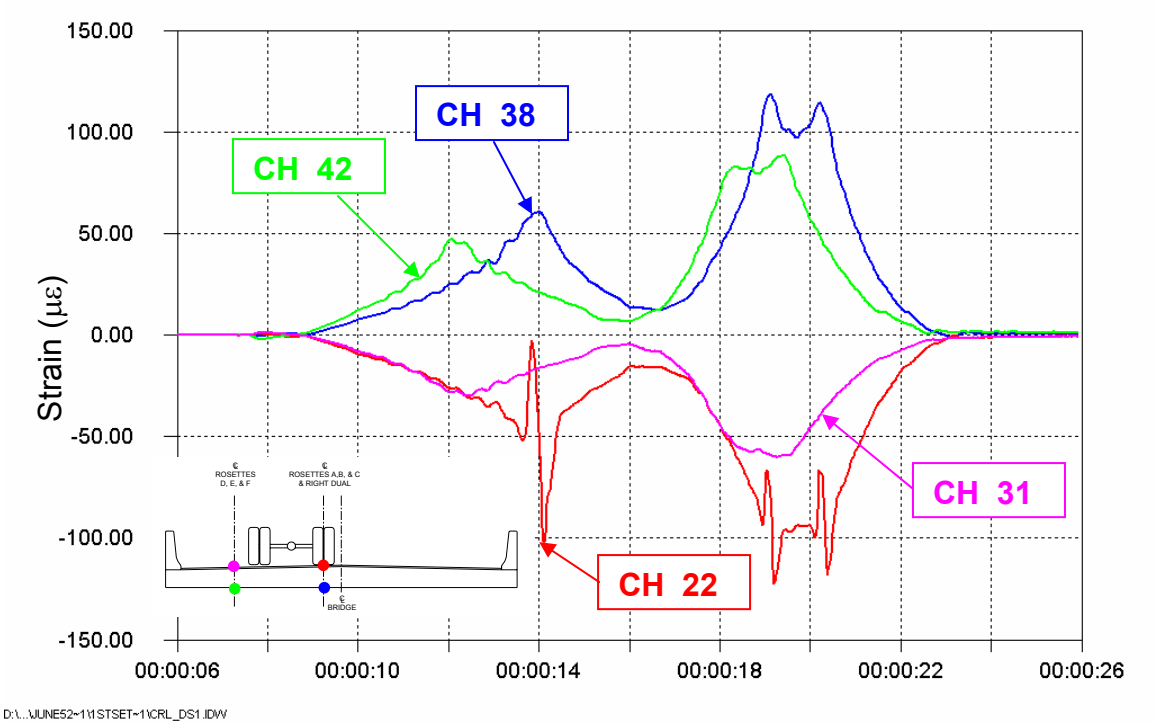

Figure 8.1 – Longitudinal strain history at midspan for load test CRL_DS1
PHASE 1 TEST
(Centerline right dual over CH_22)

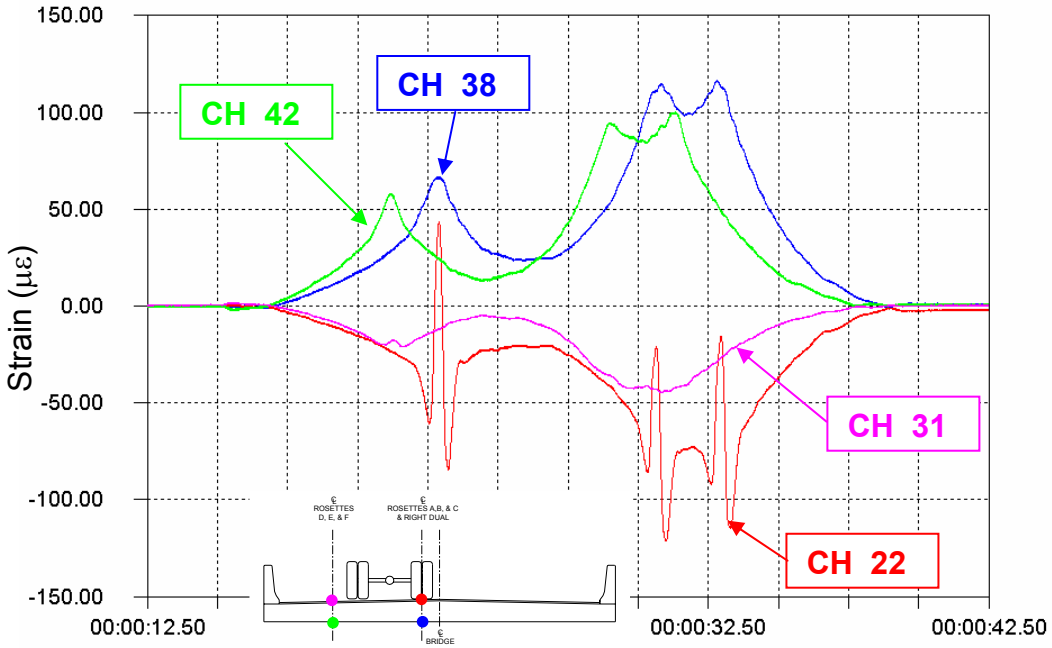

Figure 8.2 – Longitudinal strain history at midspan for load test CRL_ABC1
PHASE 2 TEST
(Centerline right dual over CH_22)

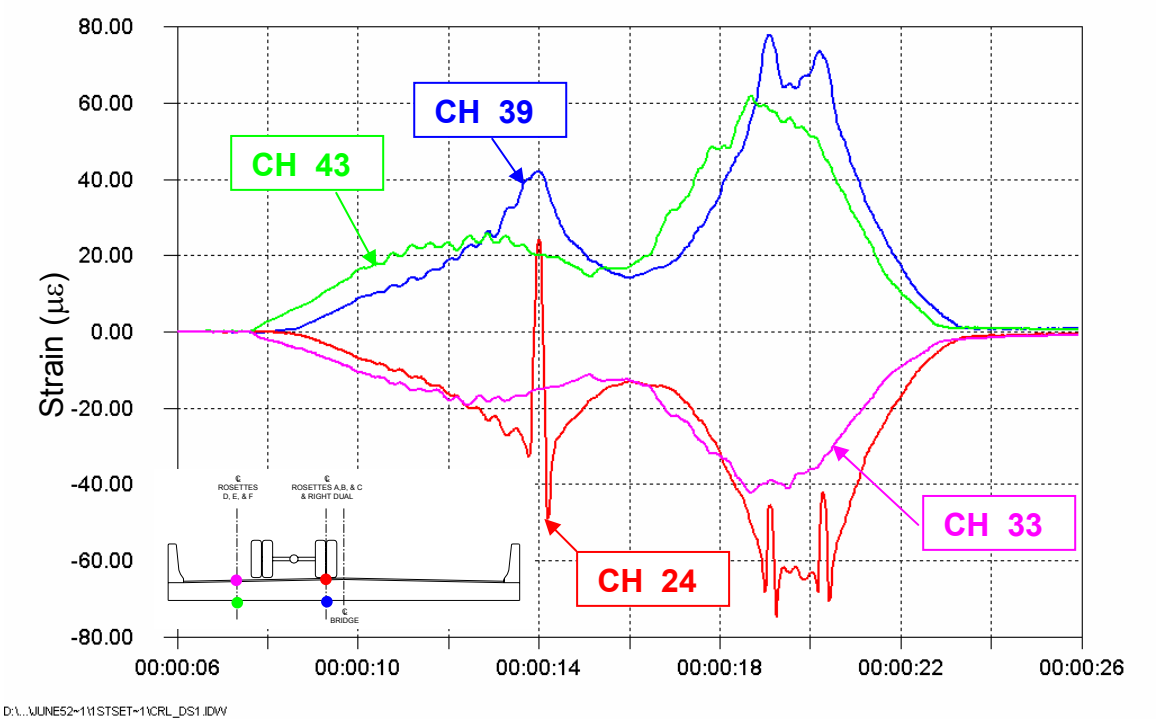

Figure 8.3 – Transverse strain history at midspan for load test CRL_DS1
PHASE 1 TEST
(Centerline right dual over CH_24)

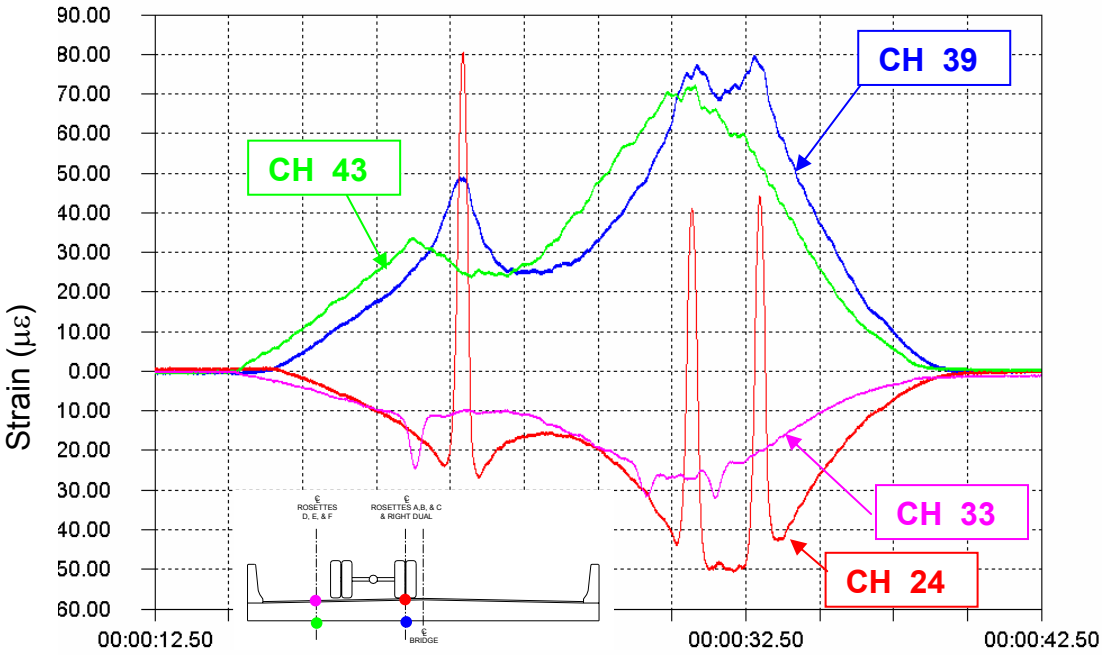

Figure 8.4 – Transverse strain history at midspan for load test CRL_ABC1
PHASE 2 TEST
(Centerline right dual over CH_24)

Measured stresses at the strain rosettes are summarized in Tables 8 and 9. Table 8 contains the maximum and minimum stresses measured at the rosettes for setup #1 of Phase 2. These stresses represent stresses in the top plate of the slab. For location and orientation of the rosettes, refer to the Phase 1 Final Interim Report. It can be seen that the peak tensile and compressive stresses of 0.64 ksi and –0.38 ksi are low, similar to peak stresses of 0.25 ksi and –0.52 ksi measured during Phase 1.

Rosette Name		*CRL_PPT1*			*CRL_DEF2*			*CRL_ABC1*			*CRL_US1*		
		σ_x (ksi)	σ_y (ksi)	τ_{xy} (ksi)	σ_x (ksi)	σ_y (ksi)	τ_{xy} (ksi)	σ_x (ksi)	σ_y (ksi)	τ_{xy} (ksi)	σ_x (ksi)	σ_y (ksi)	τ_{xy} (ksi)
C	*Max*	0.02	0.02	0.00	0.01	0.01	0.01	**0.64**	0.26	0.23	-0.01	0.01	0.00
	Min	-0.01	0.01	-0.01	-0.26	-0.08	-0.04	-0.30	-0.14	-0.03	-0.13	-0.04	-0.08
D	*Max*	0.01	0.01	0.00	0.56	0.47	0.04	0.00	0.00	0.04	0.00	0.04	0.02
	Min	0.00	0.00	0.00	**-0.38**	-0.16	-0.09	-0.26	-0.16	-0.01	-0.07	0.00	0.00
E	*Max*	0.01	0.00	0.00	0.12	0.21	0.02	0.01	0.00	0.01	0.00	0.01	0.00
	Min	-0.01	-0.01	0.00	-0.37	-0.18	-0.16	-0.21	-0.13	-0.02	-0.05	0.00	-0.02

Table 8.4 –Summary of peak rosette stresses measured during static crawl tests
Maximum tensile and compressive stresses are indicated in bold (Test Setup #2)
PHASE 2 DATA

Table 8.5 contains the maximum and minimum measured stresses for setup #2 of Phase 2 (bottle instrumentation). These stresses represent local bending response due to passage of the wheel load in the direct vicinity of the gage. The peak tensile stress of 2.7 ksi and peak compressive stress of –4.2 ksi are reasonably similar to the peak stresses of 4.6 ksi and –5.3 ksi measured during Phase 1.

Rosette		*Test CRL_CLB2*			*Test CRL_DSB2*			*Test CRL_USB1*		
		σ_x (ksi)	σ_y (ksi)	τ_{xy} (ksi)	σ_x (ksi)	σ_y (ksi)	τ_{xy} (ksi)	σ_x (ksi)	σ_y (ksi)	τ_{xy} (ksi)
Rosette 123	*Max*	0.1	0.1	0.1	0.0	0.0	0.4	0.0	0.3	0.0
	Min	-0.2	**-4.2**	-0.2	-0.2	-2.2	0.0	-0.1	0.0	-0.3
Rosette 456	*Max*	0.0	0.2	0.2	0.1	0.1	0.3	0.0	0.0	0.0
	Min	-0.7	-0.1	-0.1	-0.2	-0.1	0.0	-0.1	-0.2	-0.2
Rosette 789	*Max*	0.1	0.2	0.5	0.0	0.1	0.5	0.0	0.0	0.2
	Min	-0.3	-3.1	-0.3	-0.3	-2.4	-0.3	-0.1	0.0	-0.1
Rosette 101112	*Max*	0.1	0.2	0.4	0.0	0.1	0.4	0.1	0.1	0.0
	Min	-0.1	-3.6	-0.5	-0.3	-3.1	-0.5	0.0	0.0	-0.2
Rosette G	*Max*	**2.7**	1.4	0.0	1.4	0.7	0.0	0.0	0.0	0.0
	Min	-0.3	-0.1	-0.3	-0.2	-0.1	-0.3	-0.1	-0.2	-0.1
Rosette H	*Max*	0.5	0.3	0.0	0.2	0.1	0.0	0.0	0.0	0.0
	Min	-0.2	-0.2	-0.1	-0.2	-0.1	-0.1	-0.1	-0.2	-0.1

Table 8.5 – Summary of peak stresses in the bottle rosettes for static load tests
Maximum tensile and compressive stresses are indicated in bold (Test Setup #2)
PHASE 2 DATA

8.2 Dynamic Load Tests

As discussed above, dynamic tests were conducted similar to Phase 1. The heavier truck #2 was used for these tests (GVW=67.4 kips). This truck was 17% heavier than the Phase 1 truck. Figures 8.5 and 8.6 contain the strain history plot for bottom surface gages at midspan for the Phase 1 and 2 dynamic tests, respectively. The peak transverse strains are 68 με and 106 με, for Phase 1 and 2, respectively. This is a 55% increase. The peak longitudinal strains are 113 με and 140 με, for Phase 1 and 2, respectively. This is a 24% increase.

Figures 8.7 and 8.8 contain similar strain history plots for top surface gages at midspan for the Phase 1 and 2 dynamic tests, respectively. If the strain reversals are not considered, the peak negative (compressive) transverse strains are -66 με and -59 με, for Phase 1 and 2, respectively. Similarly, the peak negative (compressive) longitudinal strains are -150 με and -129 με, for Phase 1 and 2, respectively. Interestingly, the strain magnitudes have dropped for the Phase 2 tests, despite the heavier truck.

However, when the strain reversals are considered, the peak positive (tensile) transverse strains are +31 με (CH_24, Figure 8.7) and +104 με (CH_24, Figure 8.8), for Phase 1 and 2, respectively. Similarly, the peak positive (tensile) longitudinal strains are 0 με (CH_22, Figure 8.7) and +70 με (CH_22, Figure 8.8), for Phase 1 and 2, respectively. This is a significant change in behavior. However, it is not clear if it is the result of dynamic loading. As discussed above, there were significantly higher strain reversals observed in the static load tests. In general however, despite this apparent change in behavior, the strains in the slab due to dynamic loading do not appear to be excessive.

It can be suggested, as it was for the static tests, that the difference in behavior can be attributed to differences in geometry of the test trucks and location of the test trucks. It should be noted that one major difference between the static and dynamic tests is that the test truck position was much more carefully controlled during the static tests. Therefore, comparison of global strains between the Phase 1 and 2 dynamic tests is less accurate than for the dynamic tests. It is proposed that more careful control of the truck position during dynamic testing for the Phase 3 tests to be conducted later this summer, in order to better assess the effect of dynamic behavior of the bridge.

The observed change in behavior may also be the result of differing behavior of the wearing surface both in terms of load spreading on the slab and local composite behavior with the top plate of the FRP slab. This may be caused by the numerous repairs made the wearing surface.

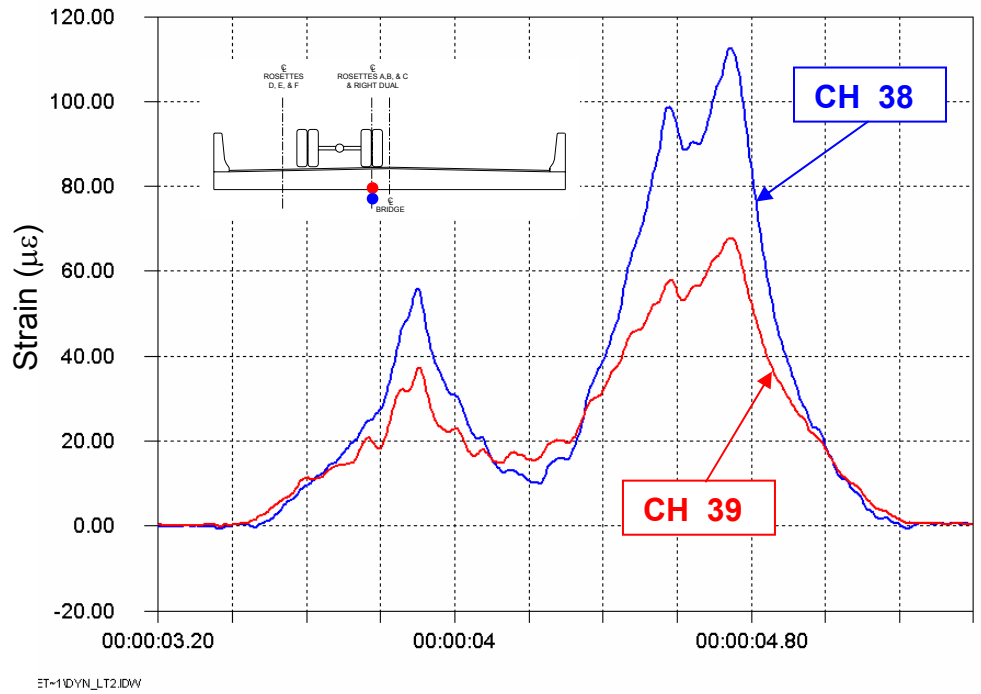

Figure 8.5 – Strain history at bottom of FRP slab at midspan for dynamic load test DYN_LT2
PHASE 1 TEST
(CH_38 is longitudinal, CH_39 is transverse)

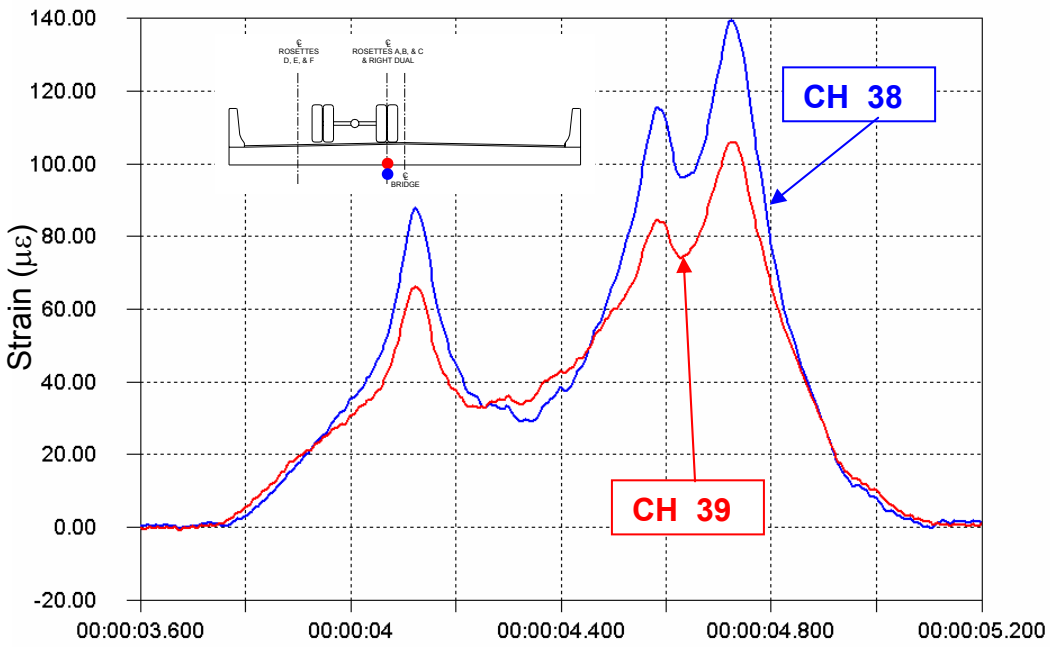

Figure 8.6 – Strain history at bottom of FRP slab at midspan for dynamic load test DYN_DS1
PHASE 2 TEST
(CH_38 is longitudinal, CH_39 is transverse)

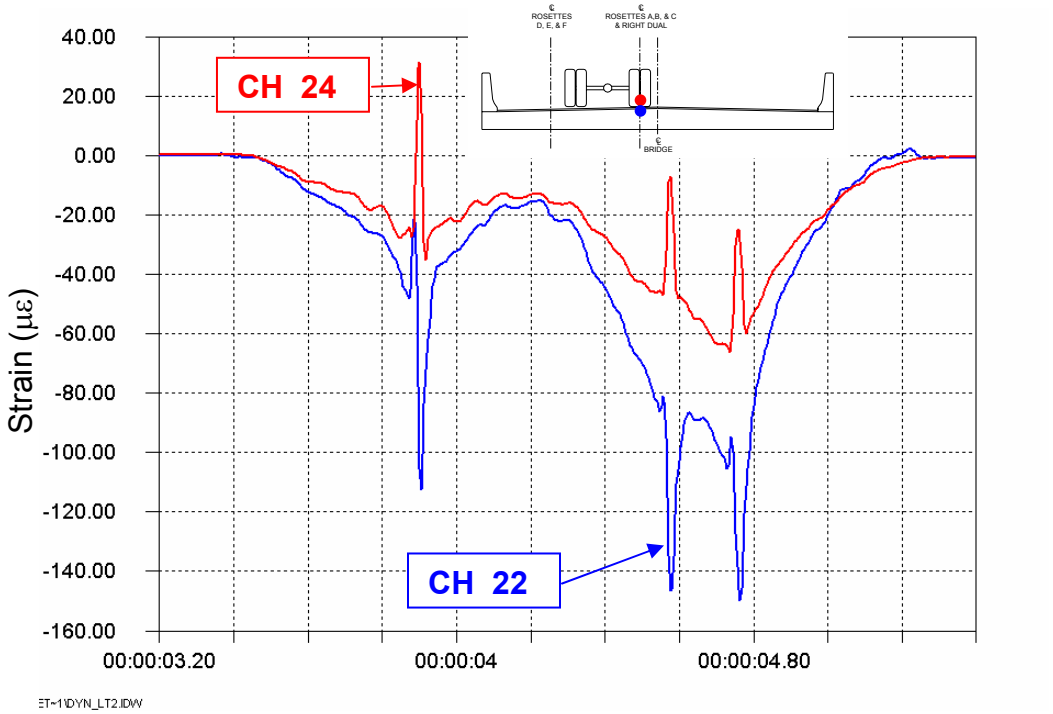

Figure 8.7 – Strain history at top of FRP slab at midspan for dynamic load test DYN_LT2
PHASE 1 TEST
(CH_22 is longitudinal, CH_24 is transverse)

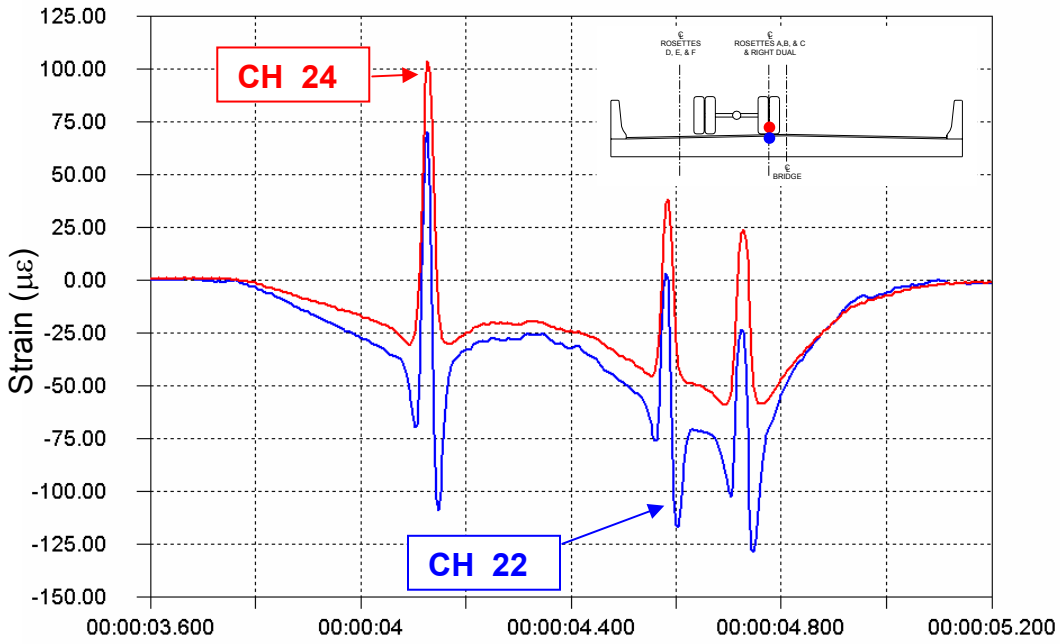

Figure 8.8 – Strain history at top of FRP slab at midspan for dynamic load test
DYN_DS1
PHASE 2 TEST
(CH_22 is longitudinal, CH_24 is transverse)

9.0 Results of Long-Term Monitoring

As reported previously, the first phase of long-term monitoring of the FRP bridge was conducted from July 1, 2002 to August 12, 2002. The second phase of long-term monitoring extended from February 25, 2003 to April 10, 2003.

9.1 Strain Monitoring

As before, a reduced number of strain gages were selected for the long-term monitoring. The channels selected are the same as those used in Phase 1. Thermocouples were also monitored.

A summary of the peak measured strains for each monitored channel, during Phase 1 and 2, is presented in Table 9.1. It can be seen from the table that most of the measured strains on the bottom of the slab are comparable for the two phases. However, on the top of the slab, it can be seen that the measured peak strains are lower for Phase 2. This may be the result of the increased strain reversal described above. It may be just a difference in the traffic passing across the bridge during the two monitoring periods.

When the Phase 2 tests were conducted, there was a significant accumulation (approximately 3-4 feet) of snow and ice along the parapets that extended into the roadway. This snow and ice was removed on the bridge for testing, however, it was not removed off the bridge. This accumulation off the bridge would have forced vehicles closer to the center of the road way. This is illustrated in Figure 9.1. Therefore, lower peak strains would be expected in strain gages closer to the parapet oriented in both the transverse and longitudinal directions. This is in agreement with the data presented in Table 9.1. The peak observed strains at channels CH_38, CH_39, and CH_40, located near the bridge centerline on the bottom slab surface were not markedly changed from Phase 1 to Phase 2. However, channels CH_42, CH_44, and CH_42, located in the downstream lane closer to the parapet showed significantly lower peak strains. In general however, it can be seen that in all cases, the measured strains are low.

Plots of all triggered events recorded during the Phase 1 and Phase 2 monitoring periods can be seen in Figures 9.2 and 9.3, respectively. During the Phase 2 monitoring period, there were 120 vehicles that crossed on the downstream side of the bridge which exceeded the trigger threshold, or about 2.6 per day. This is in good agreement with the average 2.4 per day reported for Phase 1. Furthermore, there were only six vehicles during the Phase 2 monitoring period which caused strains higher than 100 με in either of the trigger gages (there were eight such vehicles during the Phase 1 monitoring period).

Data Channel	Location	Peak Strain Phase 1 Monitoring (με)	Peak Strain Phase 2 Monitoring (με)
CH_38	Bottom of slab; near centerline; longitudinal @ midspan	132	141
CH_40	Bottom of slab; near centerline; longitudinal @ quarterspan	94	91
CH_42	Bottom of slab; in downstream lane; longitudinal @ midspan	162	87
CH_44	Bottom of slab; in downstream lane; longitudinal @ quarterspan	127	54
CH_39	Bottom of slab; near centerline; transverse @ midspan	91	83
CH_43	Bottom of slab; in downstream lane; transverse @ midspan	140	59
CH_22	Top of slab; near centerline; longitudinal @ midspan	-161 (+23)	-106 (+70)
CH_31	Top of slab; in downstream lane; longitudinal @ midspan	-120 (+17)	-51 (+8)
CH_32	Top of slab; in downstream lane; 45 deg. @ midspan	-191 (+17)	-50 (+26)
CH_33	Top of slab; in downstream lane; transverse @ midspan	-92 (+85)	-32 (+31)
CH_45	Top of parapet; longitudinal; @ midspan	-27	-19
CH_50	Bottom of parapet; longitudinal @ midspan	62	31

Table 9.1 – Summary of peak strains measured during Phase 1 and 2 long-term monitoring
(peak strain reversals are shown in parentheses)

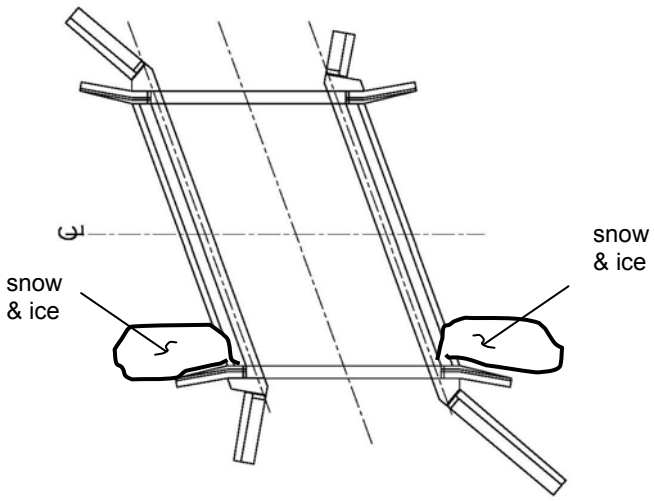

Figure 9.1 – Plan view of bridge showing accumulation of snow and ice on the roadway. This was removed on the bridge itself for testing but not on the approach roadway.

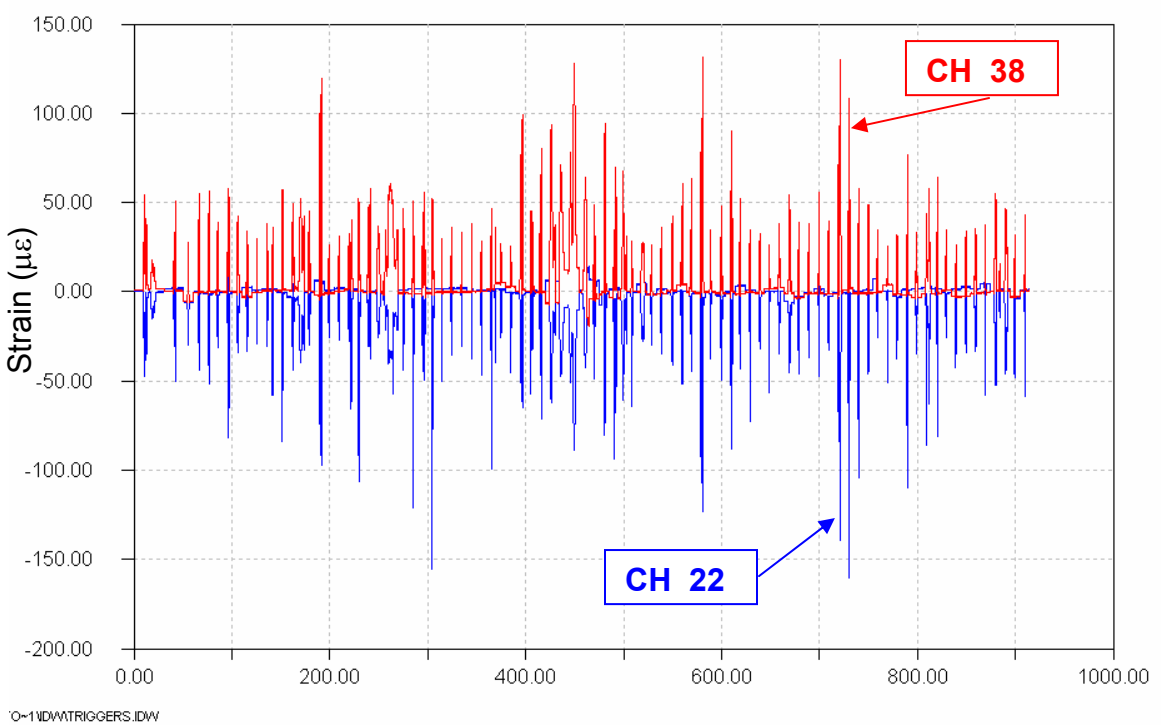

Figure 9.2 – Triggered time histories for entire PHASE 1 monitoring period

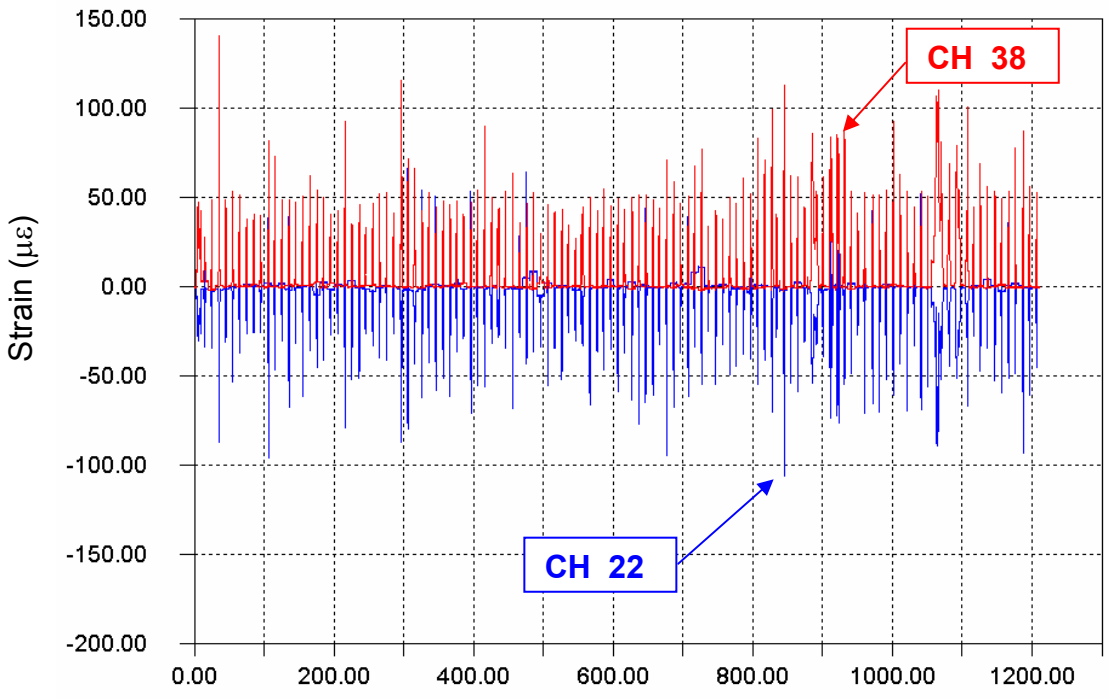

Figure 9.3 – Triggered time histories for entire PHASE 2 monitoring period

9.2 Temperature Monitoring

Temperatures in the FRP slab and outside air were monitored during Phase 2. The average temperature in the top of the slab during the entire monitoring period was 38 F. At the bottom of the slab, the average temperature was 36 F. The average ambient air temperature was 35 F. Figure 9.4 presents a temperature history plot for the entire monitoring period.

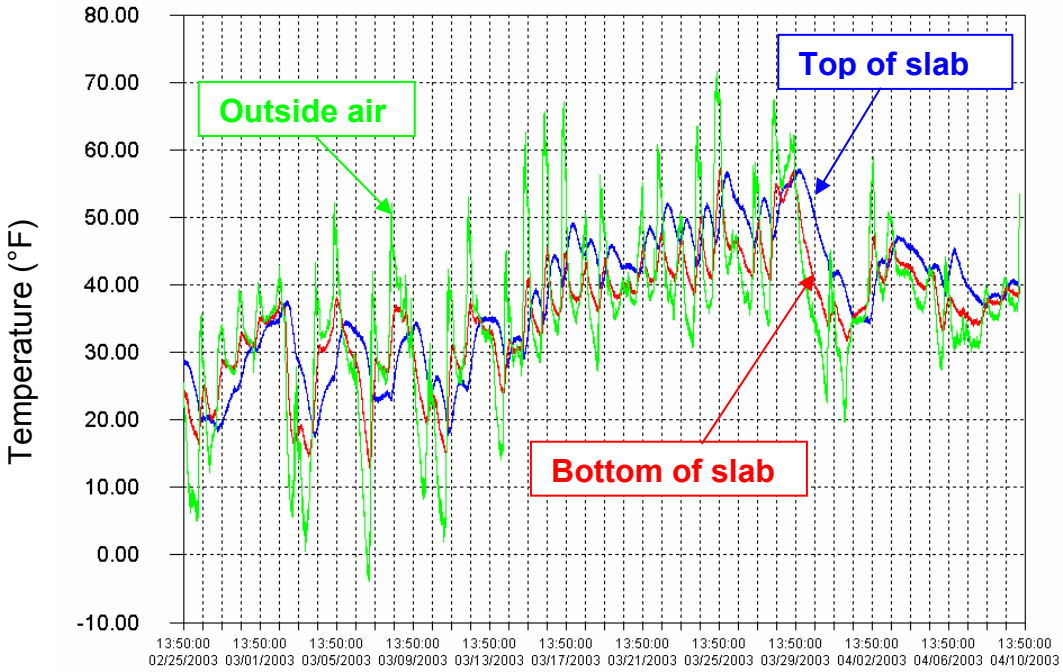

Figure 9.4– Temperature time-histories for the entire Phase 2 monitoring period

10.0 Phase 3 Testing

This section of the report discusses the results of the third and final phase of controlled load testing and long-term monitoring of the Dubois Creek FRP bridge in Great Bend, PA.

The controlled load testing was conducted on August 21, 2003, and was a follow-up to similar testing conducted in June 2002 and February 2003.

This third and final phase of testing was performed to further investigate potential changes over time in stiffness, load distribution characteristics, or general behavior of this unique new bridge. A series of load tests were performed similar to those conducted during the first and second phases of testing discussed previously. The results of Phase 1 are treated as a baseline. Therefore the results of Phase 3 are compared to those of Phase 1 in the sections below.

11.0 Phase 3 Test Program - Summary

11.1 Test Trucks

The same two test trucks used in Phase 2 were made available for the third phase of testing. New tests were conducted investigate the sensitivity of truck position on stress in the bridge. Figure 11.1 contains a photograph of test truck #2. A summary of the truck weights is given in Table 11.1. The geometry of the test trucks is contained in Table 11.2.

Test truck #2 was used for the majority of the static crawl tests and all dynamic tests. The rear tandem weight of truck #2 was 1.5% heavier than the rear tandem of the Phase 1 truck.

Test truck #1 was used for the side-by-side tests only. The rear tandem weight of this truck was 0.7% more than that of the Phase 1 test truck.

Figure 11.1 – Photograph of test truck #2 (107-8076) utilized during controlled load testing

Test Phase.	Truck No.	Truck ID No.	Rear Axle Type	Front Axle Load (lb)	Rear Tandem Load (lb)	GVW[1] (lb)	Date of Tests
1	1	N/A	Tandem	13,700	39,120	52,820	June 5, 2002
2	1	425-8076	Tandem	16,300	41,250	57,550	February 20, 2003
2	2	107-8076	Tandem	21,750	45,650	67,400	February 20, 2003
3	1	425-8076	Tandem	15,550	39,400	54,950	August 21, 2003
3	2	107-8076	Tandem	15,400	39,700	55,100	August 21, 2003

Note:
1. GVW = Gross Vehicle Weight

Table 11.1 – Test truck axle load data

Test Phase.	Truck No.	L1 (in)	L2 (in)	W_f (in)	W_r (in)	A[1] (in)	B (in)	C (in)	D[1] (in)	E (in)
1	1	192	50	84	72	-	16	24	-	11.5
2	1	163	51	84	72	-	13	22	-	9
2	2	162	51	84	73	-	12	22	-	9
3	1	163	51	84	72	-	13	22	-	9
3	2	162	51	84	73	-	12	22	-	9

Note:
1. This dimension was not measured.

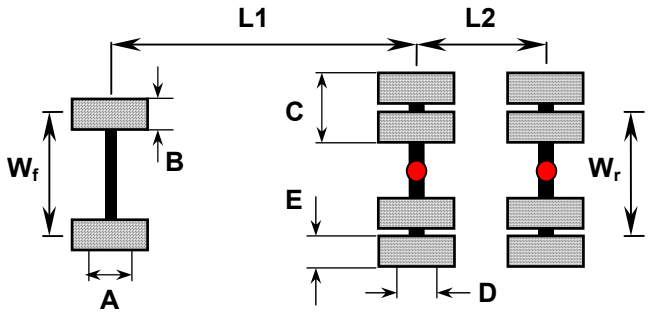

Table 11.2 - Geometry of test truck used for controlled load tests (all phases)

11.2 Test Summary

In general, the same tests were conducted for the Phase 3 tests, since the purpose of this testing was to compare the behavior with the Phase 1 and 2 testing. However, with the exception of the side-by-side park test, park tests were not conducted. New tests were conducted to investigate the sensitivity to lateral truck position. As before, two setups were used for testing since the total number of data channels was more than could be read by the data logger at one time. Tables 11.3 and 11.4 summarize the load tests which were conducted for setup #1 and #2, respectively. The tests highlighted and bold represent the tests of each type that were selected for data analysis (each test type was repeated).

Instrumentation was kept the same, however, five displacement transducers were added to record vertical displacement of the underside of the bridge during controlled load tests and long-term monitoring. These sensors were mounted to three steel braced frames spanning between the bridge abutments, as shown in Figure 11.2. A close-up photograph of the displacement sensor is shown in Figure 11.3. The sensors were located according to the plan shown in Figure 12.1, as will be discussed in Section 12.

Test #	File Name	Test Type	Travel Dir.[1]	Lane[2]	Truck Dir.[3]	Comment
1	CRL_PPT1.DAT	Crawl	S	US	F	Left tires adj. to DS PPT
2	**CRL_PPT2.DAT**	**Crawl**	**S**	**US**	**F**	**Left tires adj. to DS PPT**
3	**CRL_DEF1.DAT**	**Crawl**	**S**	**DS**	**F**	**CL left dual over rosettes D, E, F.**
4	CRL_DEF2.DAT	Crawl	S	DS	F	CL left dual over rosettes D, E, F.
5	**CRL_ABC1.DAT**	**Crawl**	**S**	**DS**	**F**	**CL right dual over rosettes A, B, C**
6	CRL_ABC2.DAT	Crawl	S	DS	F	CL right dual over rosettes A, B, C
7	CRL_US1.DAT	Crawl	N	DS	R	Truck in upstream lane CL right rear approx. 60" from FF PPT
8	**CRL_US2.DAT**	**Crawl**	**N**	**DS**	**R**	**Truck in upstream lane CL right rear approx. 60" from FF PPT**
9	**CRL_UP61.DAT**	**Crawl**	**S**	**DS**	**F**	**Left front tire 6" upstream of DEF**
10	CRL_UP62.DAT	Crawl	S	DS	F	Left front tire 6" upstream of DEF
11	CRLUP121.DAT	Crawl	S	DS	F	Left front tire 18" upstream of DEF
12	**CRLUP122.DAT**	**Crawl**	**S**	**DS**	**F**	**Left front tire 18" upstream of DEF**
13	**CRL_DS61.DAT**	**Crawl**	**S**	**DS**	**F**	**Left front tire 6" downstream of DEF**
14	CRL_DS62.DAT	Crawl	S	DS	F	Left front tire 6" downstream of DEF
15	CRLDS121.DAT	Crawl	S	DS	F	Left front tire 12" downstream of DEF
16	**CRLDS122.DAT**	**Crawl**	**S**	**DS**	**F**	**Left front tire 12" downstream of DEF**
17	SBS_1.DAT	Crawl	S	US,DS	F	Both trucks side by side (Truck #1 US; #2 DS) Truck #1 approx. 4' ahead
18	**SBS_2.DAT**	**Crawl**	**S**	**US,DS**	**F**	**Both trucks side by side; parallel to abut.**
19	SBS_3.DAT	Park	S	US,DS	F	Both trucks side by side, parallel to abut parked with rear duals at midspan.
20	DYN_DS1.DAT	Dynamic	S	DS	F	Approx. speed = 20 mph; approx. centered in normal DS travel lane
21	**DYN_DS2.DAT**	**Dynamic**	**S**	**DS**	**F**	**Approx. speed = 20 mph; approx. centered in normal DS travel lane**
22	**DYN_US1.DAT**	**Dynamic**	**S**	**US**	**F**	**Approx. speed = 20 mph; approx. centered in normal US travel lane**
23	DYN_US2.DAT	Dynamic	S	US	F	Approx. speed = 22 mph; approx. centered in normal US travel lane

Note:
1. N = north, S = south
2. DS = downstream, US = upstream
3. F= forward, R = reverse
4. Truck #2 was used for tests 1-18 and 22-25

Table 11.3 – Summary of controlled load tests (SETUP #1)

Test #	Filename	Test Type	Travel Dir	Lane	Truck Dir.	Comment
24	BOT_CL1.DAT	Crawl	S	DS	F	CL left dual over CL instrumented bottle
25	BOT_CL2.DAT	Crawl	S	DS	F	CL left dual over CL instrumented bottle
26	**BOT_CL3.DAT**	**Crawl**	**S**	**DS**	**F**	**CL left dual over CL instrumented bottle**
27	BOT_US61.DAT	Crawl	S	DS	F	CL left front tire 6" US of inst. bottle
28	**BOT_US62.DAT**	**Crawl**	**S**	**DS**	**F**	**CL left front tire 6" US, front tire only**
29	**BOTUS121.DAT**	**Crawl**	**S**	**DS**	**F**	**CL left front tire 12" US, front tire only**
30	BOTUS122.DAT	Crawl	S	DS	F	CL left front tire 12" US, front tire only
31	BOT_DS61.DAT	Crawl	S	DS	F	CL left front tire 6" DS, front tire only
32	**BOT_DS62.DAT**	**Crawl**	**S**	**DS**	**F**	**CL left front tire 6" DS, front tire only**
33	**BOTDS121.DAT**	**Crawl**	**S**	**DS**	**F**	**CL left front tire 12" DS, front tire only**
34	BOTDS122.DAT	Crawl	S	DS	F	CL left front tire 12" DS, front tire only

Note:

1. N = north, S = south
2. DS = downstream, US = upstream
3. F= forward, R = reverse
4. Truck #1 was used for tests 17-22

Table 11.4 – Summary of controlled load tests (SETUP #2)

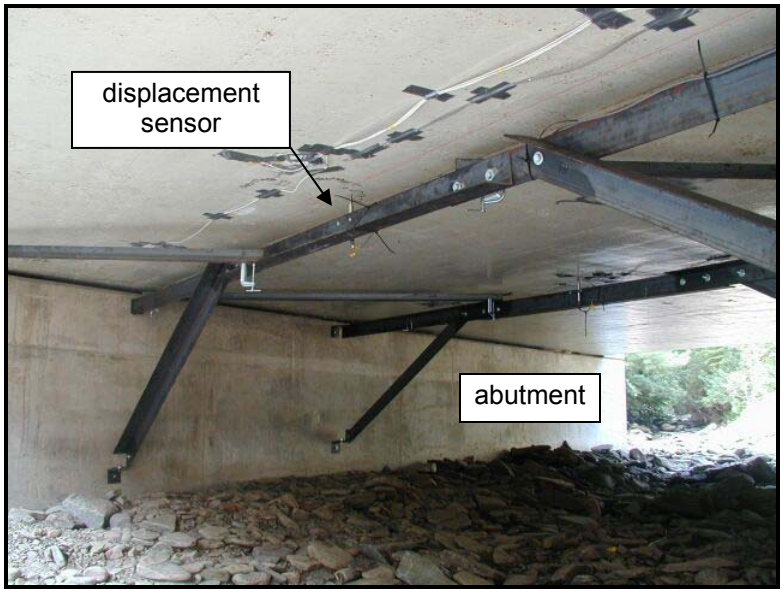

Figure 11.2 – Steel support frame installed for displacement measurements

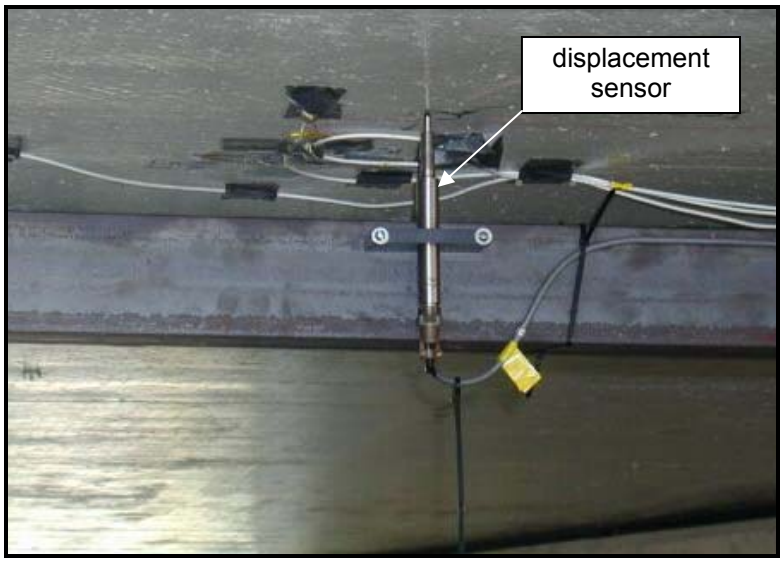

Figure 11.3 – Displacement transducer at the underside of the FRP slab

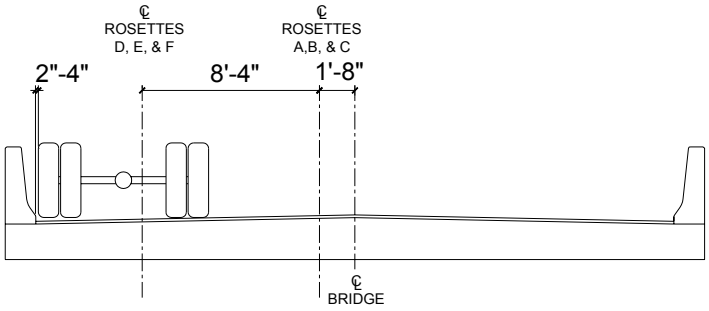

(a) Tests CRL PPT1 & CRL PPT2

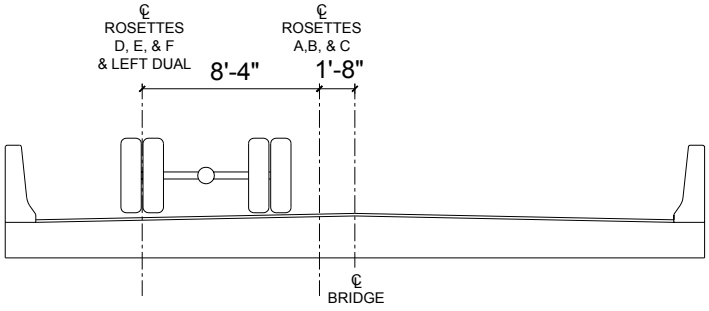

(b) Tests CRL DEF1 & CRL DEF2

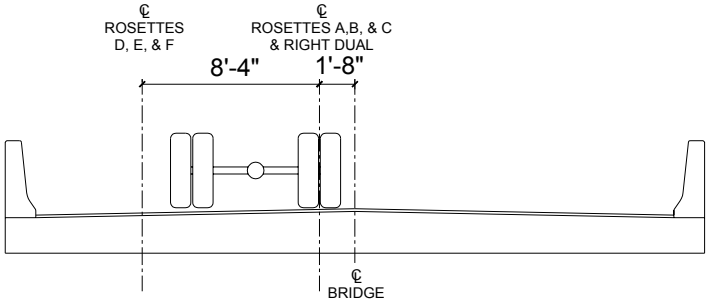

(c) Tests CRL ABC1 & CRL ABC2

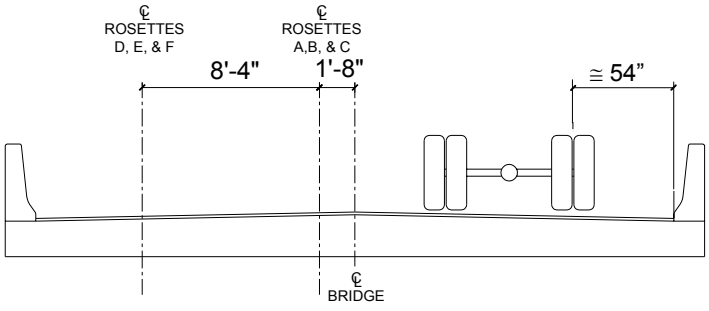

(d) Tests CRL US1 & CRL US2

Figure 11.4 – Location of test truck for the various load tests
(a) CRL_PPT1 (b) CRL_DEF2 (c) CRL_ABC1 (d) CRL_US1

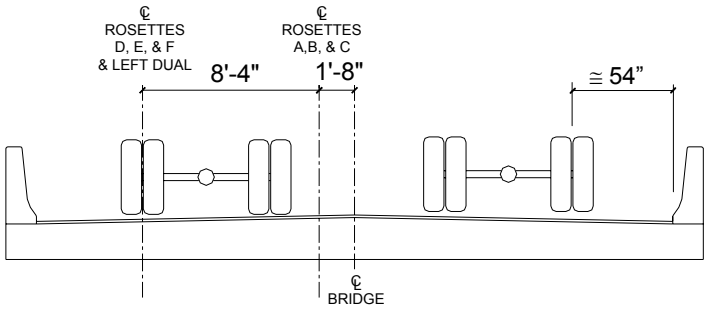

(e) Tests CRL_SBS1 & CRL_SBS2

Figure 11.4 cont’d – Location of test truck for the various load tests
(e) CRL_SBS2

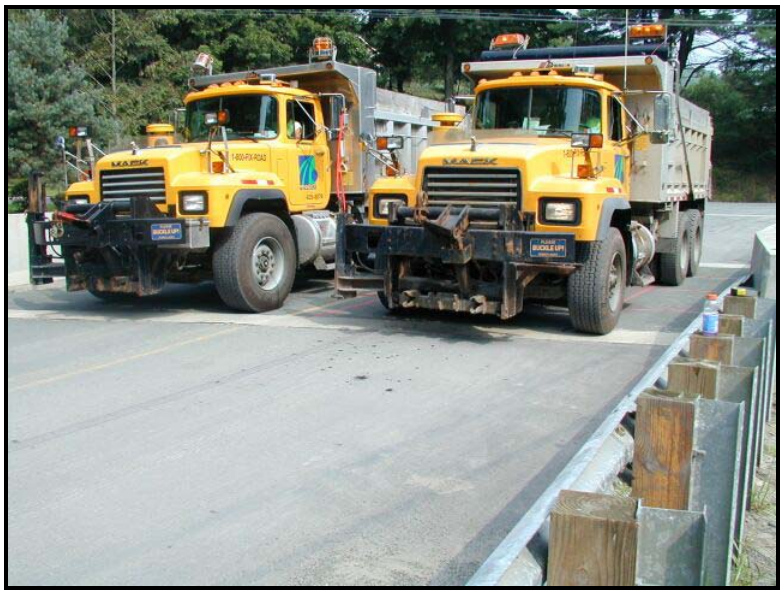

Figure 11.5- Photograph of side-by-side static crawl test

The test truck positions were kept the same, as shown in Figure 11.4. Furthermore, tests were conducted with the trucks positioned side-by-side (as in Phase 2 testing), as shown in Figures 11.4(e) and 11.5.

12.0 Results of Controlled Load Tests

In general, the behavior of the bridge during the Phase 3 tests was similar to that of the Phase 1 tests. However, two new displacement sensors were added to measure the vertical deflection of the bridge close to the abutment. It should be noted that displacements were not measured during Phase 2 testing

12.1 Static Load Tests

12.1.1 Displacements

A direct comparison between the displacement response of the bridge during Phases 1 and 3 can be made using the data presented in Tables 12.1 and 12.2, which contain the peak displacements recorded during Phases 1 and 3, respectively. The layout of the displacement sensors for Phase 3 is shown in Figure 12.1.

It can be seen that there is very good agreement between the peak displacements recorded during the two Phases of testing. As noted above, the weight of the test truck for Phase 3 was 1.5% greater than that for Phase 1, therefore, a direct comparison of the measured values can be made. In general, there is less than a 15% difference between corresponding displacements from the two phases, with the exception of the parapet displacement with the truck at the parapet (CRL_PPT1 and CRL_PPT2), and over rosettes ABC (CRL_DS1 and CRL_ABC1), where there is a 40% difference.

Of particular interest is the peak displacements recorded during Phase 3 testing at the abutments (LVDT_4 and LVDT_5). With the truck at the parapet, the peak displacement at LVDT_5 was 24 mils. When the truck was centered over rosettes ABC (CRL_ABC1) the peak displacement recorded at LVDT_4 was 21 mils. This indicates that there is significant vertical displacement of the slab at the abutment, and most likely the result of compression of the bearing pad. These displacements are not insignificant. In the case of LVDT_4, the peak displacement of 21 mils is approximately 30% of the peak displacement measured at the centerline (LVDT_3). In the case of LVDT_5, the peak displacement of 24 mils is approximately 40% of the peak displacement measured at the quarter point (LVDT_2). Hence, the deflections in tables 12.1 and 12.2 over-predict the actual deflection of the slab itself due to movement at the bearing.

Data Channel	Location	Peak Vertical Displacement (mils) (negative down)			
		CRL_PPT1	CRL_DS4	CRL_DS1	CRL_US1
CH_51	Centerline	-35.4 *(L/7290)*	-54.2 *(L/4760)*	-66.1 *(L/3900)*	-39.0 *(L/6620)*
CH_52	1/4 pt.	-57.6 *(L/4480)*	-63.6 *(L/4060)*	-58.8 *(L/4390)*	-13.9 *(L/18560)*
CH_53	Parapet	-24.8 *(L/10400)*	-16.3 *(L/15820)*	-9.8 *(L/26330)*	-0.8 *(L/322500)*

Table 12.1 – Summary of peak vertical displacements
measured during static crawl tests (PHASE 1)

Data Channel	Location	Peak Vertical Displacement (mils) (negative down)			
		CRL_PPT2	CRL_DEF1	CRL_ABC1	CRL_US2
LVDT_3	Centerline	-37.9 *(L/6810)*	-61.5 *(L/4200)*	-68.0 *(L/3790)*	-45.2 *(L/5710)*
LVDT_2	1/4 pt.	-57.3 *(L/4500)*	-62.9 *(L/4100)*	-60.5 *(L/4260)*	-15.4 *(L/16750)*
LVDT_1	Parapet	-34.8 *(L/7410)*	-18.0 *(L/14330)*	-14.0 *(L/18430)*	-0.8 *(L/322500)*
LVDT_4	Abut/CL	-10.1 *(L/25540)*	-17.7 *(L/14580)*	-20.5 *(L/12590)*	-8.3 *(L/31080)*
LVDT_5	Abut & 1/4 pt.	-23.7 *(L/10890)*	-23.8 *(L/10840)*	-21.1 *(L/12230)*	-1.5 *(L/172000)*

Table 12.2 – Summary of peak vertical displacements measured during static crawl tests (PHASE 3)

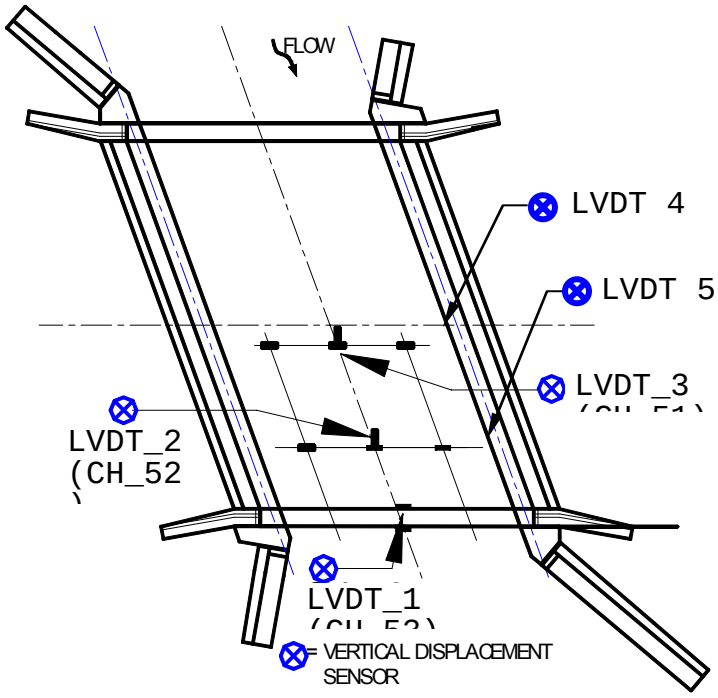

Figure 12.1 – Locations of vertical displacement sensors (used for Phase 3) located on the underside of the bridge slab.

Plots of vertical displacement for the four transverse truck positions, from the parapet to the upstream lane, are contained in Figures 12.2 through 12.5, in that order. As with the results of the Phase 1 testing, it can be seen that the displacement of the parapet is lower than the other measured displacements. Comparing with the corresponding figures for Phase 1, Figures 4.2 through 4.5, it can be seen that the response is very similar.

Figure 12.6 contains the time history plot for LVDT_4 and LVDT_5, the sensors at the abutment. These plots are very similar to an influence line plot for shear or reaction at the abutment. It can be seen that the value of displacement increases very rapidly when each axle comes onto the bridge. As noted above, the displacements at the abutment are not negligible. It should also be note that the bending deflection of the slab itself cannot be determined by subtracting the deformation at the abutment.

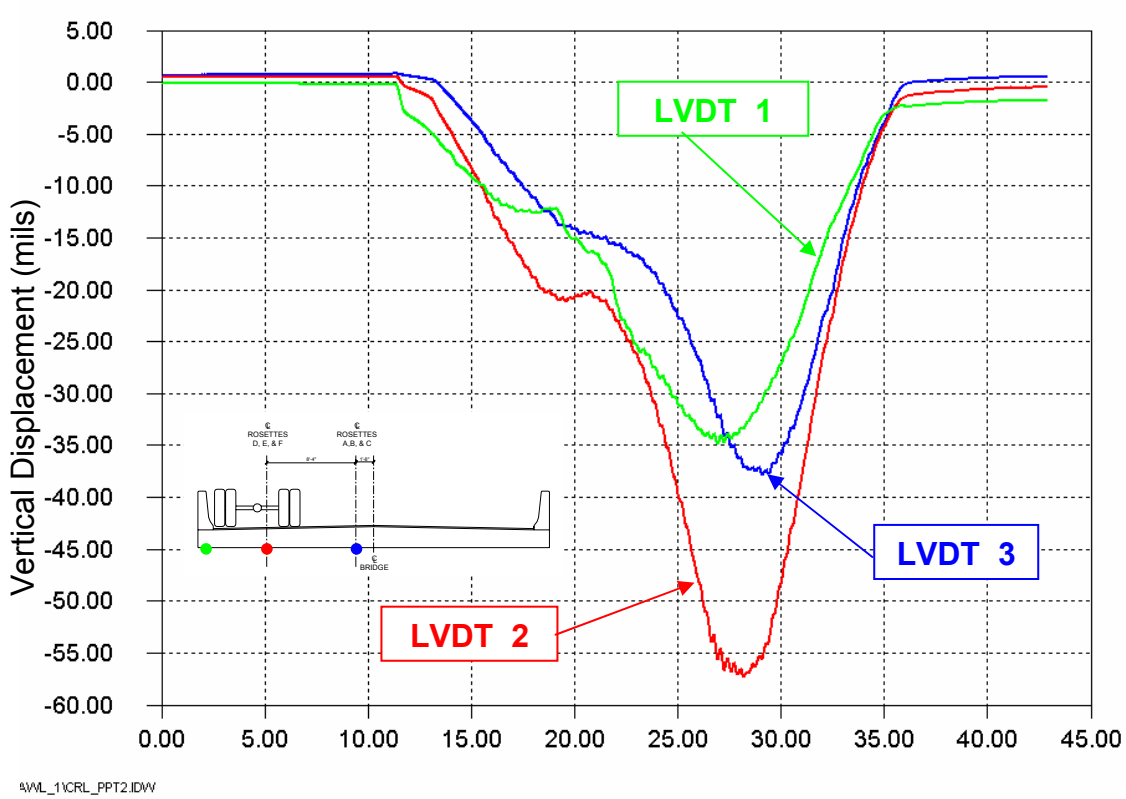

Figure 12.2 – Vertical displacement time-history for load test CRL_PPT2
(test truck located as close as possible to down stream parapet)

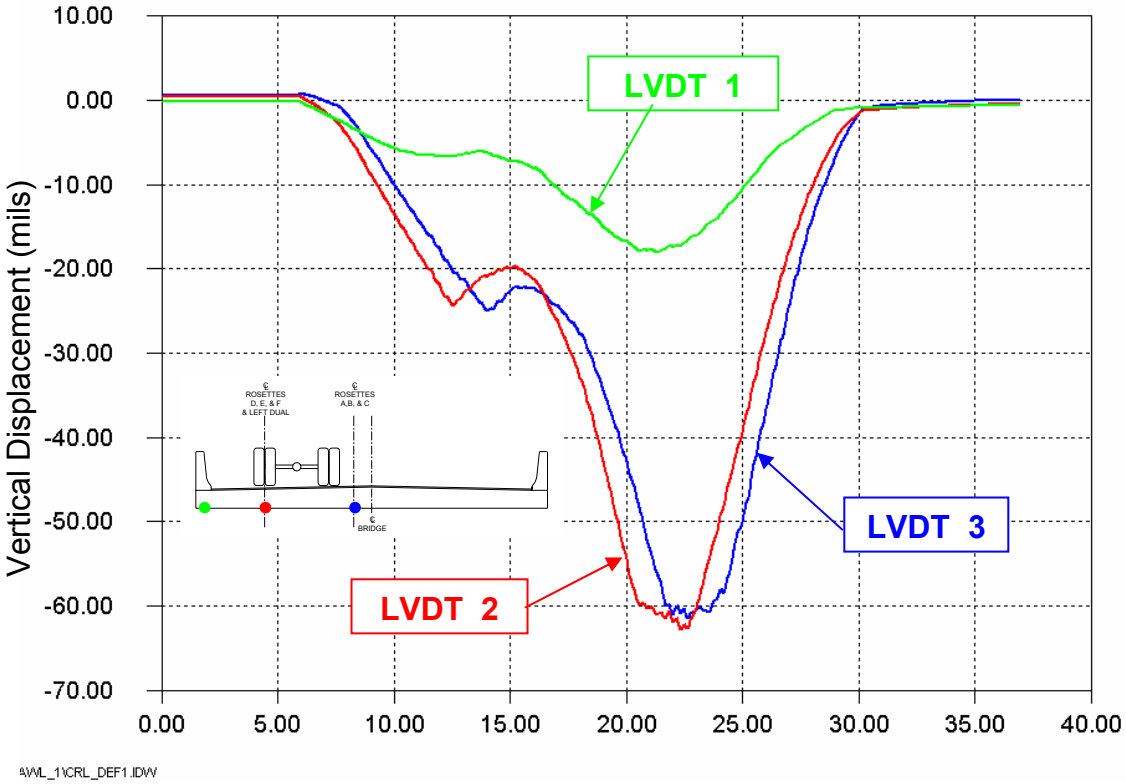

Figure 12.3 – Vertical displacement time-history for load test CRL_DEF1
(test truck located with centerline of left dual over rosettes D, E, F)

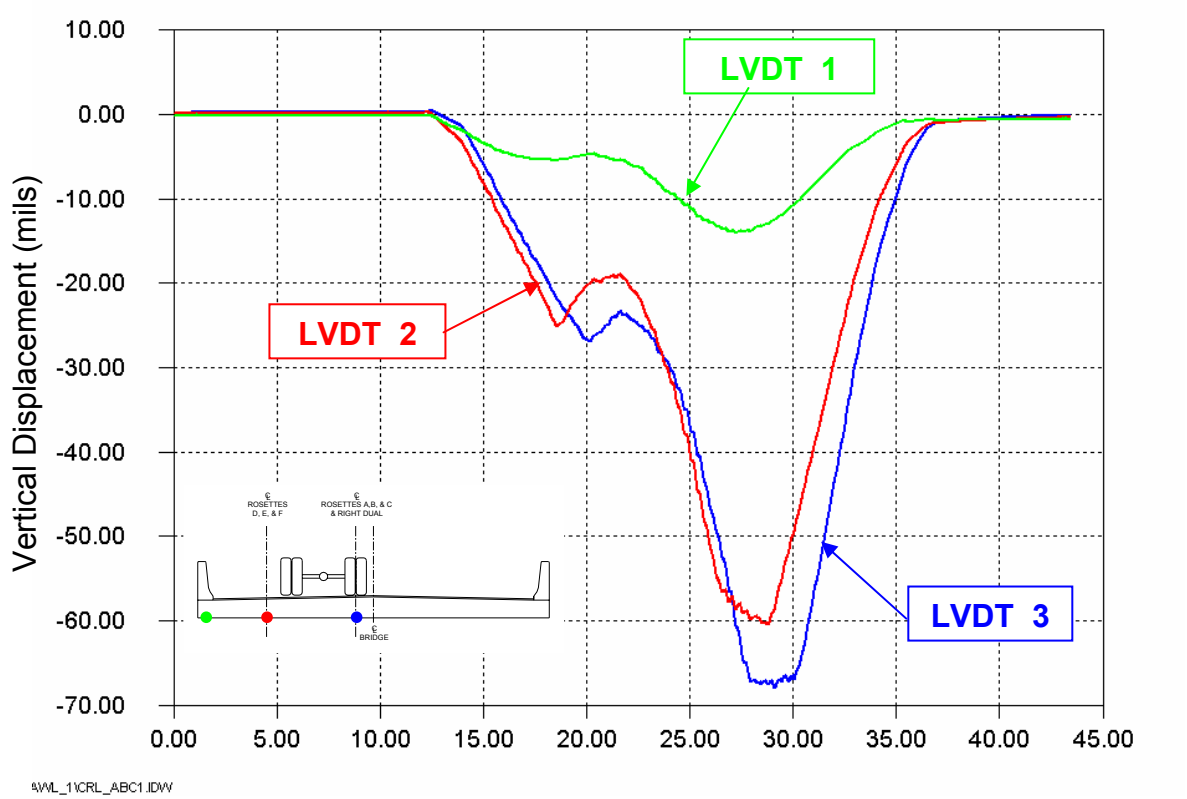

Figure 12.4 – Vertical displacement time-history for load test CRL_ABC1
(test truck located with centerline of right dual over rosettes A, B, C)

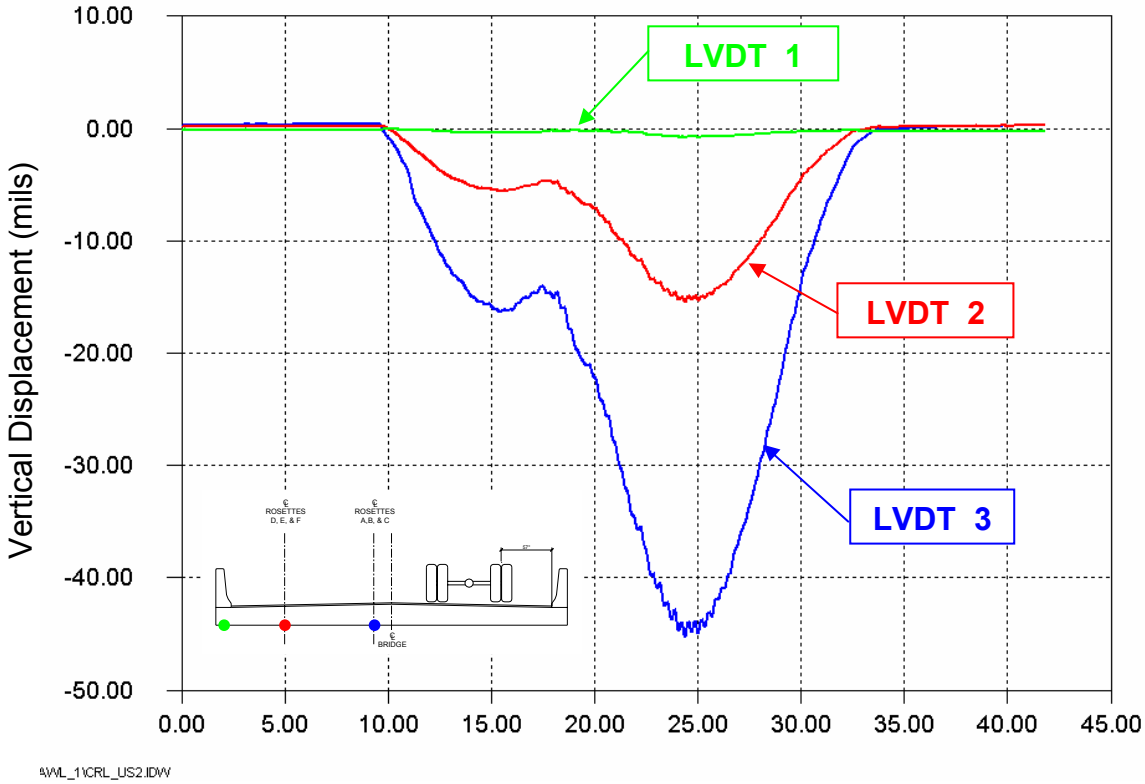

Figure 12.5 – Vertical displacement time-history for load test CRL_US2
(test truck located in upstream lane)

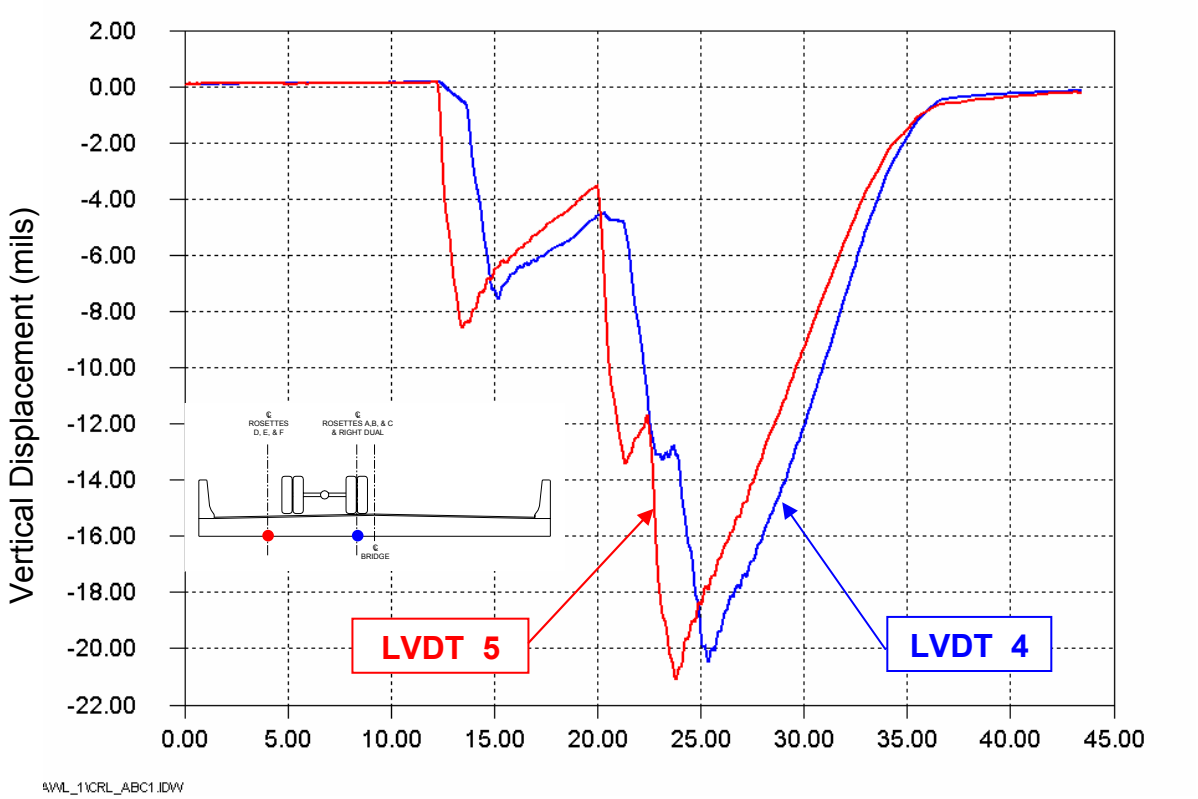

Figure 12.6 – Vertical displacement time-history of LVDT's located at the abutment for load test CRL_ABC1
(test truck located with centerline of right dual over rosettes A, B, C)

12.1.2 Strains

The magnitudes of measured strains due to global bending were similar from the two phases. Since there was only a 1.5% difference between the rear tandem axle weights of the trucks used for the static crawl tests for the two phases, direct comparison can be made between the measured strains.

A summary of the peak strains measured in Phases 1 and 3 can be seen in Tables 12.3 and 12.4, respectively. It can be seen that in general the strain magnitudes are comparable. Table 12.5 contains a summary of the peak measured strains for the side-by-side test conducted during Phase 3 only. The magnitude of the measured strains during these tests are not excessive.

Similar strain reversals to those seen in the Phase 2 data were observed in the Phase 3 data. The numbers given in parentheses in Table 12.4 are the peak positive measured strains. Again, these reversals were not observed in Phase 1.

Figures 12.7 and 12.8 contain strain time-history plots for four longitudinally oriented strain gages located at midspan for Phases 1 and 3, respectively. It can be seen by comparing these two figures, that the tension strains are very comparable. However, for the compression strains, the strain reversal is actually less in the Phase 3 test, however, the peak negative strain is greater in the Phase 3 test (-145 versus –100, for the front axle). Note that neglecting the local strains due to the passage of the wheel, the strains are comparable on the compression side as well.

Figures 12.9 and 12.10 contain strain time-history plots for four transversely oriented strain gages located at midspan for Phases 1 and 3, respectively. Again, neglecting the local strains, both the tension and compression histories are very similar.

However, the strain reversals on the compression side are much larger during the Phase 3 test.

In order to further study this phenomena, which is believed to be the result of variation in lateral position of the test truck, a series of tests were conducted as part of Phase 3, with slightly varying truck position. The test truck was driven across the bridge with the centerline of the left rear dual 6, and 12 inches downstream and 6 and 18 inches upstream of rosettes D, E, and F. Each test was repeated twice. Figures 12.11 and Figures 12.12 contain strain time history plots of the four strain gages at centerline at rosette E (both transversely and longitudinally oriented, at top and bottom) for the 12 inch and 6 inch downstream tests, respectively. It can be seen that by moving the truck just 6 inches closer to the line of interest, the behavior changes markedly, in particular, the magnitude of the local peak strains. Figures 12.13 and 12.14 contain two tests with the truck lined up on rosettes D, E, and F. Though the truck was not in the exact same position for these two tests as intended, it is within a reasonable error. These two plots indicate again that there is significant difference in the response as the front tire crosses the gage. Finally, Figures 12.15 and 12.16 contain similar plots with the truck 6 and 18 inches upstream of rosettes D, E, and F. This plots indicate that when the truck was 18 inches upstream, the local stresses cannot be seen in the data. The point of interest in all of these plots is that regardless of the truck position (within 18 inches of the intended location) the global strain behavior is very similar. However, the local strains are markedly different.

Data Channel	Location	Direction	Peak Strain (με)			
			CRL_PPT1	CRL_DS4	CRL_DS1	CRL_US1
CH_22	Top of FRP Slab	Longitudinal	-55	-81	-123	-64
CH_24		Transverse	-5	-29	*-75 (+24)*	5
CH_31		Longitudinal	-62	-98	-60	-15
CH_33		Transverse	-50	*-93 (+1)*	-42	9
CH_38	Bottom of FRP Slab	Longitudinal	55	85	119	70
CH_39		Transverse	5	27	78	-9
CH_42		Longitudinal	100	126	88	18
CH_43		Transverse	79	120	62	-11
CH_45	Parapet	Top - Long	-46	-31	-18	-2
CH_50		Bot - Trans	69	50	35	5

Table 12.3 – Summary of peak strains measured during **PHASE 1** static crawl tests

Data Channel	Location	Direction	Peak Strain (με)			
			CRL_PPT2	CRL_DEF1	CRL_ABC1	CRL_US2
CH_22	Top of FRP Slab	Longitudinal	-56	-86	-172	-75
CH_24		Transverse	-3	-42	-72 *(+67)*	-10
CH_31		Longitudinal	-61	-98	-63	-17
CH_33		Transverse	-30	-64 *(+34)*	-42	9
CH_38	Bottom of FRP Slab	Longitudinal	57	94	115	77
CH_39		Transverse	7	42	73	9
CH_42		Longitudinal	104	128	100	20
CH_43		Transverse	73	117	70	-11
CH_45	Parapet	Top - Long	Gages Damaged			
CH_50		Bot - Trans				

Table 12.4 – Summary of peak strains measured during **PHASE 3** static crawl tests

Data Channel	Location	Direction	Peak Strain (με)
			CRL_SBS2
CH_22	Top of FRP Slab	Longitudinal	-166
CH_24		Transverse	-40
CH_31		Longitudinal	-133
CH_33		Transverse	-86
CH_38	Bottom of FRP Slab	Longitudinal	163
CH_39		Transverse	28
CH_42		Longitudinal	160
CH_43		Transverse	117
CH_45	Parapet	Top - Long	Gages Damaged
CH_50		Bot - Trans	

Table 12.5 – Summary of peak strains measured during **PHASE 3** side-by-side static crawl test

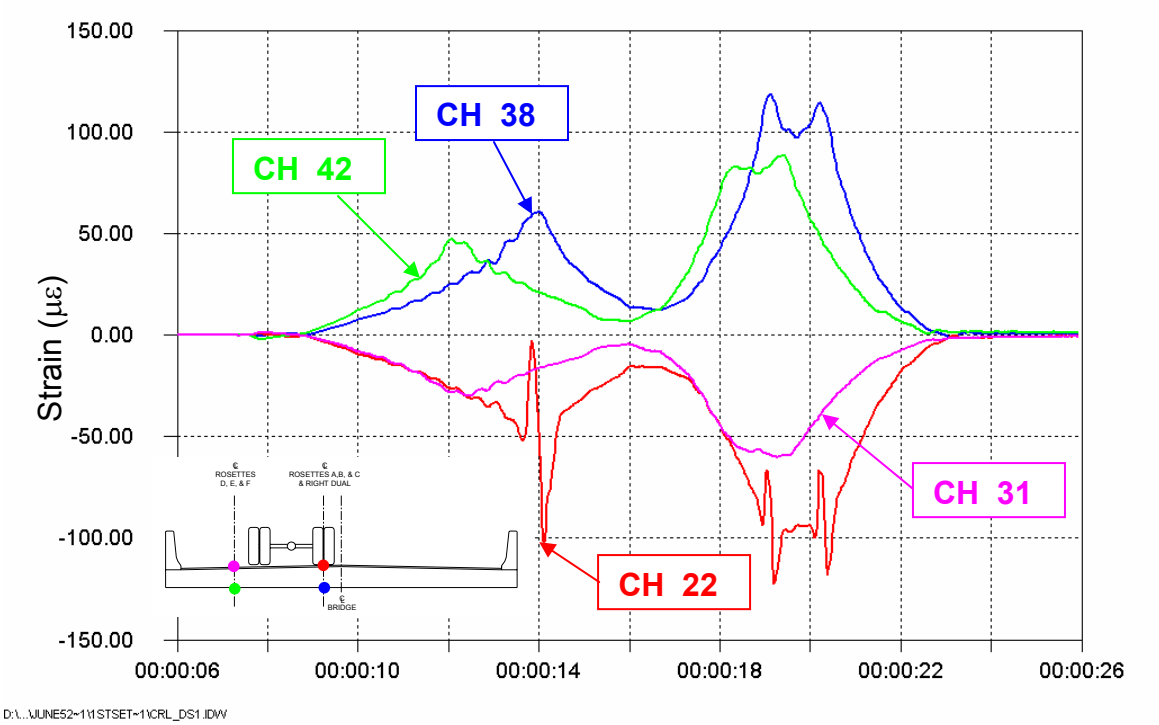

Figure 12.7 – Longitudinal strain history at midspan for load test CRL_DS1
PHASE 1 TEST
(Centerline right dual over CH_22)

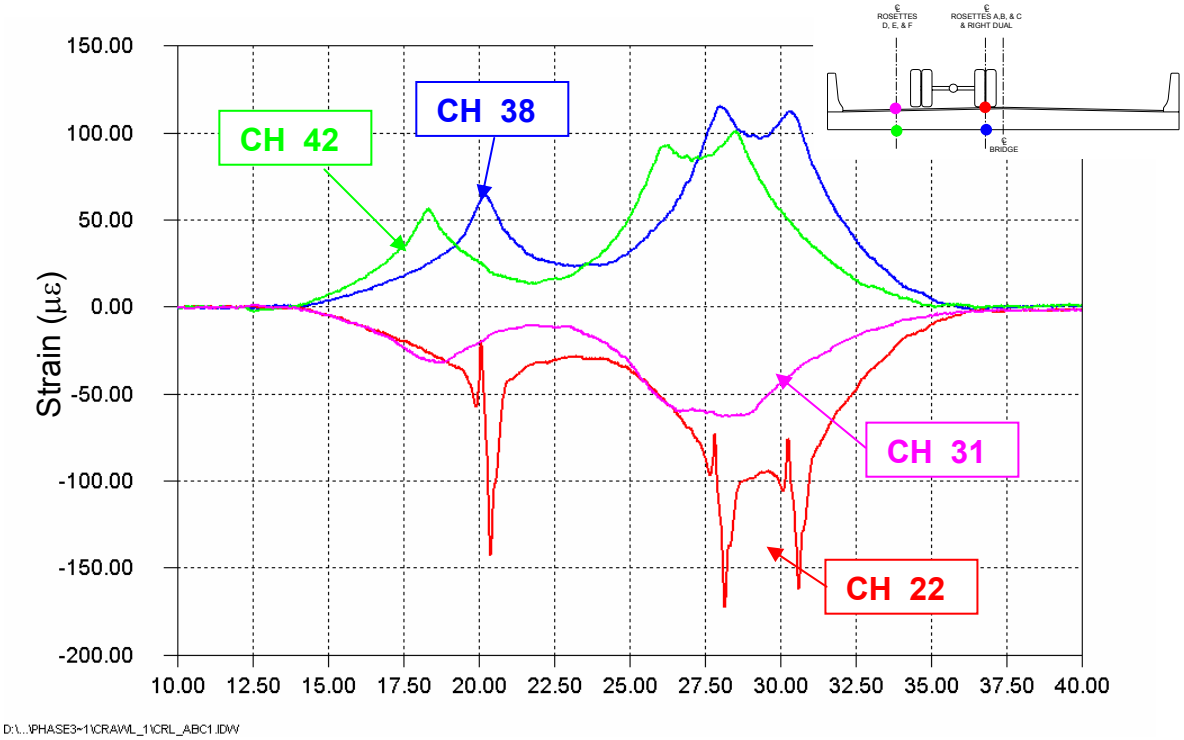

Figure 12.8 – Longitudinal strain history at midspan for load test CRL_ABC1
PHASE 3 TEST
(Centerline right dual over CH_22)

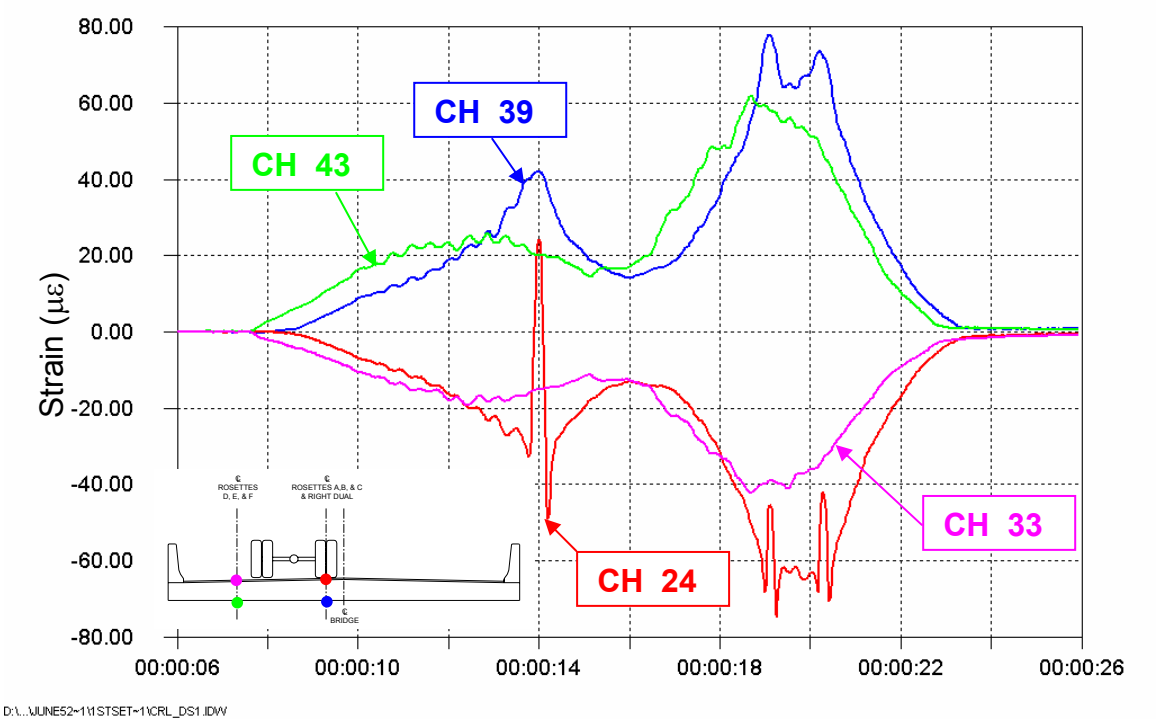

Figure 12.9 – Transverse strain history at midspan for load test CRL_DS1
PHASE 1 TEST
(Centerline right dual over CH_24)

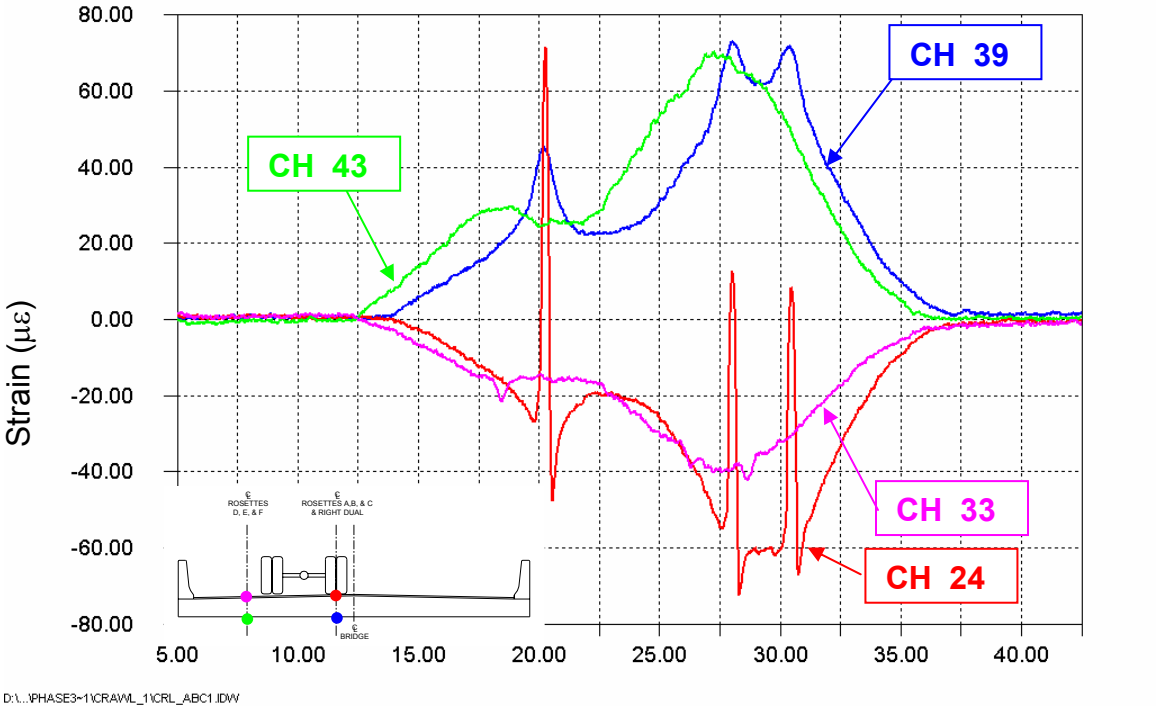

Figure 12.10 – Transverse strain history at midspan for load test CRL_ABC1
PHASE 3 TEST
(Centerline right dual over CH_24)

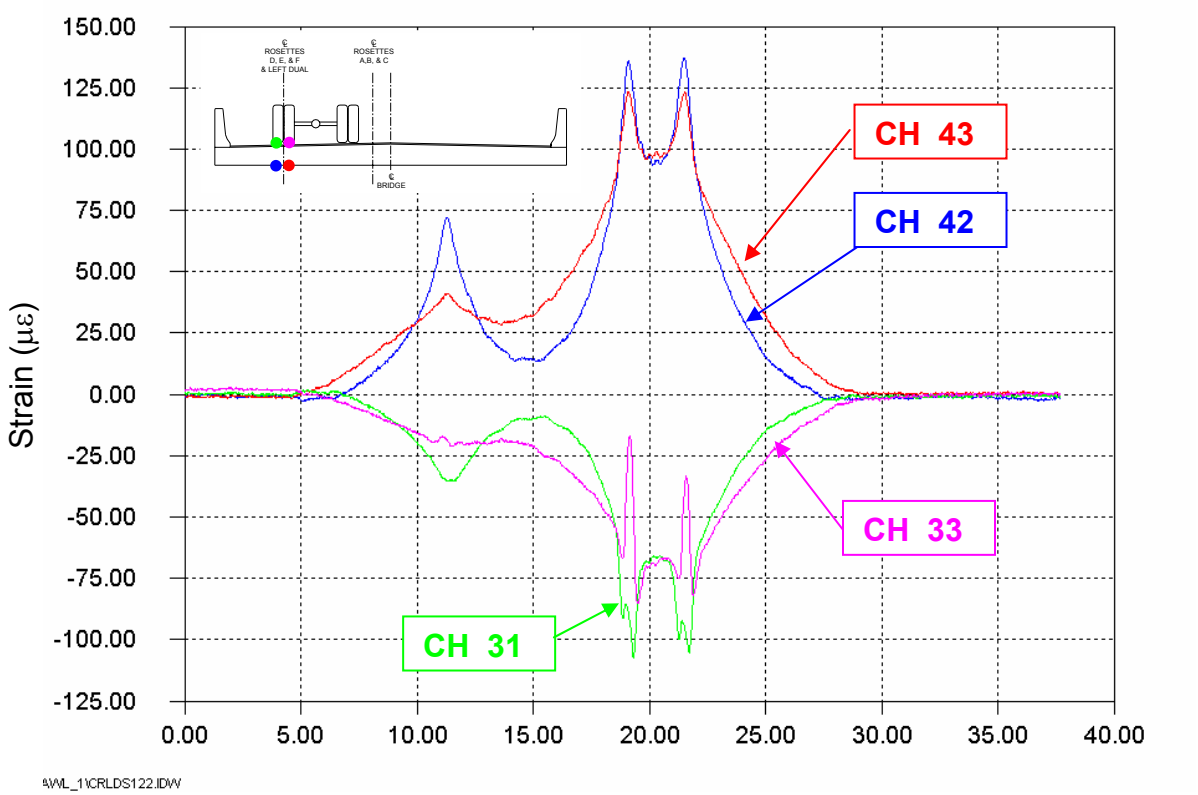

Figure 12.11 –Strain history at midspan for load test CRLDS122
Center of left dual 12” downstream of rosettes DEF
(CH_31, 42 longitudinal, CH_33, 43 transverse) PHASE 3 TEST

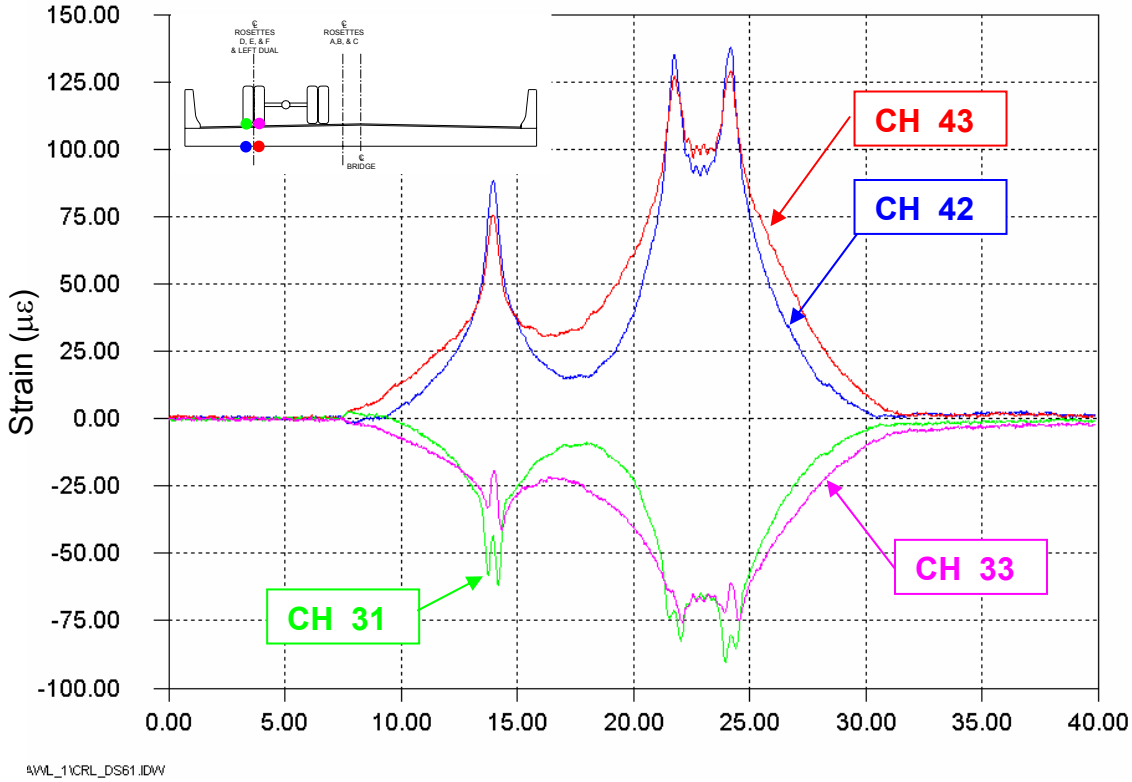

Figure 12.12 –Strain history at midspan for load test CRL_DS61
Center of left dual 6” downstream of rosettes DEF
(CH_31, 42 longitudinal, CH_33, 43 transverse) PHASE 3 TEST

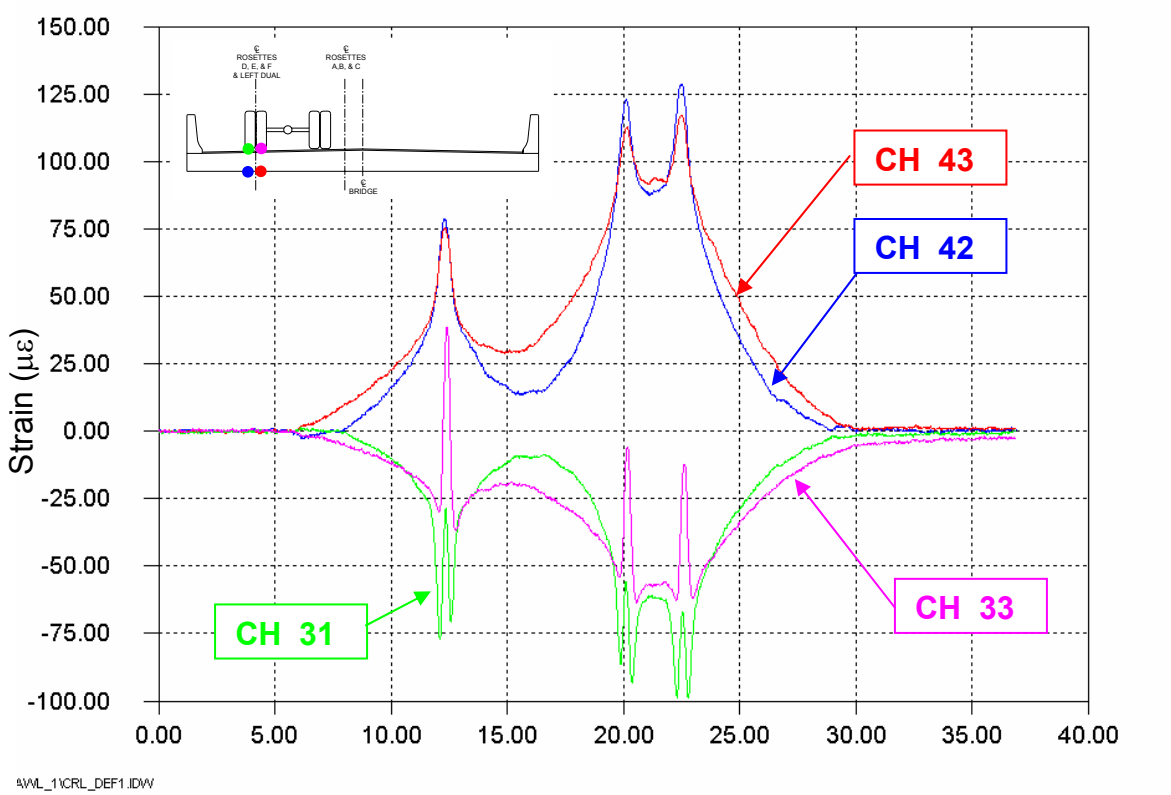

Figure 12.13 –Strain history at midspan for load test CRL_DEF1
Left dual centered on rosette DEF
(CH_31, 42 longitudinal, CH_33, 43 transverse) PHASE 3 TEST

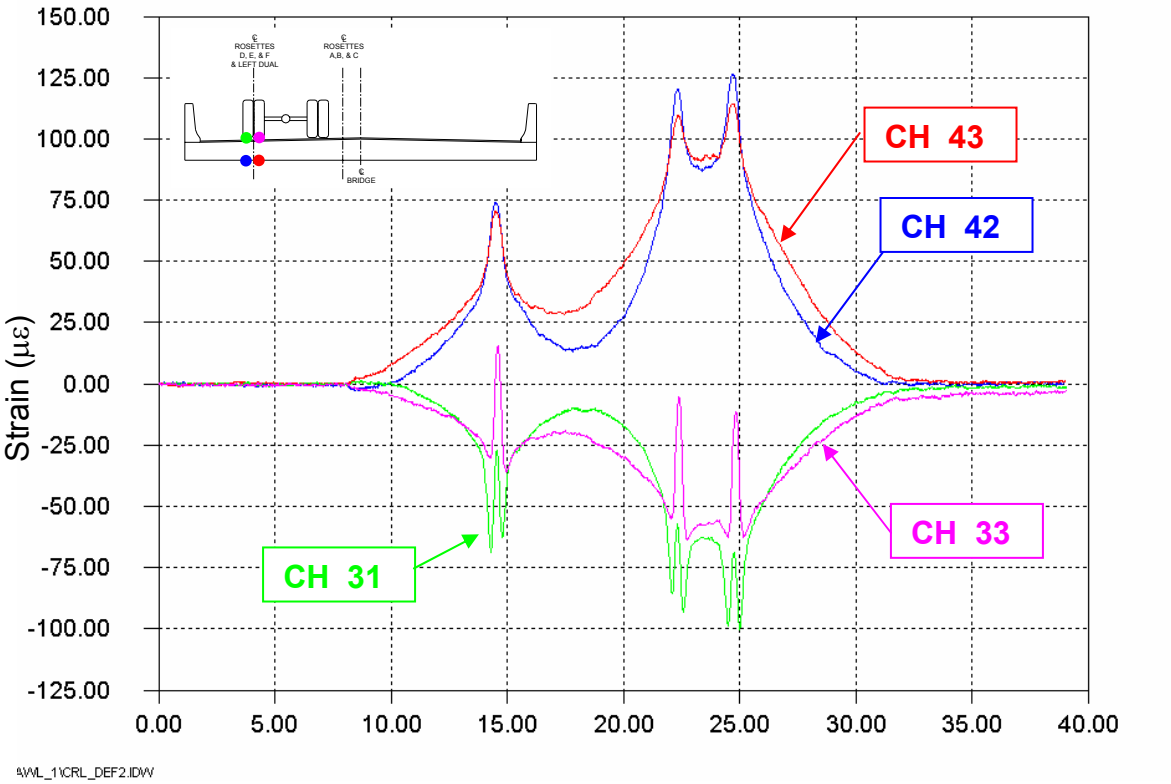

Figure 12.14 –Strain history at midspan for load test CRL_DEF2
Left dual centered on rosette DEF
(CH_31, 42 longitudinal, CH_33, 43 transverse) PHASE 3 TEST

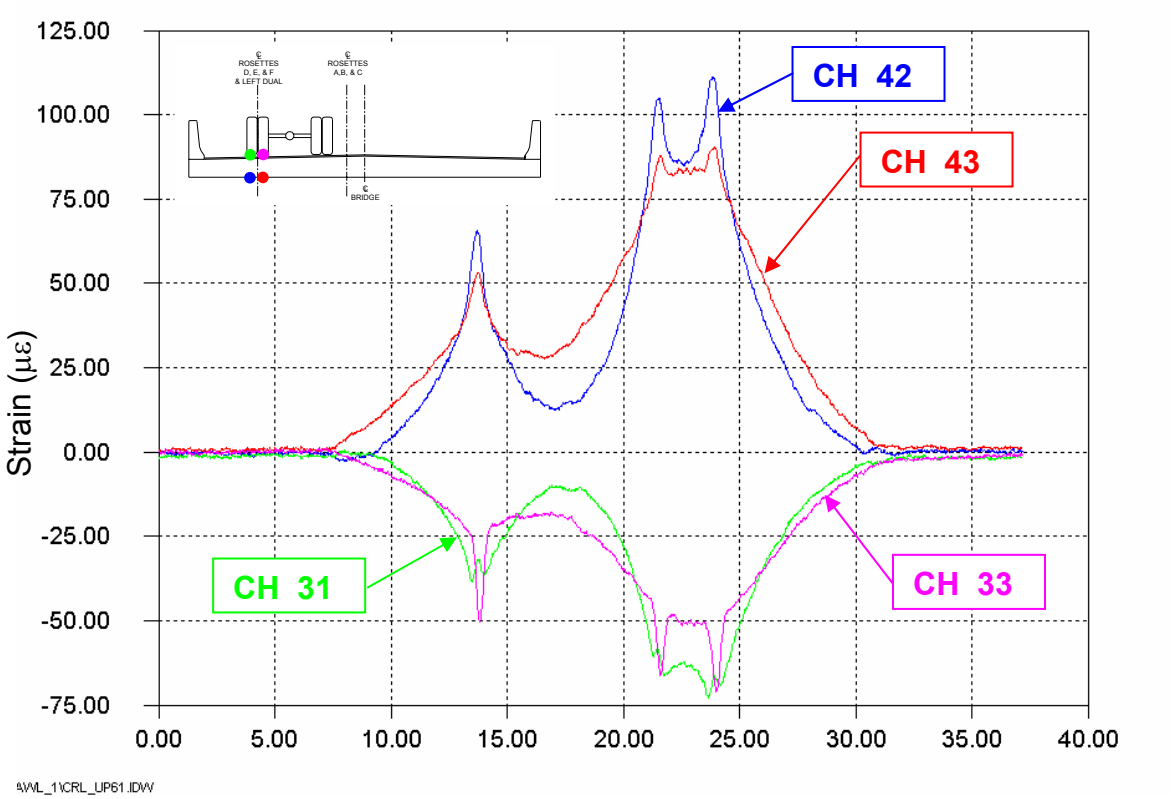

Figure 12.15 –Strain history at midspan for load test CRL_UP61
Center of left dual 6” upstream of rosettes DEF
(CH_31, 42 longitudinal, CH_33, 43 transverse) PHASE 3 TEST

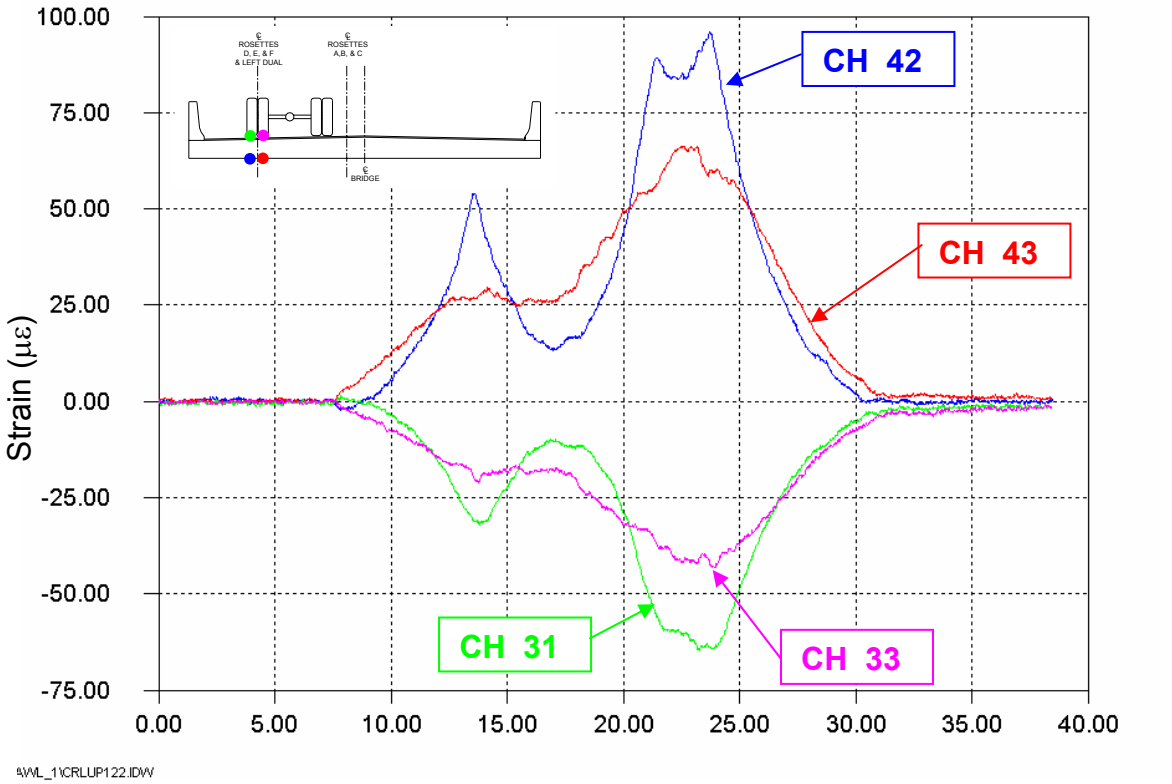

Figure 12.16 –Strain history at midspan for load test CRLUP122
Center of left dual 18” DS of rosettes DEF
(CH_31, 42 longitudinal, CH_33, 43 transverse) PHASE 3 TEST

Measured stresses at the strain rosettes are tabulated in Tables 12.6 and 12.7. Table 12.6 contains the maximum and minimum stresses measured at the rosettes for setup #1 of Phase 3. These stresses represent stresses in the top plate of the slab. (For location and orientation of the rosettes, refer to the instrumentation plan in Appendix A.) It can be seen that the peak tensile and compressive stresses of 0.74 ksi and –0.48 ksi are low. The corresponding peak stresses measured during Phase 1 were 0.25 ksi and –0.52 ksi. For Phase 2 these stresses were 0.64 ksi and –0.38 ksi. The peak compressive stresses are reasonably similar for all phases, however the peak tensile stresses appear to be highest during Phases 2 and 3.

Rosette Name		*CRL_PPT1*			*CRL_DEF2*			*CRL_ABC1*			*CRL_US1*		
		σ_x (ksi)	σ_y (ksi)	τ_{xy} (ksi)	σ_x (ksi)	σ_y (ksi)	τ_{xy} (ksi)	σ_x (ksi)	σ_y (ksi)	τ_{xy} (ksi)	σ_x (ksi)	σ_y (ksi)	τ_{xy} (ksi)
C	*Max*	0.00	0.00	0.00	0.00	0.01	0.02	**0.74**	0.19	0.29	0.00	0.03	0.21
	Min	0.00	-0.01	0.00	-0.32	-0.10	-0.05	-0.32	-0.15	-0.04	-0.14	-0.04	-0.17
D	*Max*	0.01	0.00	0.00	0.25	0.29	0.04	0.00	0.00	0.04	0.00	0.05	0.02
	Min	0.00	0.00	0.00	**-0.48**	-0.24	-0.10	-0.33	-0.15	-0.02	-0.08	-0.01	0.00
E	*Max*	0.00	0.00	0.00	0.00	0.09	0.01	0.00	0.01	0.02	0.00	0.02	0.00
	Min	0.00	-0.01	0.00	-0.46	-0.27	-0.16	-0.29	-0.18	-0.05	-0.06	-0.01	-0.02

Table 12.6 –Summary of peak rosette stresses measured during static crawl tests
Maximum tensile and compressive stresses are indicated in bold (Test Setup #2)
PHASE 3 DATA

Table 12.7 contains the maximum and minimum measured stresses for Setup #2 of Phase 2 (bottle instrumentation). These stresses represent local bending response due to passage of the wheel load in the direct vicinity of the gage. The peak tensile stress of 5.2 ksi and peak compressive stress of –5.9 ksi are reasonably similar to the peak stresses of 4.6 ksi and –5.3 ksi measured during Phase 1. However the peak stresses of 2.7 and –4.2 measured during Phase 2 are somewhat lower.

Rosette		*Test CRL_CL3*			*Test CRL_US62*			*Test CRL_DS62*		
		σ_x (ksi)	σ_y (ksi)	τ_{xy} (ksi)	σ_x (ksi)	σ_y (ksi)	τ_{xy} (ksi)	σ_x (ksi)	σ_y (ksi)	τ_{xy} (ksi)
Rosette 123	*Max*	0.3	0.2	0.0	0.4	0.1	0.0	0.0	0.0	0.4
	Min	-0.4	**-5.9**	-0.2	-0.4	-4.7	-0.6	-0.2	-0.6	0.0
Rosette 456	*Max*	0.1	0.4	0.1	0.1	0.2	0.0	0.0	0.0	0.2
	Min	0.0	-0.1	-0.3	0.0	-0.1	-0.6	0.0	0.0	0.0
Rosette 789	*Max*	0.0	0.2	0.4	0.0	0.2	0.2	0.3	0.2	0.5
	Min	-0.3	-3.3	-0.4	-0.1	-1.4	-0.2	-0.3	-2.8	-0.3
Rosette 101112	*Max*	0.3	0.3	0.3	0.5	0.2	0.1	0.1	0.3	0.6
	Min	-0.1	-3.4	-0.5	0.0	-1.1	-0.3	-1.3	-5.2	-0.4
Rosette G	*Max*	**5.2**	2.5	0.0	4.0	1.8	0.0	0.4	0.0	0.0
	Min	-0.5	-0.2	-0.7	-0.4	-0.2	-0.5	-0.2	-0.2	-0.1
Rosette H	*Max*	0.1	0.0	0.1	0.0	0.0	0.1	0.0	0.0	0.0
	Min	-0.2	-0.3	-0.2	-0.2	-0.2	-0.1	-0.2	-0.1	-0.1

Table 12.7 – Summary of peak stresses in the bottle rosettes for static load tests
Maximum tensile and compressive stresses are indicated in bold (Test Setup #2)
PHASE 3 DATA

12.2 Dynamic Load Tests

As discussed above, dynamic tests were conducted similar to Phase 1. Truck #2 was used for these tests (GVW=55.1 kips). This truck was only 1.5% heavier than the Phase 1 truck. Figures 12.17 and 12.18 contain the strain history plot for bottom surface gages at midspan for the Phase 1 and 3 dynamic tests, respectively. As can be seen, there is very good agreement in the response between the two phases. The peak transverse strains are 68 με and 62 με, for Phase 1 and 3, respectively. This is a 9% decrease. The peak longitudinal strains are 113 με and 112 με, for Phase 1 and 3, respectively. This is a 1% decrease.

Figures 12.19 and 12.20 contain similar strain history plots for top surface gages at midspan for the Phase 1 and 3 dynamic tests, respectively. If the strain reversals are not considered, the peak negative (compressive) transverse strains are -66 με and -64 με, for Phase 1 and 3, respectively. Similarly, the peak negative (compressive) longitudinal strains are -150 με and -104 με, for Phase 1 and 3, respectively. It can be seen that the plots look very different in that the Phase 3 plot does not have sharp peaks at the crossing of each truck axle. This can be attributed to the fact that the truck probably did not cross directly over the gage. Interestingly, if the peaks in the longitudinal gages at the crossing of the rear dual in Figure 12.19 are ignored, the peak stress is approximately -106 με, which is very close to the –104 με observed in the Phase 3 test. This behavior was observed in the lateral sensitivity tests described previously.

In general, with the exception of the local strain behavior, the dynamic test results of Phase 3 are comparable with those of Phase 1.

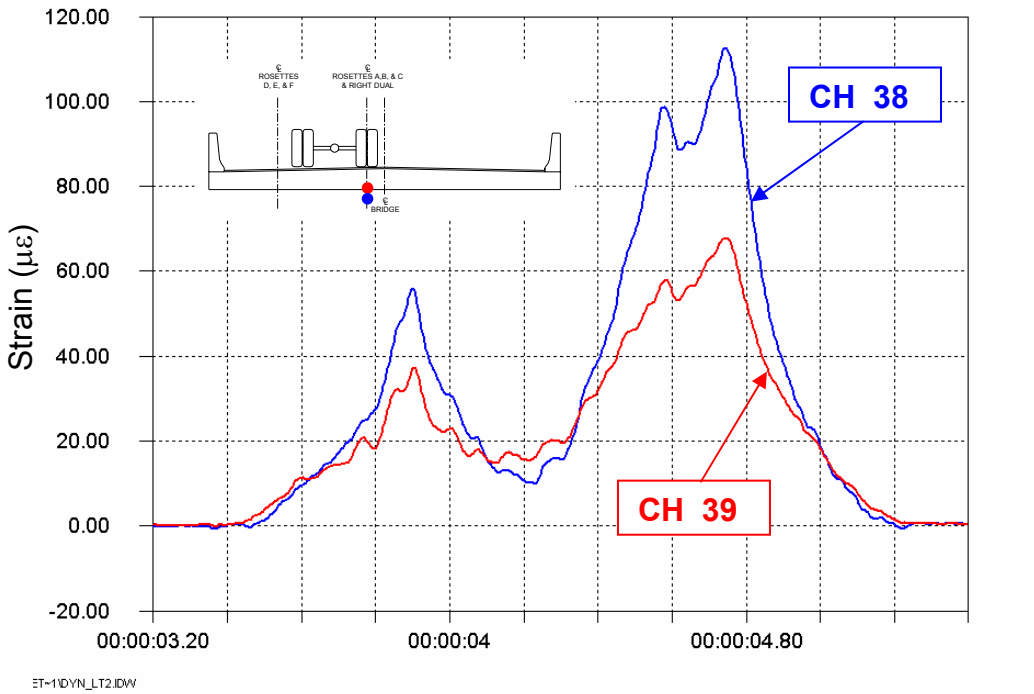

Figure 12.17 – Strain history at bottom of FRP slab at midspan
for dynamic load test DYN_LT2
PHASE 1 TEST
(CH_38 is longitudinal, CH_39 is transverse)

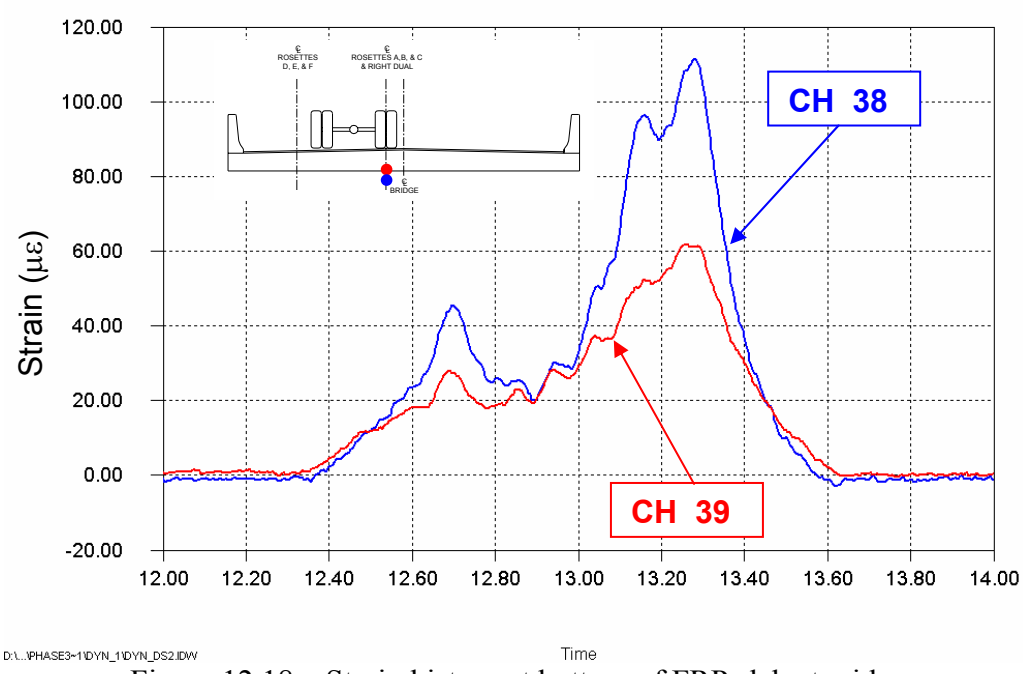

Figure 12.18 – Strain history at bottom of FRP slab at midspan
for dynamic load test DYN_DS2
PHASE 3 TEST
(CH_38 is longitudinal, CH_39 is transverse)

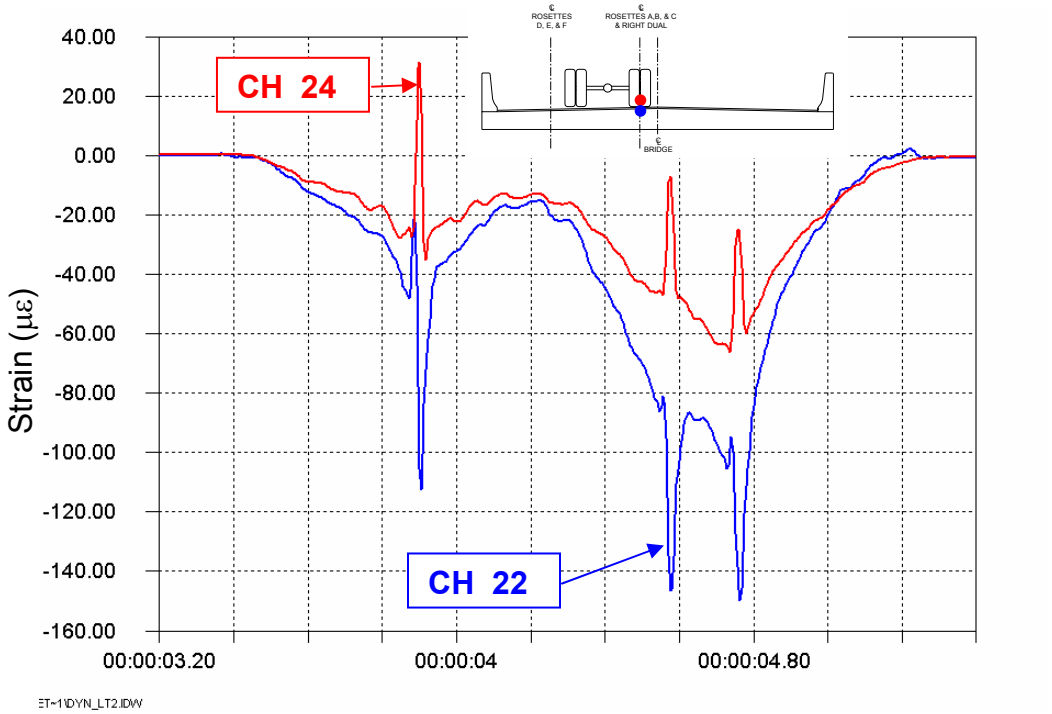

Figure 12.19 – Strain history at top of FRP slab at midspan
for dynamic load test DYN_LT2
PHASE 1 TEST
(CH_22 is longitudinal, CH_24 is transverse)

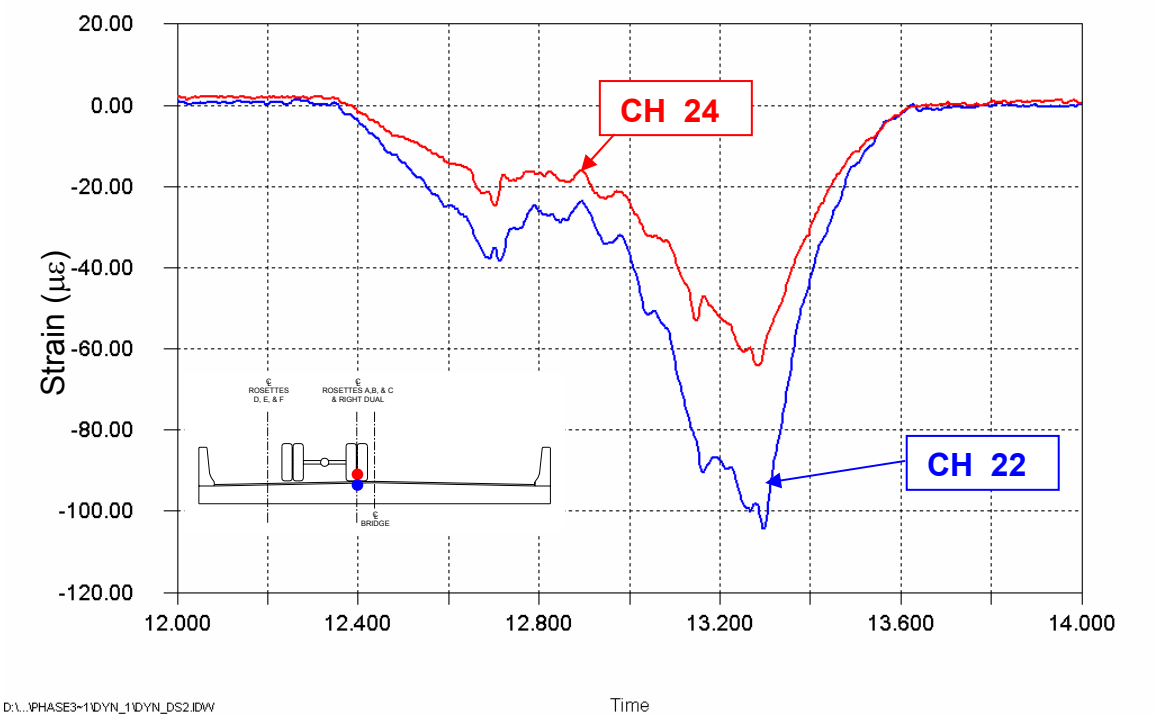

Figure 12.20 – Strain history at top of FRP slab at midspan
for dynamic load test DYN_DS2
PHASE 3 TEST
(CH_22 is longitudinal, CH_24 is transverse)

13.0 Long-Term Monitoring

As reported previously, the first phase of long-term monitoring of the FRP bridge was conducted from July 1, 2002 to August 12, 2002. The second phase of long-term monitoring extended from February 25, 2003 to April 10, 2003. The third and final phase of long-term monitoring began on August 21, 2003 and continued until October 28, 2003.

13.1 Strain Monitoring

As before, a reduced number of strain gages were selected for the long-term monitoring. The channels selected are the same as those used in Phase 1. However, the gages on the parapet were not included since they were no longer functional. Thermocouples installed within the FRP slab measured the temperature of the structure. One sensor was located outside to measure the ambient temperature.

A summary of the peak measured strains for each monitored channel, during Phase 1 and 3, is presented in Table 13.1. It can be seen from the table that most of the measured strains on the bottom of the slab are comparable for the two phases. However, on the top of the slab, it can be seen that the measured peak strains are much higher for Phase 3, in particular, gages CH_22, CH_31, and CH_32. This appears to have been caused by a single-event heavy truck. If this truck is ignored, the peak compressive strain was measured at CH_22, equal to –184 με, similar to the peak of –191 με from Phase 1. Furthermore, there is significantly more variability in the top surface gages due to sensitivity to wheel loads. In general however, it can be seen that in all cases, the measured strains are low.

Plots of all triggered events recorded during the Phase 1 and Phase 3 monitoring periods can be seen in Figures 13.1 and 13.2, respectively. During the Phase 3 monitoring period, there were 200 vehicles that crossed on the downstream side of the bridge which exceeded the trigger threshold, or about 4.3 per day. This is higher than the average 2.4 per day reported for Phase 1. Furthermore, there were only five vehicles during the Phase 3 monitoring period which caused strains higher than 100 με in either of the trigger gages (there were eight such vehicles during the Phase 1 monitoring period). It should be noted that with such a low number of heavy vehicles crossing the bridge, small events can influence the overall traffic.

It should also be noted that on October 24, 2003, the bridge was resurfaced with an asphalt topping. The continued presence of the construction vehicles on the bridge caused the data logger to trigger continuously during the resurfacing work. This is evident in the triggered time-history plot shown in Figure 13.2.

Data Channel	Location	Peak Strain Phase 1 Monitoring (με)	Peak Strain Phase 3 Monitoring (με)
CH_38	Bottom of slab; near centerline; longitudinal @ midspan	132	125
CH_40	Bottom of slab; near centerline; longitudinal @ quarterspan	94	99
CH_42	Bottom of slab; in downstream lane; longitudinal @ midspan	162	172
CH_44	Bottom of slab; in downstream lane; longitudinal @ quarterspan	127	166
CH_39	Bottom of slab; near centerline; transverse @ midspan	91	68
CH_43	Bottom of slab; in downstream lane; transverse @ midspan	140	146
CH_22	Top of slab; near centerline; longitudinal @ midspan	-161 (+23)	-184 (+72)
CH_31	Top of slab; in downstream lane; longitudinal @ midspan	-120 (+17)	-280 (+25)
CH_32	Top of slab; in downstream lane; 45 deg. @ midspan	-191 (+17)	-249 (+97)
CH_33	Top of slab; in downstream lane; transverse @ midspan	-92 (+85)	-62 (+67)
CH_45	Top of parapet; longitudinal; @ midspan	-27	-
CH_50	Bottom of parapet; longitudinal @ midspan	62	-

Table 13.1 – Summary of peak strains
measured during Phase 1 and 3 long-term monitoring
(peak strain reversals are shown in parentheses)

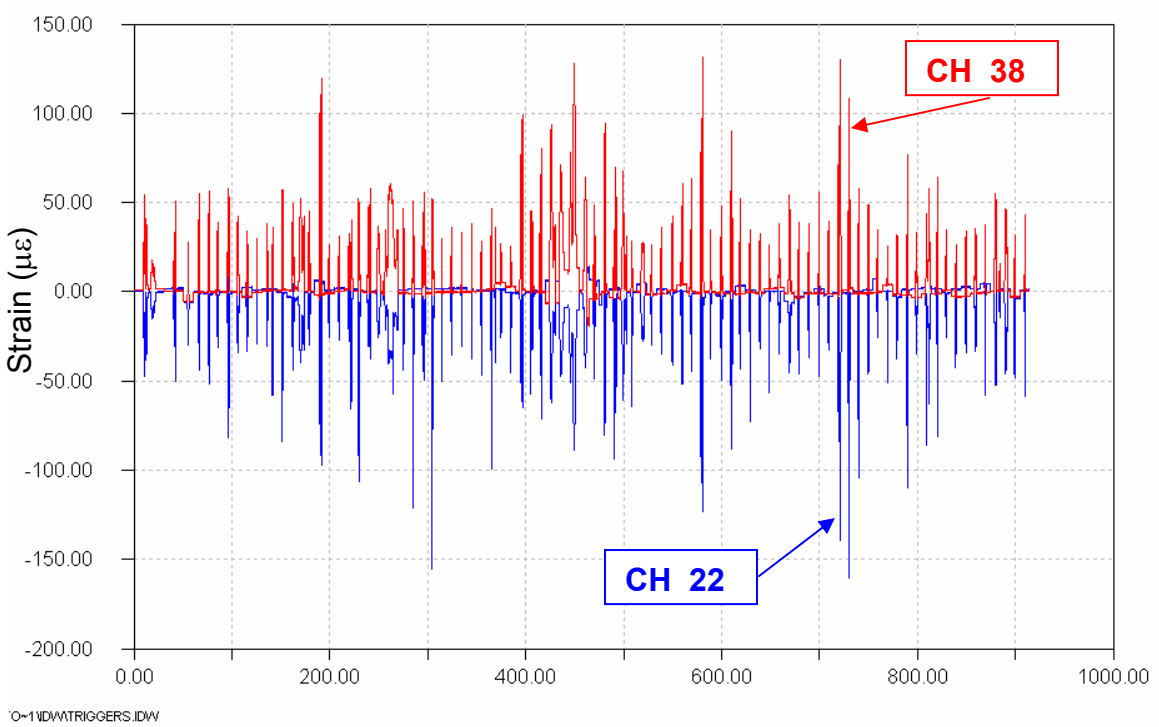

Figure 13.1 – Triggered time histories for entire PHASE 1 monitoring period

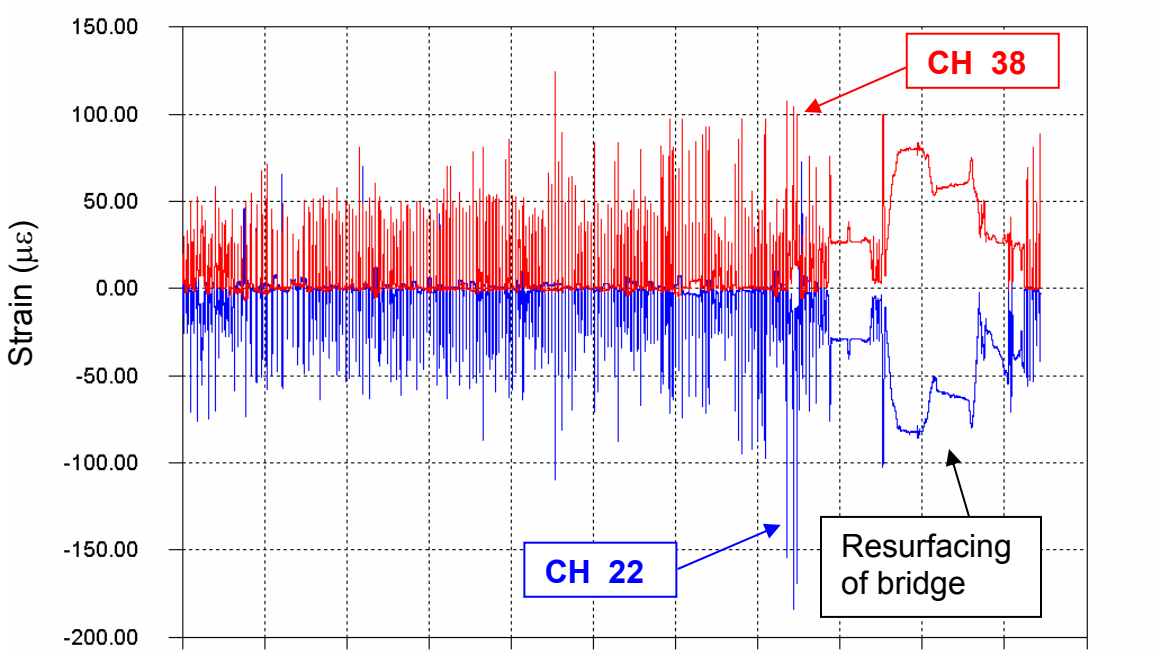

Figure 13.2 – Triggered time histories for entire PHASE 3 monitoring period

13.2 Temperature Monitoring

Temperatures in the FRP slab and outside air were monitored during Phase 3 testing. The average temperature in the top of the slab during the entire monitoring period was 59 F. At the bottom of the slab, the average temperature was 61 F. The average ambient air temperature was 58 F. Figure 13.3 presents a temperature history plot for the entire monitoring period. Note that the date the bridge was resurfaced (October 24 ,2003) is highlighted on Figure 13.3. The data show that the temperature in the top and bottom of the slab were not excessive during placement of the asphalt surface, which was a issue during the initial design phase for the bridge. The original epoxy topping was used due to concern that high temperature would damage the FRP material.

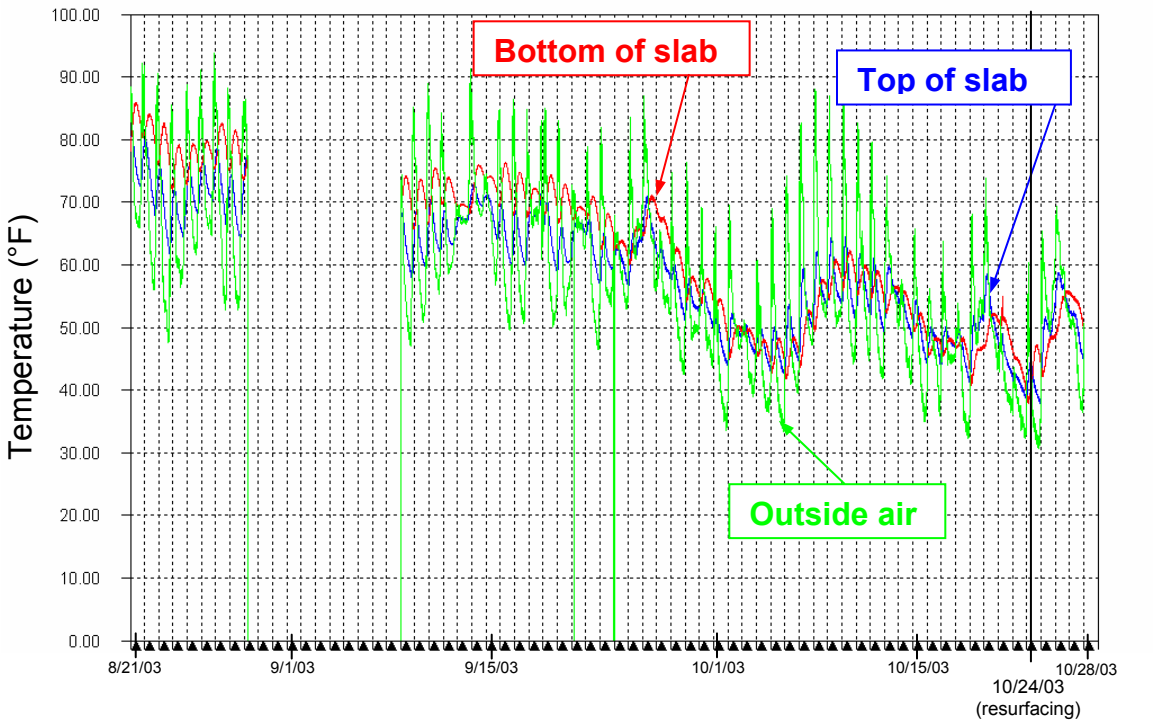

Figure 13.3 – Temperature time-histories for the entire Phase 3 monitoring period

14.0 Summary of Findings

14.1 Phase 1 Testing

The following conclusions can be drawn from the results of the Phase 1 controlled load testing presented above for this FRP bridge.

1. For the test truck load and geometry presented, the vertical displacement of the bridge is very low. The peak displacement of the bridge during the tests was approximately 0.07 inches (note that this deformation includes deformation of the bearing pads). During testing, these displacements were not perceptible to the naked eye. Peak displacements were significantly less than the design specified maximum of L/800.
2. The test truck produced low global strains in the bridge, for all load cases investigated, which are believed to encompass all expected normal service conditions. Peak global strains were on the order of 130 microstrain. Higher

strains would be expected (and were measured) when the random variable load spectrum is considered. This is because trucks heavier than the test truck (GVW = 52,820 lbs) exist.

3. Peak global stresses in the slab were on the order of 0.5 ksi.
4. The parapet behaves as a structural component of the bridge. As a result, the FRP slab is supported on all four edges. Comparable slab strains were observed in both the longitudinal and transverse directions.
5. The longitudinal joint in the FRP slab, between the two panel sections does not appear to provide full continuity across the joint.
6. The location of neutral axis varied with transverse position in the bridge cross-section. This is a result of the participation of the parapet in the vertical load-carrying system. The assumption of plane sections remaining plane is not valid when analyzing the entire bridge cross-section.
7. There was a dynamic amplification of local strains in the slab directly under the wheels of approximately 25%.
8. The concentrated wheel loads produce local stresses in the FRP material up to approximately 5 ksi in tension and 5 ksi in compression.
9. Concentrated loads on the FRP slab cause bending in both directions in both the top plate and web plates.
10. Out-of-plane bending of the parapet due to the test truck load was observed. However, the magnitude of strains caused by this bending is low.

14.2 Phase 2 Testing

The following conclusions can be drawn from the results of the Phase 2 testing.

1. The global strain magnitudes in both the transverse and longitudinal directions observed during the Phase 1 and 2 tests were very similar.
2. The peak strain measured during the Phase 2 controlled load tests was 132 με, while for Phase 1 it was 126 με.
3. The local behavior in the top of the deck directly under the truck tire during the Phase 2 tests was noticeably different from the response during the Phase 1 tests. There was significantly higher strain reversal (into tension) observed during the Phase 2 tests. This can be attributed to differences in truck geometry, possibly inaccurate placement of the test truck, and differences in behavior of the wearing surface.
4. The peak measured stress at the strain rosettes was approximately –4.2 ksi, which is very similar to the peak of -5.3 ksi measured during the Phase 1 tests.
5. During the dynamic tests, significant strain reversals were observed, similar to the static tests. However, the peak strains do not appear to be excessive, and do not seem to be the result of dynamic amplification.
6. Peak strains measured during the Phase 2 long-term monitoring was 141 με, less than the peak strain observed during Phase 1 of 191 με. Such reductions in peak measured strains may be the result of snow and ice accumulation along the roadway adjacent to the bridge which would have prevented vehicles from crossing the bridge close to the parapet, thereby reducing the strains measured in gages closer to the parapet.
7. An average of 2.6 vehicles per day crossed the bridge which exceeded the strain trigger threshold during the Phase 2 monitoring period, which is very close to the value of 2.4 vehicles per day observed during Phase 1.

8. The average air temperature during the Phase 2 long-term monitoring was 35 degrees. During Phase 1 it was 74 degrees.
9. In general, the behavior of the bridge does not appear to be significantly affected by average air temperature. Furthermore, the bridge behavior does not appear to have changed over the time period elapsed between the Phase 1 and 2 testing.
10. As discussed, the local behavior of the bridge under concentrated wheel loads differs from Phase 1 to Phase 2.

14.3 Phase 3 Testing

The following conclusions can be drawn from the results of the Phase 3 testing.

1. For the test truck load and geometry presented, the vertical displacement of the bridge is very low. The peak displacement of the bridge during the tests was approximately 0.07 inches (note that this deformation includes deformation of the bearing pads). During testing, these displacements were not perceptible to the naked eye. Peak displacements were significantly less than the design specified maximum of L/800.
2. The global strain magnitudes in both the transverse and longitudinal directions observed during the Phase 1 and 3 tests were very similar.
3. The peak strain measured during the Phase 3 controlled load tests was -172 με, while for Phase 1 it was 126 με. These readings were taken at different locations.
4. The local behavior in the top of the deck directly under the truck tire during the Phase 3 tests was noticeably different from the response during the Phase 1 tests, yet similar to the Phase 2 tests. This can be attributed to differences in truck geometry, possibly inaccurate placement of the test truck, and differences in behavior of the wearing surface.
5. The peak measured stress at the strain rosettes was approximately –5.9 ksi, which is very similar to the peak of -5.3 ksi measured during the Phase 1 tests.
6. During the dynamic tests, strain reversals were not observed, unlike the Phase 1 and 2 tests. This was attributed to the sensitivity to transverse truck position. It was shown that there is significant variability in the top surface strain readings with slightly changing wheel position.
7. Peak strains measured during the Phase 3 long-term monitoring was -280 με, significantly more than the peak strain observed during Phase 1 of -191 με. In the bottom (tension) side gages, the peak strains were very similar to those of Phase 1. This high strain recorded during Phase 3 was the result of a single heavy vehicle. If this vehicle is ignored, the next highest strain was –184 με, which is comparable to the results from Phase 1.
8. An average of 4.3 vehicles per day crossed the bridge which exceeded the strain trigger threshold during the Phase 3 monitoring period, which is somewhat higher than the value of 2.4 vehicles per day observed during Phase 1.
9. The average air temperature during the Phase 3 long-term monitoring was 58 degrees. During Phase 1 it was 74 degrees.
10. In general, the behavior of the bridge does not appear to be significantly affected by average air temperature. Furthermore, the bridge behavior does not appear to have changed over the time period elapsed between the Phase 1 and 3 testing.

11. As discussed, the local behavior of the bridge under concentrated wheel loads differs from Phase 1 to Phase 2. Tests were conducted with slightly varying transverse truck positions. It was confirmed that small variations in the position of the truck can drastically change the local strain behavior, but not the global strain behavior.

15.0 References

1. Hardcore Composites, “Analysis of Dubois Creek Bridge, Susquehanna County Analysis Report (Rev. B)” July 10, 2001.

APPENDIX A

Instrumentation Plans

FRP Bridge
SR1037 Over Dubois Creek
Great Bend Township, PA
Susquehanna County

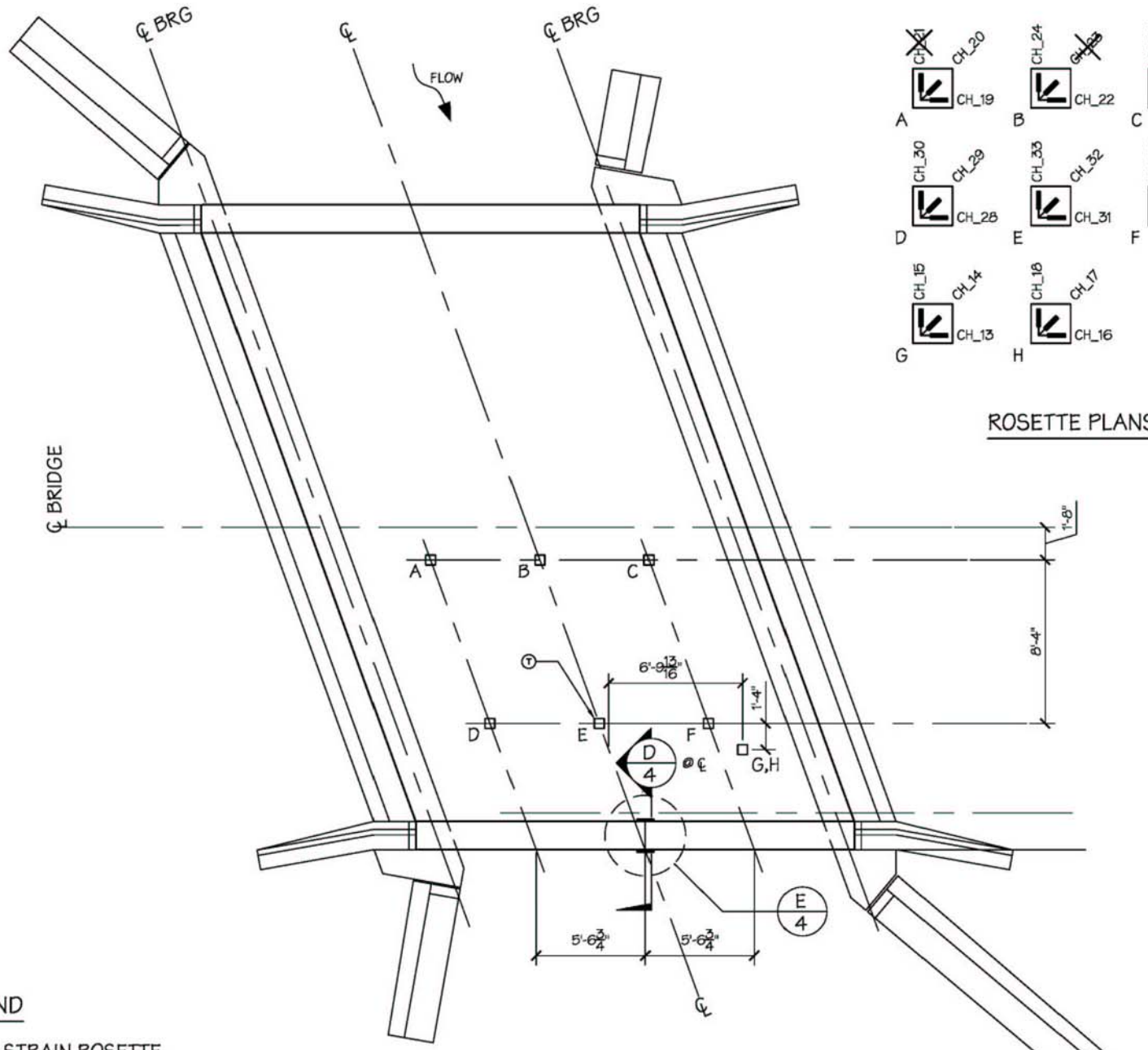

ROSETTE PLANS

LEGEND

□ = STRAIN ROSETTE

▬ = STRAIN GAGE

Ⓣ = THERMOCOUPLE

PLAN - TOP OF DECK

A/—

ATLSS

ADVANCED TECHNOLOGY FOR LARGE STRUCTURAL SYSTEMS
117 ATLSS Drive
Lehigh University
Bethlehem, PA 18015
610-758-3500 FAX 610-758-5553

PROJECT:

FRP BRIDGE

SHEET NOTES:

1. SEE ROSETTE PLANS FOR CHANNEL IDENTIFICATION.
2. ROSETTES "G" & "H" ARE LOCATED ON THE TOP SURFACE OF BOTTLE #3 (SEE SHT. 3 OF 5).
3. ALL STRAIN GAGES TO BE MICRO MEASUREMENTS N2A-06-20CBW-350.
4. ALL ROSETTES TO BE MICRO MEASUREMENTS CEA-06-250UR-350.

NO.	DESCRIPTION	DATE	BY
3	FIELD MONITORING	6/26/02	ICH
2	AS BUILT	6/19/02	GCP
1	INITIAL PLAN	5/17/02	ICH

DESIGNED BY:	ICH
DRAWN BY:	ICH
CHECKED BY:	ICH
SCALE:	1/8" = 1'-0"
DATE:	5/17/02
PROJECT NO.:	
SHEET TITLE:	

INSTRUMENTATION PLAN

SHEET NO.:

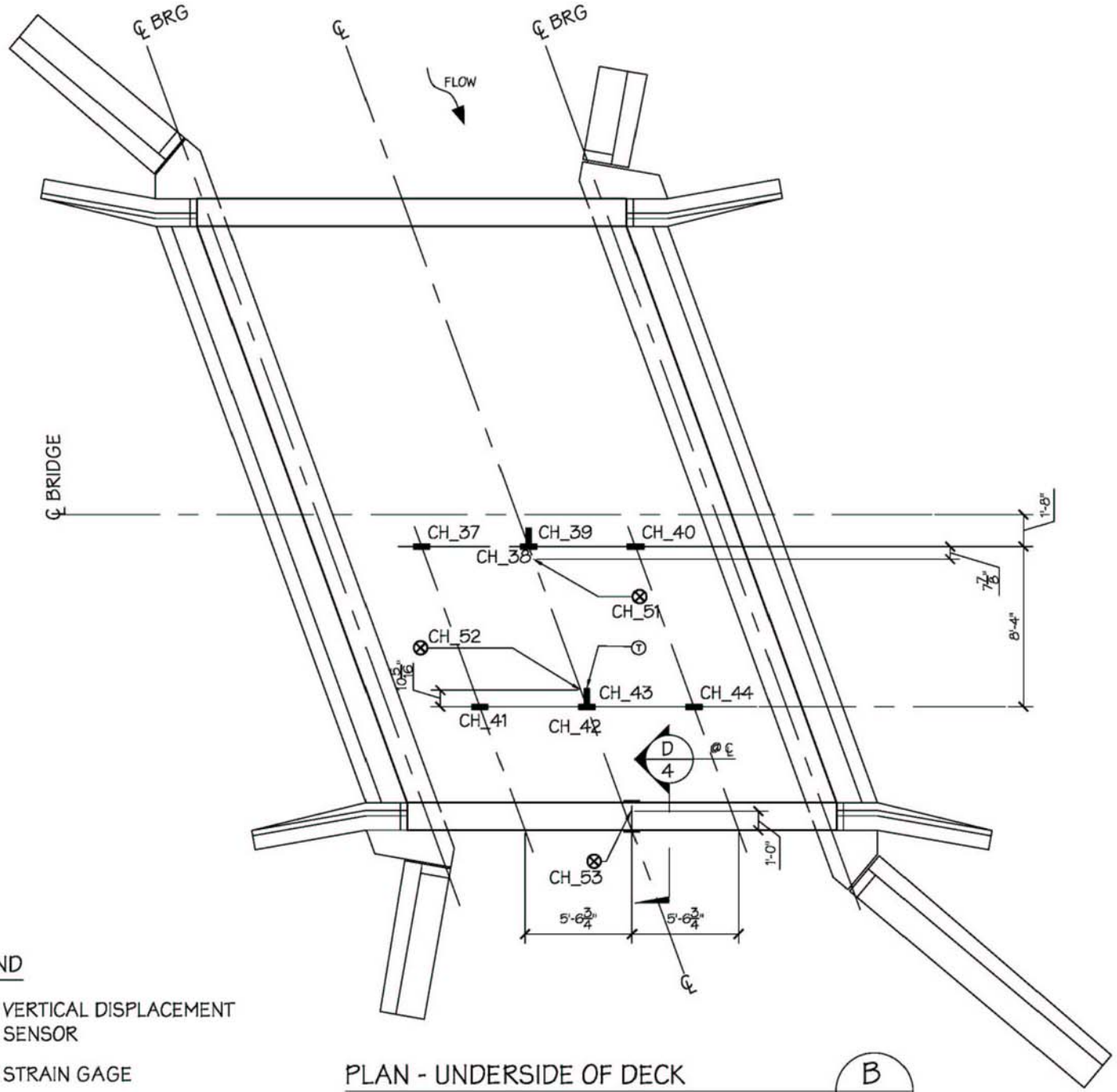

LEGEND

⊗ = VERTICAL DISPLACEMENT SENSOR

▬ = STRAIN GAGE

Ⓣ = THERMOCOUPLE

PLAN - UNDERSIDE OF DECK

B
—

ATLSS

ADVANCED TECHNOLOGY FOR LARGE STRUCTURAL SYSTEMS
117 ATLSS Drive
Lehigh University
Bethlehem, PA 18015
610-758-3500 FAX 610-758-5553

PROJECT:

FRP BRIDGE

SHEET NOTES:

1. STRAIN GAGES SHOWN ARE TO BE INSTALLED ON THE UNDERSIDE OF THE FRP DECK.
2. ALL STRAIN GAGES TO BE MICRO MEASUREMENTS N2A-06-20CBW-350.

NO.	DESCRIPTION	DATE	BY
3	FIELD MONITORING	6/26/02	ICH
2	AS BUILT	6/19/02	GCP
1	INITIAL PLAN	5/17/02	ICH

DESIGNED BY:	ICH
DRAWN BY:	ICH
CHECKED BY:	ICH
SCALE:	1/8" = 1'-0"
DATE:	5/17/02
PROJECT NO.:	
SHEET TITLE:	

INSTRUMENTATION PLAN

SHEET NO.:

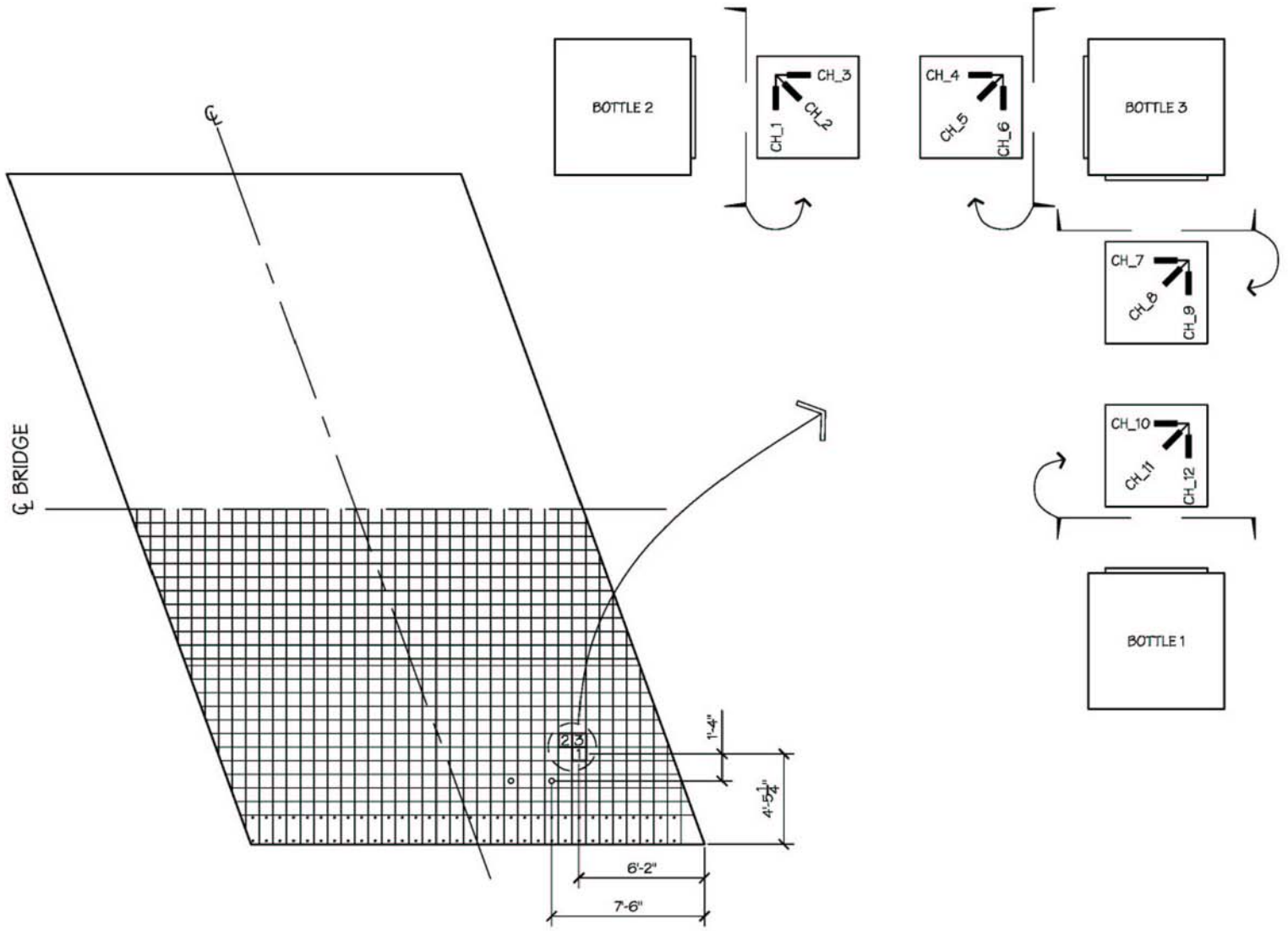

PLAN - BOTTLE INSTRUMENTATION C

ATLSS
ADVANCED TECHNOLOGY FOR LARGE STRUCTURAL SYSTEMS
117 ATLSS Drive
Lehigh University
Bethlehem, PA 18015
610-758-3500 FAX 610-758-5553

PROJECT:

FRP BRIDGE

SHEET NOTES:

1. STRAIN GAGES SHOWN ARE TO BE INSTALLED ON THE BOTTLES INDICATED.
2. ALL STRAIN GAGES TO BE MICRO MEASUREMENTS N2A-06-20CBW-350.
3. ALL ROSETTES TO BE MICRO MEASUREMENTS CEA-06-250UR-350.

NO.	DESCRIPTION	DATE	BY
3	FIELD MONITORING	6/26/02	ICH
2	AS BUILT	6/19/02	GCP
1	INITIAL PLAN	5/17/02	ICH

DESIGNED BY:	ICH
DRAWN BY:	ICH
CHECKED BY:	ICH
SCALE:	1/8" = 1'-0"
DATE:	5/17/02
PROJECT NO.:	
SHEET TITLE:	

INSTRUMENTATION PLAN

SHEET NO.:

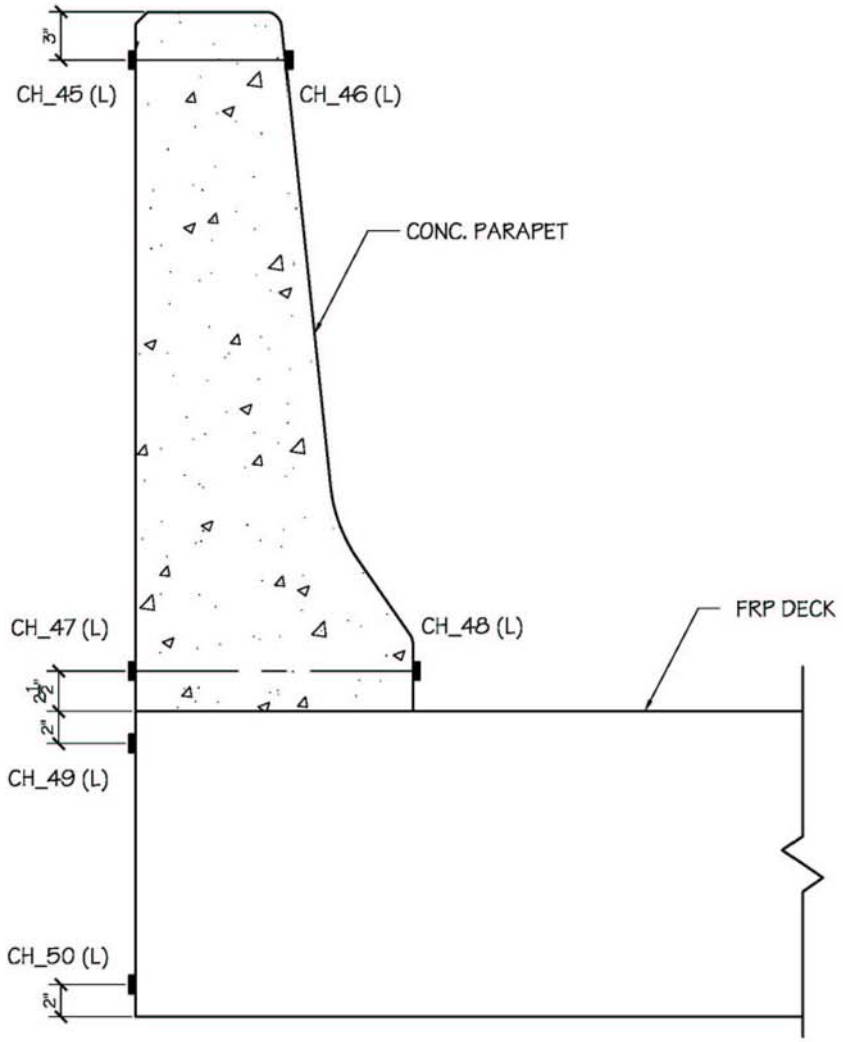

SECTION D

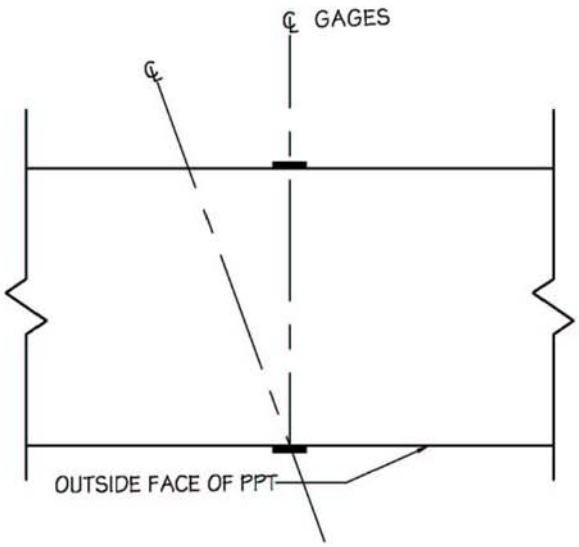

DETAIL E

ATLSS
ADVANCED TECHNOLOGY FOR LARGE STRUCTURAL SYSTEMS
117 ATLSS Drive
Lehigh University
Bethlehem, PA 18015
610-758-3500 FAX 610-758-5553

PROJECT:

FRP BRIDGE

SHEET NOTES:

1. "L" DENOTES LONGITUDINAL ORIENTATION.
2. "T" DENOTES TRANSVERSE ORIENTATION.
3. ALL STRAIN GAGES TO BE MICRO MEASUREMENTS N2A-06-20CBW-350.

NO.	DESCRIPTION	DATE	BY
3	FIELD MONITORING	6/26/02	ICH
2	AS BUILT	6/19/02	GCP
1	INITIAL PLAN	5/17/02	ICH

DESIGNED BY:	ICH
DRAWN BY:	ICH
CHECKED BY:	ICH
SCALE:	1" = 1'-0"
DATE:	5/17/02
PROJECT NO.:	
SHEET TITLE:	

INSTRUMENTATION PLAN (DETAIL)

SHEET NO.:

NO.	CHANNEL	LOCATION	DIRECTION	DATA TYPE
1	-	BOTTOM	-	TEMP
2	-	TOP	-	TEMP
3	-	AMBIENT	-	TEMP
4	38	BOTTOM	LONGITUDINAL	STRAIN
5	40	BOTTOM	LONGITUDINAL	STRAIN
6	42	BOTTOM	LONGITUDINAL	STRAIN
7	44	BOTTOM	LONGITUDINAL	STRAIN
8	39	BOTTOM	TRANSVERSE	STRAIN
9	43	BOTTOM	TRANSVERSE	STRAIN
10	22	TOP	LONGITUDINAL	STRAIN
11	31	TOP	LONGITUDINAL	STRAIN
12	32	TOP	45°	STRAIN
13	33	TOP	TRANSVERSE	STRAIN
14	45	PARAPET	LONGITUDINAL	STRAIN
15	50	PARAPET	LONGITUDINAL	STRAIN

LONG-TERM MONITORING
INSTRUMENTATION SCHEDULE

F
—

ATLSS
ADVANCED TECHNOLOGY FOR
LARGE STRUCTURAL SYSTEMS
117 ATLSS Drive
Lehigh University
Bethlehem, PA 18015
610-758-3500 FAX 610-758-5553

PROJECT:

FRP BRIDGE

SHEET NOTES:

NO.	DESCRIPTION	DATE	BY
3	FIELD MONITORING	6/26/02	ICH
2	AS BUILT	6/19/02	GCP
1	INITIAL PLAN	5/17/02	ICH

DESIGNED BY:	ICH
DRAWN BY:	ICH
CHECKED BY:	ICH
SCALE:	N.T.S.
DATE:	5/17/02
PROJECT NO.:	
SHEET TITLE:	

LONG-TERM MONITORING PLAN

SHEET NO.:

APPENDIX B

- **Overlay Specification**
- **History of Overlay Repairs**

FRP Bridge
SR1037 Over Dubois Creek
Great Bend Township, PA
Susquehanna County

CASTEK® INC.
A TRANSPO INDUSTRIES COMPANY

Technical Data Sheet

Low Modulus Polysulfide Epoxy Overlay

T-48

T-48 is a premium quality, two-component, polysulfide epoxy based wearing course used for restoring bridge decks and other pavements. It is a completely impervious overlay that will prevent any ingress of moisture, chlorides, salts, and other corrosion inducing substances. Transpo T-48 system is typically applied at the thickness of only ¼" – ½", eliminating the need to relocate joints, end dams, drain structures or catch basins. It will add less than 3-4 pounds of deadweight load per square foot of deck area, an important consideration for older structures.

Application Procedure

Surface Preparation: It is strongly recommended that all surfaces that are to receive Transpo T-48 be thoroughly clean and free of all dirt, grease, rust and other contaminates that might interfere with the proper adhesion of the polymer overlay. All damaged or deteriorated concrete shall be removed, cut back to sound concrete, and repaired with appropriate materials and methods. All surfaces, including those that are patched, must be thoroughly shot-blasted to ICRI concrete surface profile (CSP-5). Steel bridge decks (orthotropic) should be blasted to steel structures painting council SSPC–SP5 (white metal) finish. FRP bridge decks should be sandblasted to a medium sandpaper finish. To verify that the surface preparation is adequate, ACI 503R tensile adhesion tests should be performed.

Mixing: Transpo T-48 resin comes in two components (T-48A resin and T-48B hardener). Thorough and complete mixing of these two components is vital for uniform curing and performance. Mix parts A & B together in a 2:1 volume for 2-3 minutes using a Jiffy mixer (or equal) powered by low speed (400-650 rpm) electric drill until blend is uniform.

Transpo T-48 is applied using either a Broom-and-Seed or a Slurry method. It is recommended that the ambient and deck temperature be between 50 ºF and 100 ºF at the time of application.

Broom-and-Seed Method

Transpo T-48 epoxy overlay can be applied in a two-coat (1/4") or three-coat (3/8") application.

Resin Application: The first coat of T-48 resin is applied using notched squeegees or rollers at the rate of 40-50 square feet per gallon on the prepared surface.

Broadcast: Immediately after resin application, a very light broadcast is applied to break any air bubbles that may have formed during the priming process. A heavy broadcast can then be applied after 15-20 minutes (depending on temperature) until refusal. Standard basalt (dry, dust-free, and having a Mohs Hardness of 6 or above) or any other similar material can be used as a cover aggregate. Broadcasting can be accomplished either by hand or by the use of mechanical spreading machines. After cure, the excess aggregate can be broomed off for reuse.

The second and third coats must be applied after the initial set of the previous coat. The T-48 resin for the second and third coats are applied at the rate of 20-25 square feet per gallon and broadcast aggregate at approximately 1.5 lbs. per square foot.

Slurry Method

Priming: Transpo T-48 resin is applied using either notched squeegees or rollers at the rate of 30-35 square feet per gallon (100 square feet per gallon for steel and FRP decks). Temperature of Transpo T-48 resin must be above 50 °F for mixing.

Slurry-Base Coat Application: The base coat consists of T-48 epoxy resin and blended powder component. A unit mix consists of the following:

Material Component	Quantity
T-48A resin	2 gallon
T-48B hardener	1 gallon
T-48 powder (52.5 lb. bags)	2 bags

These components can be mixed using drill powered paddles, mortar mixers or special high volume continuous mixing equipment. It is recommended that the base resin components (T-48A and T-48B) be mixed thoroughly prior to adding the T-48 powder. Mixing can also be done in any multiple of the above unit mix ratio. The base coat can be spread to its desired thickness by trowels, gauge rakes, screed or automatic equipment.

Broadcast: Immediately after base coat application, a very light broadcast is applied to break any air bubbles that may have formed during the above process. A heavy broadcast can then be applied after 15-20 minutes (depending on temperature) until refusal. Standard basalt (having a Mohs Hardness of 6 or above) or any other similar material can be used as a cover aggregate. Broadcasting can be accomplished either by hand or by the use of mechanical spreading machines. After cure, the excess aggregate can be broomed off for reuse.

Packaging

	Part A	Part B
55 Gallon Drum		
Gross Weight (lbs.)	537	430
Net Weight (lbs.)	500	393
Nominal Volume(gal.)	50	50
5 Gallon Pail		
Gross Weight (lbs.)	53.1	42.4
Net Weight (lbs.)	50	39.3
Nominal Volume(gal.)	5	5

Storage

Transpo T-48 should be stored in tightly sealed containers in a dry location and at normal room temperatures (50°F-85°F). Some epoxy materials may crystallize during storage at low temperatures. The epoxy can be used once it has reached desired application temperatures.

Caution

Transpo T-48B (hardener component) contains an alkaline amine. Prolonged or repeated contact may cause sensitivity in some individuals.

It is recommended that all persons involved in mixing and application wear protective clothing such as goggles, rubber boots, rubber gloves. As with all chemicals, read MSDS prior to use.

Properties*

Property	Unit of Measure	Test
Neat Resin		
Mix Ratio	2:1 by volume	
Viscosity	1200 - 1600 cps (MPa-sec)	Brookfield
Density	8.8 lbs/gal (1.05 gms/ml) min.	ASTM D2849
Pot Life (@ 70 ºF)	15 - 30 minutes	AASHTO T237
Flash Point	200 ºF (93 ºC) min.	ASTM D1310
Solids Content	100%	ASTM D1644
Compressive Strength	5000 psi (34 MPa) min.	ASTM D695
Tensile Strength	1800 psi (12 MPa) min.	ASTM D638
Tensile Adhesion (to concrete)	250 psi (1.7 MPa) min.	ACI 503R
Tensile Elongation	45% min.	ASTM D638
Shore D Hardness	60 min.	ASTM D2240
Filled System (Mortar)		
Compressive Strength	5000 psi (34 MPa) min.	ASTM C109
Flexural Strength	1800 psi (12 MPa) min.	ASTM D790
Tensile Strength	1800 psi (12 MPa) min.	ASTM C307
Tensile Modulus of Elasticity	600,000 psi (4.10 GPa) max.	ASTM D638
Flexural Modulus of Elasticity	440,000 psi (3.0 GPa) max.	ASTM D790
Tensile Adhesion (pull-off concrete)	250 psi (1.7 MPa) min.	ACI 503R
Bond Strength	100% substrate failure	ACI 503R
Coefficient of Thermal Expansion	20-24 x 10^{-6} in./in./ ºF (11-13 x 10^{-6} mm/mm/ºC)	ASTM C531
Freeze-Thaw Resistance	Pass (no change)	ASTM C666
Wet Skid Resistance	50 min.	ASTM E274

* To be used as general guidelines only

Warranty

The following warranty is made in lieu of all other warranties, either expressed or implied. This product is manufactured of selected raw materials by skilled technicians. Neither seller nor manufacturer has any knowledge or control concerning the purchaser's use of either product and no warranty is made as to the results of any use. The only obligation of either seller or manufacturer shall be to replace any quantity of this product that proves to be defective. Neither seller nor manufacturer assumes any liability for injury, loss or damage resulting from use of this product.

01/03

20 Jones Street, New Rochelle, NY 10801

Tel: 914-636-1000 Fax: 914-636-1282
Web: http://www.transpo.com Email: info@transpo.com

November 20, 2003

Dubois Creek FRP Bridge – Overlay Repairs

A 3/8" epoxy overlay, Transpo T-48 supplied by Castek, was used for the wearing surface. The wearing surface was shop applied with the longitudinal joint and lift points being applied in the field after installation. The overlay was placed by the slurry method in the shop. The slurry method is a one-coat application, which consists of a slurry-base coat application of the two-component T-48 epoxy resin and a blended powder component followed by the broadcasting of aggregate. The blended powder is added as filler and consists mostly of sand and silica.

The method of application of the overlay for the longitudinal joint and lift points was the broom-and-seed method, which calls for the overlay to be applied in three 1/8" coats. Each coat consisted of the application of a two-component resin followed by the broadcasting of aggregate.

The FRP panels were installed in December 2001. The bridge was opened to traffic in June 2002. The bridge has a total of 750sf of riding surface area.

The manufacturer has been on the site twice since the installation to repair the overlay. The first time a total of 110.5sf was repaired. The first set of repairs was made in May 2002 prior to opening the bridge to traffic. The second time 60sf was repaired. The second set of repairs was made in August 2002 just 2 months after the bridge was opened to traffic.

The first time the manufacture determined that there were three types of failure that occurred. The first type was a delamination of 1/8" of the top treatment of the overlay. A total of 70sf of delamination occurred only on the east panel. A large part of the failure was almost the whole width of the east panel closer to the far abutment. Then there were smaller patches sporadically located on the east panel. Hardcore stated that the delamination most likely occurred due to improper surface treatment prior to applying the top coat.

The second type of failure was described as uncured areas totaling 36sf. Hardcore believed this occurred because of inadequate mixing of the overlay slurry and that there were pockets of unmixed slurry. All of the uncured failures happened on the west panel and were located in a random pattern.

The third type of failure was a full-depth failure that was at the center splice joint. The area was 4.5sf. The entire 3/8" depth of overlay delaminated at this location. Also, it was determined that there were low areas on the deck totaling 35sf, which were filled in using the same method as the repairs.

All repairs were made with the Broom-and-Seed Method. In some cases where only 1/8" of overlay was removed only one coat of the Broom-and-Seed Method was applied.

For the second set of repairs made in August 2002, Hardcore identified only one type of failure of the overlay material. The failure was delamination of the overlay from the deck. This occurred at the center splice joint and the east panel. A lot of the delamination on the east panel was on the edge of the panel along the backwalls. There was a total of 60sf that was repaired. Under the direction of a Hardcore Composites representative the aggregate was mixed in with the two-component resin. The mixture was placed with hand trowels to the blend with the top of the surrounding overlay. After the completion of the second set of repairs, a total of 23% of the original epoxy overlay was repaired to date.

In May of 2003 it was discovered that there were areas of delamination of the wearing surface again. It was determined that the best course of action would be to totally replace the epoxy overlay with a bituminous wearing surface.

Hardcore Composites began removal of the entire epoxy overlay using jackhammers and scrappers on October 21, 2003. Removal of the overlay was completed on October 23, 2003. An ID-2 wearing surface was placed on the FRP structure on October 24, 2003. The bituminous wearing surface depth varied from ¾” to 1 ½” due to field conditions. All work was completed under the construction contract that required a two-year guarantee from the fabricator.